DIMENSIONALITY REDUCTION IN CONTROL AND COORDINATION OF HUMAN HAND

by

Ramana Kumar Vinjamuri

B. Tech in Electrical and Electronics Engineering, Kakatiya University, 2002

MS in Electrical Engineering, Villanova University, 2004

Submitted to the Graduate Faculty of

Swanson School of Engineering in partial fulfillment

of the requirements for the degree of

Doctor of Philosophy

University of Pittsburgh

2008

UNIVERSITY OF PITTSBURGH

SWANSON SCHOOL OF ENGINEERING

This dissertation was presented

by

Ramana Kumar Vinjamuri

It was defended on

July 7, 2008

and approved by

Dr. Robert Boston, Professor, Department of Electrical and Computer Engineering

Dr. Heung-no Lee, Assistant Professor, Department of Electrical and Computer Engineering

Dr. Patrick Loughlin, Professor, Department of Electrical and Computer Engineering

Dr. Robert J. Sclabassi, Professor, Department of Neurological Surgery

Dr. Mingui Sun, Professor, Department of Electrical and Computer Engineering

Dissertation Director: Dr. Zhi-Hong Mao, Assistant Professor, Department of Electrical and Computer Engineering

DIMENSIONALITY REDUCTION IN CONTROL AND COORDINATION OF HUMAN HAND

Ramana Kumar Vinjamuri, Ph.D.

University of Pittsburgh, 2008

The human hand is an excellent example of versatile architecture which can easily accomplish numerous tasks with very least effort possible. Researchers have been trying to analyze the complex architecture of the human hand. It is an unsolved mystery even today how Central Nervous System (CNS) controls the high degree of freedom (DoF) of the human hand. Investigators have put forth numerous theories which support movement planning both at higher and lower levels of the neural system as well as the bio mechanical system. This planning is hypothesized to happen in a reduced dimensionality space of tiny modules of movement called movement primitives often referred to as **synergies**. These synergies are physiologically significant in planning and control of movement.

This dissertation presents time-varying kinematic synergies which linearly combine to generate the entire movement. The decomposition of these synergies becomes an exciting optimization problem and even more fascinating as it addresses two most important problems of motor control—coordination and dimensionality reduction. In this dissertation, a new model of convolutive mixtures for generation of joint movements is proposed. According to this model, an impulse originated in the higher-level neural system evokes the activation of some circuits in the lower-level neural system, then stimulates certain biomechanical structures, and eventually creates a stereotyped angular change at each finger-joint of the hand. Current model enabled greater access to existing blind source separation algorithms which reduce the computational

complexity. First, kinematic synergies were extracted from a well known matrix factorization method, namely principal component analysis. By using the above kinematic synergies, a method to obtain temporal postural synergies is established. These temporal postural synergies were further used in the model of convolutive mixtures. An optimal selection of these temporal synergies which can reconstruct movements is then achieved by l_1-minimization. The realization of the model by l_1-minimization out performed the previous models which use steepest descent gradient methods. Synergies have received increased attention in the fields of robotics, human computer interface, telesurgery and rehabilitation. Improved performance and new computational model to decompose synergies presented here might enable them to be appropriate for real time applications.

TABLE OF CONTENTS

LIST OF TABLES

LIST OF FIGURES

1.0 INTRODUCTION

1.1 DEGREES OF FREEDOM: AN OPTIMIZATION PROBLEM

Miraculous architecture of the hand always makes one wonder and leaves every one in awe and reverence for the controller, the central nervous system (CNS). A significant portion of primary motor cortex is attributed to the control of hand and fingers (see homunculus in Fig. 1.) emphasizing the complexity involved in control and coordination of the human hand. How is the CNS able to control the hand which has over 25 degrees of freedom? How many independently controlled variables, the degrees of freedom (DoF) are available for the controller? If this number is greater than the number of independent parameters describing a motor task, one confronts a genuine Bernstein problem (Bernstein, 1967). In other words, if number of DoF for peripheral apparatus is greater than the necessary DoF to execute a motor task or to unambiguously describe its motion, then it is classified as Bernstein's DoF problem. In robotics, when redundancy is encountered, there are often constraints levied on them called optimization principles that enable them to reduce the problem of abundance.

To understand motor synergies, it is helpful to first understand the "degrees of freedom" problem. Biological motor systems typically have many degrees of freedom, where the degrees of freedom in a system are the number of dimensions in which the system can independently vary. Because the number of degrees of freedom of a system carrying out a task often exceeds

the number of degrees of freedom needed to specify the task, the degrees of freedom are typically redundant.

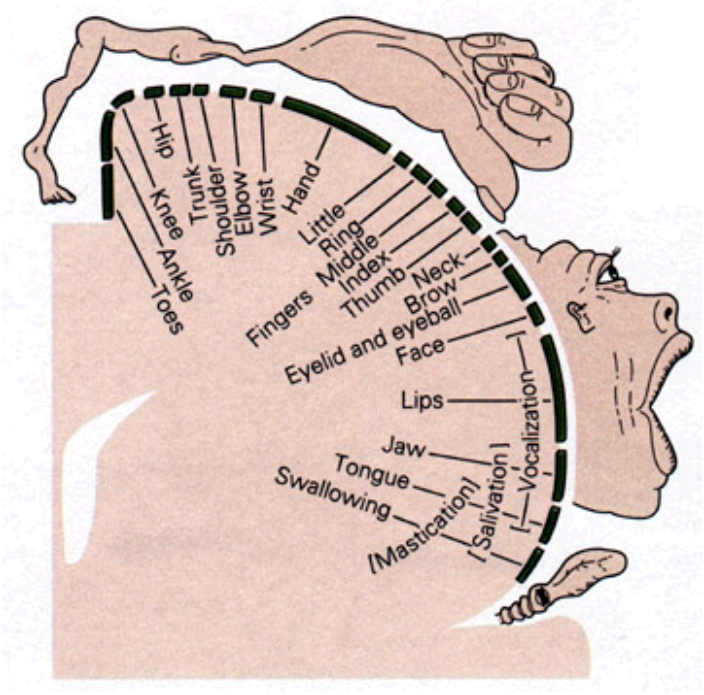

Figure 1. Topographical representation of primary motor cortex (Mackenzie and Iberall, 1994)

Consider, for example, moving human arm from a point to a point in a three dimensional plane. The location of destination has three degrees of freedom (x, y, and z position in Cartesian coordinates), but human arm have seven degrees of freedom (the shoulder has three degrees of freedom, and the elbow and wrist each have two). Obviously, there are multiple different choices of arm's joint positions that allow us to move to destination. Which one should you use? A solution to this problem is to create motor synergies, which are dependencies among dimensions of the motor system. For example, a motor synergy might be a coupling of the motions of shoulder and elbow. Motor synergies provide two types of benefits to motor systems. First, synergies restructure the problem of redundancy. Synergies can constrain the set of possible shoulder, elbow, and wrist positions that allow us to reach destination. Second, synergies reduce the number of degrees of freedom that must be independently controlled, thereby making it

easier to control a motor system. Because synergies enable motor systems easier to control, they are often hypothesized to serve as motor primitives, building blocks, or basis motor functions that are fundamental units of motor behavior that can be linearly combined to form more complex units of behavior. Investigators of motor control are attempting to develop a comprehensive understanding of biological motor synergies. Typically, researchers analyze neuro-scientific or behavioral data using mathematical techniques in order to derive the motor synergies.

Decomposition of synergies from numerous behavioral tasks is a complex optimization problem. Researchers seek for a good set of primitives, how they can be mathematically extracted and formalized? These synergies are selected such that the reconstruction error is as small as possible, while reproducing all the behavioral tasks under test by only a few synergies. I have investigated hand movements at joint level kinematics and presented here, the time varying kinematic synergies in angular velocities of finger joints during reach and grasp. Much similar to d' Avella et al., (2003), synergies are defined as tiny modules of movement which can linearly combine in different proportions and at different times to form entire movement profile. Synergies are hypothesized to exist in a space of joint level kinematics, in angular velocities. Although many such similar definitions of synergies exist, a unique numerical approach to derive these synergies from behavioral data is adapted here. Moreover, these kinematic synergies were transformed into postural synergies by extracting the postural information from the joint angle variations obtained across time and thus obtained temporal postural synergies. These were further used in a new model of convolutive mixtures for generation of movement. Selection of synergies for this model is done by l_1-minimization

1.2 SYNERGIES

Our central nervous system contains about 10^{12} neurons and neuronal connections and the human body alone consists of over 790 muscles and 100 joints. Thus, any ordinary human activity requires the cooperation among very many structurally diverse elements. It is hypothesized that in such complex living systems the elements are organized into synergies defined as functional groupings of structural elements (e.g. neurons, muscles, joints) that are temporarily constrained to act as a single unit as defined by Kelso (1982). The synergy hypothesis is therefore a way to handle biological complexity. Synergies may appear in many contexts. One of the reasons for underrating of synergies is their numerous interpretations. Synergies have no single definition. They have been used in the context of anatomy by Sherrington, a high level programming principle by Bernstein (1967), as tiny modules of movement by Mussa-Ivaldi et al., (1994), as postural synergies by Mason et al., (2001) and as muscular synergies by d'Avella and Bizzi (2003). Besides the existence of various concepts, no scientific explanations exist about their existence and how they collectively act for managing the biological complexity of motor control. Here, existing and widely accepted theories of synergies are presented.

Sir Charles Sherrington (1906) an imminent neurophysiologist who was awarded Nobel prize for his famous works like "The reflex activity of the spinal cord" proposed synergies as an anatomical-morphological concept. He observed experimentally that low level control of muscles was grouped within a reflex. He hypothesized that muscle synergies were laid down in the spinal cord and that reflex arc was the basis of synergic muscle grouping. In his words "The reflex arc is the unit mechanism of the nervous system when the system is regarded in its integrative functions. The unit reaction in nervous integration is the reflex, because every reflex is an integrative reaction and no nervous action short of reflex is a complete act of integration.

Coordination, therefore, is in part the compounding of reflexes". The conception of a reflex embraces three units 1) an effector organ – muscle cells, 2) a conducting nervous path – conductor (at least two nerve cells one with receptor and one with effector) and 3) an initiating organ where reaction starts – receptor. Main function of receptor is to lower the threshold of excitability to some and heighten to some.

Nicolas Bernstein (1935) gave a functional and operational concept for synergies. He has the credit to coin the word synergies for the first time. He described this concept as a high level control of kinematic parameters. He defined synergy as a high level organizing principle of movements. A mathematical conception was given by defining it as degree of freedom problem. It was hypothesized that CNS groups several variables into functional synergies and each synergy was controlled by a central command.

Muscle synergies (Lee, 1984; Wing, 1996) were defined as muscles acting together. Spatial synergies meant stable coactivation of a group of muscles. To address the synchronization of their activity, temporal synergies were defined. By numerous experiments scaling of synergies were observed where spatial and temporal synergies covary with modulations of task parameters like the distance to reach and grasp and sizes of grasping objects.

With the advent of virtual reality, postural synergies were widely proposed in recent times. By using matrix factorization methods like PCA (principal component analysis) and SVD (singular value decomposition) a few principal postures were obtained that could account for the variance of a wide range of postures recorded over numerous reach and grasp tasks. These postures were called eigen postures in some contexts. By extrapolating these postures, postures of the hand across the time line of reach and grasp were obtained. Though using PCA a unique way to obtain postural synergies is presented which preserves the temporal information in 4.1.

Therefore, what synergies imply still remains debatable. Moreover, the existing studies still cannot provide clear answers to the following questions: What are the physiological processes underlying a synergy? If the neural system bases its control of the hand on synergies, which part of the neural system is responsible for the generation of a synergy? How can we computationally identify the task-independent kinematic synergies from the spatiotemporal profiles of general hand movements (rather than observe the synergies from some carefully designed motion tasks)? This dissertation attempts to answer some of these questions and targets at the application of synergies in robotics and rehabilitation.

1.3 DEFINITION OF SYNERGIES

Synergies have been subject to different interpretations and have been used differently in different contexts. Numerous concepts of synergies have already been discussed in the previous section; although science today is left with the question—do these synergies really exist? If so in what spaces— muscles, joints (peripheral) or higher levels of nervous system (central) or both?

The synergies presented in this thesis are purely kinematic synergies. These are the synergies derived from angular velocities of the finger joints of human hand collected during prehension tasks. Fig.2 depicts how three synergies (left) linearly combine with three different delays and amplitudes (right bottom) to reconstruct the angular velocities at three joints. Note that the number of joints or rows is same for all synergies and the velocity profile under reconstruction. Each synergy is basically an angular velocity profile which is a coordinated sub movement. The synergy may or may not be of same duration as the velocity profile that is to be reconstructed.

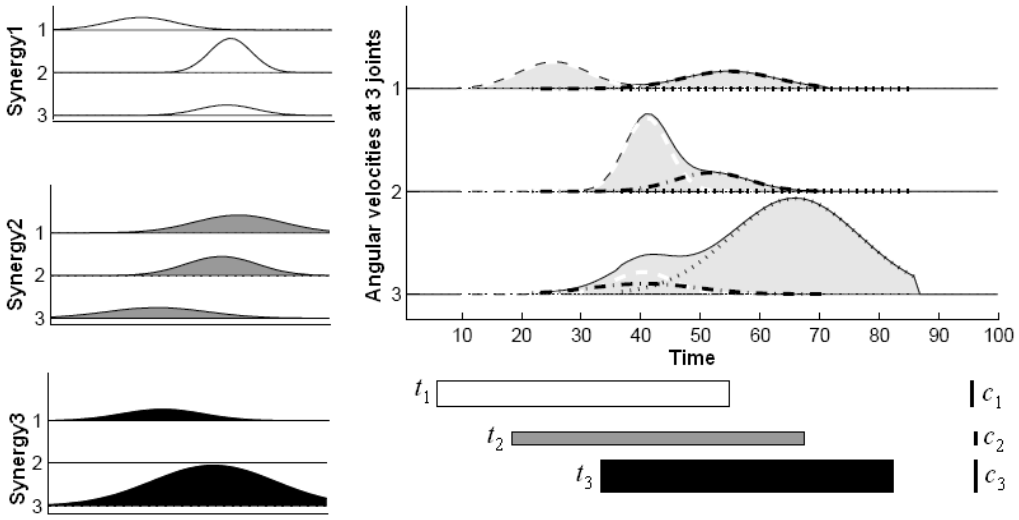

Figure 2. Synergies

These kinematic synergies are derived from the experimental recordings of prehension (reaching and grasping) tasks performed by human hand. A training data comprising hundreds of velocity profiles collected during reach and grasp experiments are used to extract these kinematic synergies using various dimensionality reduction and optimization methods.

Are these synergies task dependent or task independent? During the experiment, the tasks performed are categorically same yet they are different tasks; meaning although all the tasks can be grouped under reach and grasp tasks, each task involved reaching and grasping objects of various sizes and shapes. By decomposing all these tasks, synergies are obtained. Hence these can be called as task independent synergies as they are not meant for reconstructing grasping for a particular object. If these synergies are task independent then they must be able to reconstruct the velocity profiles during different tasks like typing, writing. To address this issue new strategies adapted are presented in 4.3.

1.4 SYNERGIES IN REHABILITATION

Apart from neuro-physiological significance, synergies are viewed to be crucial design elements in future generation robotic and prosthetic hands. Biologically inspired synergies have already taken prime place in artificial hands (Popovic and Popovic, 2001). Synergies based on the principles of data reduction and dimensionality reduction, are soon to find place in telesurgery and telerobotics (Vinjamuri et al., 2007). Synergies are projected to be miniature windows to provide immense help in next generation rehabilitation. Applying similar concepts of synergies for the behavioral data of patients with movement disorders, the sources that contain tremor were isolated. Blind source separation of convoluted mixtures model (see Chapter 4) used in modeling the tremor contained data of Essential Tremor patients led to extraction of sources containing tremor.

Biologically inspired synergies are being used in for balance control of humanoid robots (Hauser et al., 2007). Based on the principle that biological organisms recruit kinematic synergies that manage several joints, a control strategy for balance of humanoid robots is developed. This control strategy reduced computational complexity while operating in real time following a biological framework that CNS reduces the computational complexity of managing numerous degrees of freedom by effectively utilizing the synergies.

Biologically inspired neural network controllers (Benrabucci et al., 2007) have been developed which can manage ballistic arm movements. The model simulates the kinematic aspects, with bell-shaped wrist velocity profiles, and generates movement specific muscular synergies for the execution of movements.

Bimanual coordination is damaged in brain lesions and brain disorders. Postural debilitation is evidently seen in patients with movement disorders such as Parkinson's disease,

essential tremor, and multiple sclerosis. Differences in postural control and movement performance during goal directed reaching in children with developmental coordination disorders have been studied (Johnston et al., 2002). Eigen postures or postural synergies were reported to have physiological and anatomical significance by Mason et al., (2001). Study of the eigen postures in normal subjects during bimanual coordination and comparing them with bimanual eigen postures of patients might have a potential contribution for rehabilitation (Vinjamuri et al., 2008a). By training, if such lacking eigen postures are learnt by patients, it might be possible to bring back the missing bimanual coordination.

Bizzi et al., (2003) have extensively investigated muscle synergies and their modular organization in spinal motor systems (Bizzi et al., 2000) that play a significant role in kinematics (arm movements) and dynamics (force fields) of movement in vertebrates. The study (Bizzi, 2007) was extended to examine the EMG patterns in patients with stroke. They examined whether the motor disturbances following a stroke are the result of missing one or more synergies, or a failure of supraspinal structures to provide the correct coefficient of activation to one or more synergies, or a failure to select the proper synergies to accomplish a specific goal and /or a change in the balance of individual muscles within a given synergy. This study can enhance the current understanding of the role of the CNS in motor control and also be beneficial to patients in developing specific therapeutic intervention.

Using a reduced set of movements, control policies or actuator synergies have attracted great interest in robotics research. A limited set of primitives can considerably reduce the high dimensionality and complexity associated with robot control problems. Thus, several robotic studies have focused on, for example, what is a good set of primitives, how they can be mathematically extracted and formalized, and how they can be used for robot learning by

imitating human movements. Using a small set of modifiable and adjustable primitives tremendously simplifies the task of learning new skills or adapting to new environments. Constructing internal neural representations from a linear combination of a reduced set of basis functions might be crucial for generalizing to novel tasks and new environmental conditions.

1.5 OVERVIEW OF THESIS

In this thesis a time varying synergies model, experimental results in support of the model and numerical/ optimization methods to achieve the results are presented. Angular velocity of a joint of the human hand can be expressed as a linear combination of movement primitives. The decomposition of these synergies from a large set of experimental data poses dimensionality reduction problems. I investigated several numerical models and methods to achieve these synergies in this thesis. This thesis is organized as follows.

The first chapter (Chapter 1) begins by introducing the existing problems and contemporary theories about synergies. Although there are many interpretations of synergies, this thesis focuses on kinematic synergies. For the benefit of readers a definition of synergies is presented. Also, some practical applications of these synergies are listed.

The second chapter (Chapter 2) discusses the significance of synergies in the context of dimensionality reduction. By using numerical methods like principal component analysis (PCA) and steepest descent method physiological insights in human hand prehension were obtained. Limitations of surface EMG signals of extrinsic muscles of the forearm in predicting postures of human hand are presented. A model of time-varying kinematic synergies is presented and

improvements are suggesting in succeeding chapters. The presence of inherent postural synergies in bimanual coordination is demonstrated by using PCA.

The third chapter (Chapter 3) presents convolutive mixture model. Interesting neuro-physiological evidences are annexed in this chapter in support of the model. These evidences imply that the model presented is of physiological and anatomical significance and not simple curve fitting.

The fourth chapter (Chapter 4) presents realizing the above model in different experimental paradigms. As a first practical medical application this model was implemented in extraction of tremor in patients with movement disorders. Temporal postural synergies were extracted by using principal component analysis. These synergies were then selected by using l_1 norm minimization. The optimal selection of the synergies necessitates reconstruction error of the testing movements to be minimal.

2.0 SYNERGIES TOWARD DIMENSIONALITY REDUCTION

2.1 EXISTING THEORIES OF SYNERGIES

The complex and versatile architecture of the hand has attracted increasing attention in a variety of research areas such as medicine, physiology, and engineering. Investigators with mixed backgrounds have joined the study of the hand. Their work ranges from experiments of reach and grasp to theoretical analysis of coordination and dimensionality reduction. While experimental approaches offer close observations of the articulate hand, analytic methods have helped researchers as tools to ease computational complexities and aid in system modeling. In this section, a review the existing studies on the dimensionality reduction problem in the control of the human hand is presented, especially on "**synergies**"—a concept proposed by Bernstein (1967), referring originally to some task-specific strategies that may simplify the coordination of redundant musculature. This line of research has benefited from and further encouraged crosstalk between experimental studies and systems-level modeling and analysis.

The coordination patterns of the hand have been examined with multivariate statistical techniques (Santello et al., 2002). These techniques have been used to search for synergies in hand movements at several levels of investigation. Based on the principal component analysis, Jerde et al. (2003a) found support for the existence of static postural synergies of angular configuration: The shape of human hand can be predicted using a reduced set of variables and

postural synergies. Similarly, Santello and Soechting (1997) showed that a small number of postural static synergies were sufficient to describe how human subjects grasped a large set of different objects. Moreover, Mason et al. (2001) used singular value decomposition (SVD) analysis to demonstrate that a large number of hand postures during reach-to-grasp can be constructed by a small number of principal components or eigen postures.

Static postural synergies are not the only type of synergies. Kinematic synergies have also been described in various experimental situations (Grinyagin et al., 2005). These synergies refer to the stable correlations between joint angles during multi-joint movements. With PCA, Braido and Zhang (2004) examined the temporal co variation between finger-joint angles. Their results supported the view that the multi-joint acts of the hand are subject to stereotypical motion patterns controlled via simplifying kinematic synergies. In the above mentioned study of eigen postures, Mason et al. (2001) also investigated the temporal evolutions of the eigen postures and observed similar kinematic synergies across subjects and grasps. In addition, kinematic synergies have been observed in the spatiotemporal coordination between thumb and index finger movements (Paulignan et al., 1997) and coordination of tip-to-tip finger movements (Cole and Abbs, 1986).

Another concept of synergies was proposed by d'Avella et al. 2003. Although their work was not directly related to hand movements, they inspired a theme of current research study on the movement primitives of the hand. They investigated the muscle synergies of frogs during a variety of motor behaviors such as kicking. Using gradient descent method, they decomposed the muscle activities into linear combinations of three task-independent time-varying synergies. They also observed that these synergies were very much related to movement kinematics and

that similarities existed between synergies in different tasks. This suggests the dimensionality reduction as a strategy adopted by the CNS while recruiting synergies for a particular task.

Compared with the muscle synergies derived from motor behaviors in frogs (d'Avella et al., 2003), muscle synergies in human hands were far less stable and more complicated (Grinyagin et al., 2005). Most studies reported variable and individually different patterns of muscle coordination (Cooney et al., 1985; Maier and Hepp-Reymond, 1995; Weiss and Flanders, 2004), while few studies were able to show subject-independent muscle synergies (Valero-Cuevas et al., 1998). The muscle synergies can be associated with kinematic synergies. Ginyagin et al. (2005) demonstrated a convergence between these two types of synergies by identifying the so-called dynamic synergies in human precision-grip movements. They used a biomechanical model for calculating joint torques from experimentally obtained angular variations, and indicated that dynamic synergies seem to be remarkably simple compared with the kinematic synergies.

Different from the above interpretations of synergies, Todorov and Ghahramani (2004) suggested that synergistic control may not mean dimensionality reduction or simplification, but might imply task optimization. This opinion was consistent with the view in (Todorov and Jordon, 2002), where the authors applied optimal feedback control as a theory of motor coordination. From a control theoretic point of view, Todorov and Jordon tried to explain the apparent conflict in two fundamental properties of motor system: ability to accomplish high level goals reliably and repeatedly versus variability in movement. They showed that optimal strategy of the motor system is to allow variability in redundant dimensions. This strategy does not enforce any desired trajectory but uses feedback more intelligently correcting only those deviations that interfere with task goals.

2.2 LIMITATIONS OF SURFACE EMG SIGNALS

Although the synergies have a long history in physiology and medicine, they have been underrated for a long time, for a number of reasons. These include their different interpretations. Synergies are not just theoretical concepts but are of significant importance in prosthesis. Biologically inspired synergies have been already put into use for prosthetic hands (Popovic et al., 2001). Here practical problems encountered in reproduction of postures using the muscular information are considered. How these can be compensated by synergies? This chapter explores the limitations of sEMG (surface Electromyography) signals collected from the extrinsic muscles in the forearm in predicting the postures of human hand. Four subjects were asked to try ten extreme postures of hand which need high effort. Two of these four subjects were asked to try ten more normal postures which did not need effort. During the experiments, muscle activity and static postures of the hand were measured. The data obtained were analyzed by principal component analysis. The results obtained inferred that sEMG signals of extrinsic muscles cannot reproduce all postures of the hand. In such cases depending on the available muscular information may not lead to realistic reconstruction of the hand movement with prosthetic hands.

The extrinsic muscles which stretch over the forearm and the intrinsic muscles which are within the hand are responsible for all the actions of the hand. In most cases normal postures of the hand do not need much effort when compared to extreme postures which involve full extension or full flexion of fingers. For instance, American Sign Language (ASL) characters do

---

This work was published as R. Vinjamuri, Z. -H. Mao, R. Sclabassi, and M. Sun. Limitations of surface EMG signals of extrinsic muscles in predicting postures of human hand in Proceedings of the 28th IEEE EMBS Annual International Conference, NY, USA, pp. 5491- 5494, 2006.

not need much effort of muscles when compared to the extreme postures that are used here. In other words, extreme postures require high magnitudes of potentials generated in muscles where as for normal postures very low magnitudes of potentials are generated which are not easily detectable by surface electrodes of EMG machine. Surface Electromyography (sEMG) has many advantages in the sense that it is noninvasive but it has many limitations because its reach to the muscles is very limited.

This raises the question of how far can sEMG signals of extrinsic muscles in the forearm be dependable in prediction of static postures of hand. Here it was evident that zero or very low values of sEMG potentials were generated in 8 different muscles for normal static postures of hand (in this study ASL numerical characters from 0-9 were used). Also for the same set of 8 muscles but for ten extreme postures higher magnitudes of potentials were detected by the surface electrodes. This finding is also in agreement with the anatomy of human hand that extrinsic muscles and also intrinsic muscles affect the functionality of hand. To be precise, extrinsic muscles form the dominant set of muscles but not the complete set of muscles responsible for all the postures of human hand. In similar studies done by Sebelius et al., (2005) sEMG signals collected from the phantom hand of an amputee are used in predicting the postures. Amputees successfully predicted ten different postures through a trained artificial neural network. But not all static postures of human hand can be predicted in this way with sEMG signals of just the extrinsic muscles.

Two matrices were obtained, one for the sEMG signals vs. postures and the other for joint angles (measured by CyberGlove®) vs. postures for both cases of ten and twenty postures. These matrices were analyzed using Principal Component Analysis (PCA). Studies based on PCA were also done by Braido and Zhang (2004) to examine the temporal co variation between

joint angles. From the experiment, it was found that number of principal components (PC's) of sEMG signals in the case of ten extreme postures was same when compared to number of PC's in the case of twenty postures and the number of PC's of joint angles in the case of ten extreme postures was less when compared to the number of PC's in the case of twenty postures. . Results imply that surface EMG signals failed to predict normal postures. The physiological interpretation of the problem was supported quantitatively by PCA. Also, eigen vectors corresponding to PC's revealed information which was in sync with anatomy of hand.

The experimental setup consists of CyberGlove® equipped with 22 sensors which can measure angles at all the finger joints including distal inter phalangeal, proximal inter phalangeal and meta carpo phalangeal joints. Also in the setup is Delsys® EMG machine (Bagnoli 8) with 8 single differential surface electrodes (non invasive).

The selection of the extrinsic muscles for the experiment was based on several criteria. Firstly, the selected muscles must be playing a key role in particular posture of the hand chosen for a task. Secondly, muscles of interest were to be detectable by surface electrodes. For these reasons, the following eight muscles were selected – Flexor Digitorum Superficialis (FDS), Flexor Pollis Longus (FPL), Flexor Digitorum Profundus (FDP), Extensor Digitorum (ED), Extensor Indicis (EI), Extensor Digiti Minimi (EDM), Abductor Pollis Longus (APL) and Extensor Pollis Longus (EPL). These muscles are responsible for flexion, extension and abduction at most of the fingers and joints.

Four subjects participated in this experiment. Before the experiment started there was a trial period where subjects practiced all postures. The subjects were asked to try ten different extreme postures as depicted in Fig. 3. These postures are called extreme because they involve extreme flexion and extreme extension of one or multiple fingers depending on the posture. For

instance, in posture P1 all fingers are extended at their MCP joints. These postures are different from normal postures. See Fig. 3.

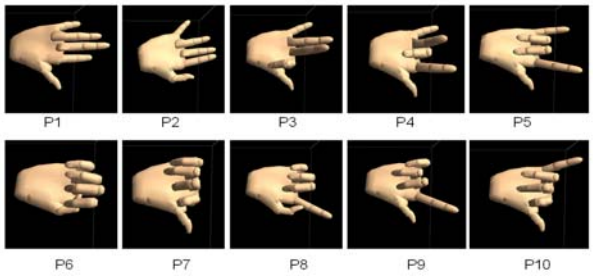

Figure 3. Ten extreme postures (P1-P10)

Of the four subjects two subjects were asked to try ten more normal postures. For the experiment numerical ASL characters as shown in Fig. 4 were adapted, as normal postures which need a little or less effort. These postures are quite different from extreme postures. There is a lot of effort on muscles in extreme postures but not in the case of normal postures. During the experiment subjects were asked to try these 20 different postures one after the other with a delay of 1-2 minutes in between postures. After ten extreme postures a recess of approximately 10 minutes was given in order to avoid effects of extreme postures. This recess was long enough for the subjects to forget the effort of muscles in the extreme postures.

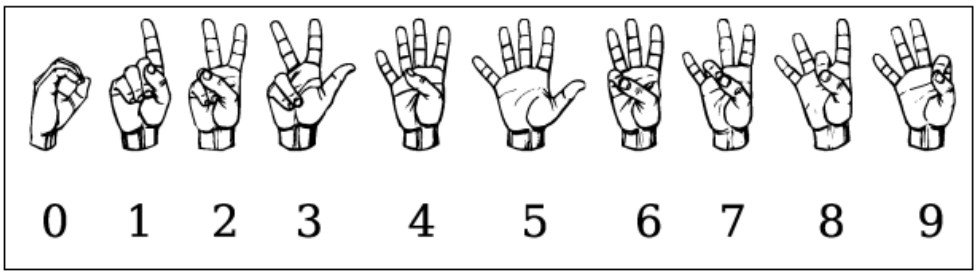

Figure 4. Normal postures—ASL numerical characters (adapted from www.wikepedia.org)

Through out the experiment muscle activity was recorded with eight surface electrodes measuring the activation potentials of the muscles listed in the setup. Each posture lasted for 15

seconds, meaning EMG and Glove data were recorded for 15 seconds. In this experiment, only 15 sensors of CyberGlove® were used that correspond to joints of all the five fingers. EMG data were analyzed using Delsys® EMGWorks Version 3.0 and information about 15 angles corresponding to joints of all the five fingers in a vector of radians are obtained from CyberGlove®.

It was observed during all the postures that the subjects used various efforts at the beginning of the task but they stabilized in last 5 seconds. Though they were trying the same posture for all the 15 seconds the EMG activity was not same through out the task. RMS values of the voltages were calculated using Delsys® EMGWorks Version 3.0. When considering RMS voltages of the activation potentials, an average of last 5 seconds of the task was considered to be the measure of RMS voltage of activation potential. There was not much difference in CyberGlove® data in 15 seconds. For all subjects, for each posture two different matrices were obtained. One is EMG matrix of dimensions 8x10 where 8 muscles (in the same order as mentioned in the setup) correspond to 8 rows and 10 postures correspond to 10 columns. The other is Glove matrix of dimensions 15x10 where 15 angles of joints of the five fingers (three for each finger) correspond to 15 rows and 10 postures correspond to 10 columns. For two of the subjects similar matrices were obtained but with dimensions 8x20 and 15x20 for EMG and Glove matrices respectively. Change in the dimensions reflects 20 postures taken into consideration for two subjects.

The above matrices were normalized such that their mean equals 0. This was done by subtracting mean of each row from every element of the row. For each of the normalized matrices covariance matrices were calculated. The eigen values and eigen vectors of covariance

matrices were computed. The number of synergies or the number of PC's was computed using the following equation:

$$\frac{\lambda_1 + \lambda_2 + \ldots + \lambda_r}{\lambda_1 + \lambda_2 + \ldots + \lambda_m}, \quad (1)$$

where λ_1, …, λ_r correspond to first r largest eigen values written in the descending order of any covariance matrix, and r is no greater than m, the total number of eigen values. If this fraction exceeds 90% for least possible number of largest eigen values, then the number of eigen values is equal to number of PC's. The computation behind PCA roots from (Jolliffe, 2002).

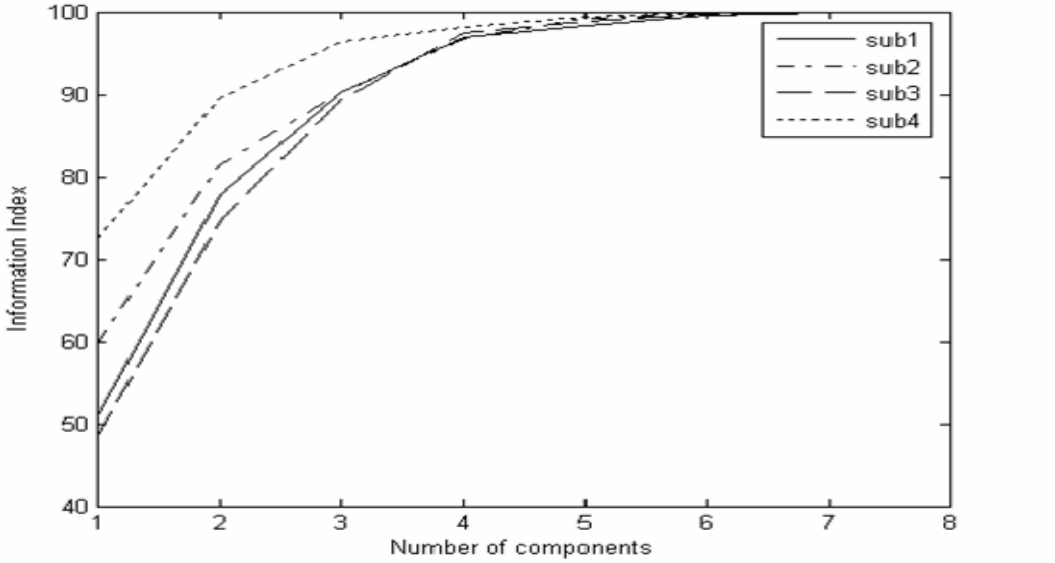

Figure 5. Information Index plots for four subjects to represent number PC's in sEMG signals

From the analysis of ten extreme postures for four subjects the following results were obtained. Fig. 5 is a comparison of number of PC's of sEMG signals for different subjects. It is observed here that for the first three subjects the number of PC's (where the curve crosses 90%) is 3 and for the subject 4 it equals 2.

For Glove signals, similar patterns of variations were observed for all the four subjects and about 3 PC's were needed for all the four subjects as shown in Fig. 6. Maximum number of

PC's that can be obtained for Glove signals is 15 but only 8 are illustrated here because the remaining 7 values did not make difference.

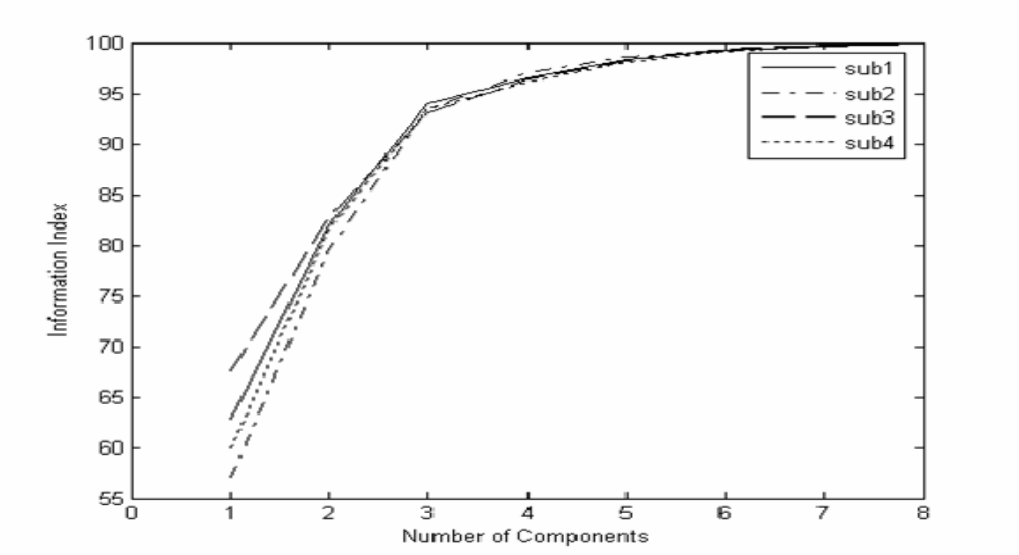

Figure 6. Information Index plots for four subjects to represent number PC's in Glove signals

Interesting results were obtained from the analysis of twenty postures for two of the subjects. For sEMG signals, the number of PC's for 10 postures was same as the number of PC's for 20 postures. For Glove signals, the number of PC's for 10 postures was less than the number of PC's for 20 postures. In order to plot Information Index for both sEMG and Glove signals in the same graphs only first eight eigen values of the Glove signals were considered. As shown in Fig. 7 for subject3 the number of PC's for sEMG signals for both ten and twenty postures is three. For Glove signals, it is clearly evident that the number of PC's in case of twenty postures was 4, which is greater than the number of PC's in the case of ten postures which is 3. Similar patterns were observed for subject4 as illustrated in Fig. 8.

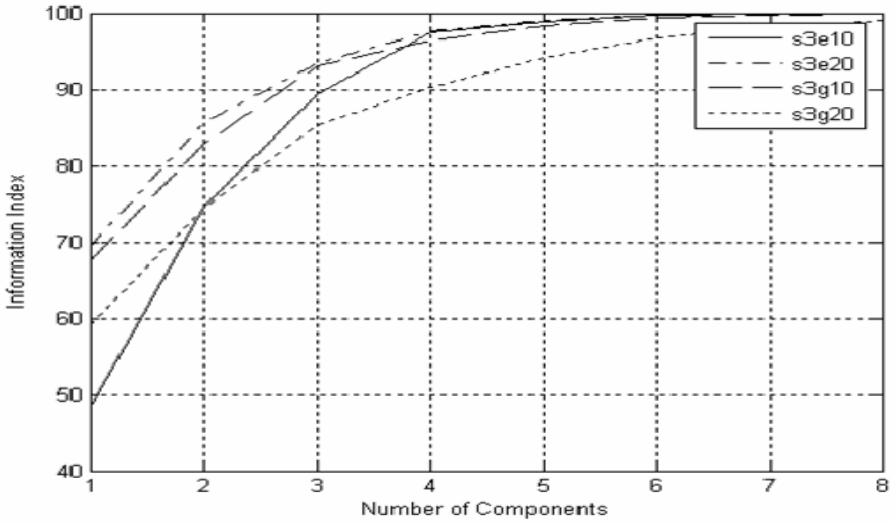

Figure 7. Number of PC's for 10 and 20 postures for sEMG and glove signals for subject3

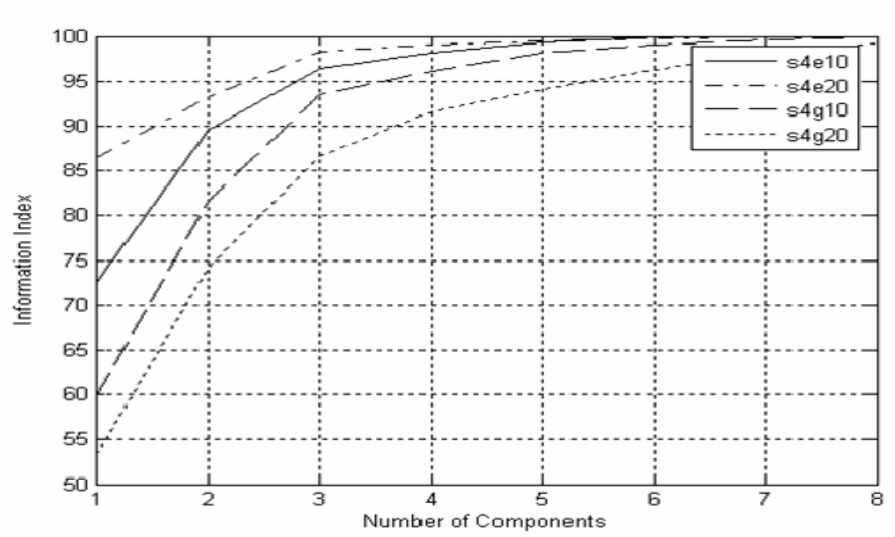

Figure 8. Number of PC's for 10 and 20 postures for sEMG and glove signals for subject4

These results suggest that even though there was an increase in the number of PC's from ten to twenty postures in the case of Glove signals there was no such increase in the case of sEMG signals which further suggests that there was no additional variance obtained from normal postures as they did not produce sufficient activation potentials in the muscles which can differentiate them from extreme postures.

Above results depict that the sEMG signals are not capable of predicting all postures of human hand. One can argue that this can be disproved with a better sophisticated EMG machine. But one cannot deny the fact that there are some natural postures of human hand which do not need much effort of the muscles. Also, there are some postures of the hand which differ only in activation potentials of intrinsic muscles in which cases postures cannot be predicted by measuring the activation potentials of just the extrinsic muscles. Many postures which include abduction and flexion of the fingers involve only intrinsic muscles which are local to the palm.

In eigen vectors of covariance of sEMG signals it was consistently observed in almost all the subjects that last four muscles which are EI, EDM, APL and EPL had higher weights and same positive polarity for first PC. This suggests that thumb, index finger and little finger played a dominant role in these tested 20 postures. This is not just because the above listed four muscles are dedicated to these three fingers. All subjects felt more stress on these fingers. It is opined in the literature (Mackenzie and Iberall, 1994) that thumb always plays an important role in many actions of hand. These results were supported by PCA in analysis. Finding the dominant muscles not only helps quantify physiological facts of hand but also helps in prosthetics. This can reduce the number of muscles to be considered prosthetics.

Surface EMG signals of the extrinsic muscles in the forearm cannot by themselves predict all postures of the human hand. The number of PC's of sEMG signals remained same where as the number of PC's of Glove signals which directly depict postures increased. This was successfully proved by PCA. Readers should consider the following points: Normal postures of the hand which are frequently used involuntarily by hand do not involve much effort of muscles. Even if they produce some lower magnitudes of activation potential in muscles they are not detectable by noninvasive surface electrodes. Some postures of the hand involve only internal

muscles of the hand which do not differ from each other in activation potentials of just extrinsic muscles. Afore said reasons limit the functionality of prosthetic hands if they are dependent on only the extrinsic muscles present in the forearm. Intrinsic muscles cannot be compensated by such prosthetic hands. On the other hand, synergy based prosthetic hands can do better. Though they depend on extrinsic muscles, synergies supply the lacking information by exploiting the interdependence among the joints. Postural synergies in chapter 4.1 will help further in this aspect.

2.3 TIME VARYING SYNERGIES

The concept of synergies has received increasing attention in motor control as it presents the two most interesting problems of coordination and dimensionality reduction by central nervous system. The study of synergies has high significance in many fields, including human computer interface and robotics. For example, in telesurgery, robotic hands are utilized to perform surgical manipulations by a surgeon at a remote site. An efficient data representation by synergies provide improved control by reducing the delay and jitter during data transmission over the network.

The term synergy, originally coined by Bernstein (1967), has been defined differently in different contexts. Here, synergies in velocity profiles are defined based on the numerical

---

This work was published as R. Vinjamuri, Z. -H. Mao, R. Sclabassi, and M. Sun. Time-varying synergies in velocity profiles of finger joints of the hand during reach and grasp in Proceedings of the 29th IEEE EMBS Annual International Conference, France, pp. 4846- 4849, 2007.

interpretation by d'Avella et al. (2002, 2003). Specifically, the angular velocity profile of each joint is represented as a combination of different time-varying velocity components which are defined as synergies. In the literature of hand movement studies, few reports have addressed the concept of time-varying kinematic synergies observed in joint movements (e.g. Grinyaginl et. al., 2005 and Cole et al., 1986). Postural synergies have been widely proposed where a small number of dominant postures or eigen postures can represent a large set of postures recorded either at discrete times of a task or during different tasks (Mason et al., 2001 and Santello et al., 2002). The former case is similar to a time-varying synergy but the latter deals with static postures. Yet another concept of synergies was proposed by Todorov and Ghahramani (2004) where they described using postural synergies that synergistic control may not mean dimensionality reduction or simplification, but might imply task optimization. What synergies imply, still remains debatable. In the current section, I still stress on dimensionality reduction and moving a step forward "time-varying" kinematic synergies in the angular velocity profiles are demonstrated. As reported in literature (Cole et al., 1986), single peak velocity profiles and increased velocities at proximal joints for larger apertures were observed in this study. During reach and grasp, opening of palm arc was observed to be faster and closing was slower.

Time varying synergies:

Angular velocity profile $\mathbf{v}(t)$ (consisting of rows which correspond to the angular velocity profiles of joints) is modeled as a linear combination of N movement patterns represented by $\mathbf{w}_i(t - t_{si})$, $i = 1, \ldots, N$. These movement patterns are called synergies, which vary with time, with shift denoted by $t - t_{si}$ and objects denoted by subscript s. For instance, $\mathbf{w}_i(\tau)$ is a column vector that denotes the angular velocities of 10 joints at time τ for i^{th} synergy . Each angular velocity

profile obtained while grasping an object is called an episode. Thus the angular velocity profile of an episode *s* is given by

$$\mathbf{v}_s(t) = \sum_{i=1}^{N} c_{si}\,\mathbf{w}_i(t - t_{si}) \tag{2}$$

where N refers to the number of synergies. In the above equation, c_{si} and t_{si} refer to the coefficient and time shift, respectively. They are unique for one particular synergy and one particular episode. This is illustrated in Fig. 9 (same as Fig. 2) where three synergies (left) with different coefficients and shifts (right bottom) combine to reproduce velocities (right top) at 3 joints.

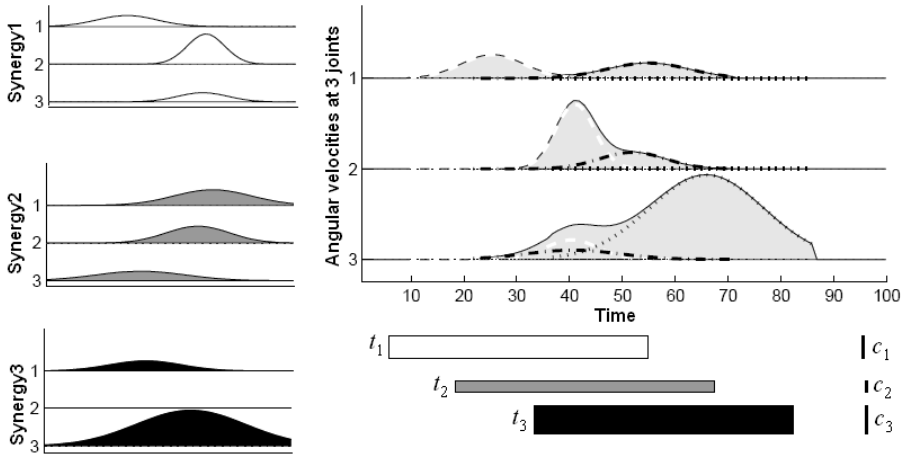

Figure 9. A reconstruction of joint velocities at 3 joints by linear combination of 3 synergies

The experimental setup consists of CyberGlove® equipped with 22 sensors which can measure angles at all the finger joints including distal, proximal and metacarpal joints. For the purpose of this experiment only ten of the sensors which correspond to metacarpal (flexion/extension) and proximal joints of five fingers are used because distal interphalangeal joints did not move significantly. Twenty eight objects (wooden and plastic) of different shapes (spheres, circular discs, rectangles, pentagons, nuts and bolts) and different dimensions (1.5

cm−11.8 cm) as shown in Fig. 10 were selected based on two strategies. One was gradually increasing sizes of similar shaped objects and the other was different shapes to isolate proximal and metacarpal joints. Some similar sized/shaped objects were intentionally used to observe trends in reach and grasp movements.

Figure 10. CyberGlove with grasping objects, sensors used (dark) and custom grasp

A typical experiment consists of reaching and grasping 28 objects. Each task has 10 trials where subjects repeated the reach and grasp for the same object 10 times. After a short recess of about 2-3 minutes, the next task was started. The start and stop times of each task were signaled by computer-generated beeps. In each task, the subject was in a seated position, resting his/her hand at corner of a table and then, upon hearing the beep, reached and grasped the object placed approximately 40 cm away on the edge of the table. Each task lasted for 2.3 seconds.

After obtaining the joint angles at various times from the experiment, angular velocities were calculated. Ten trials were collected for each task. These angular velocities were filtered from noise. Since the 10 trials did not start exactly at the same time, one profile was fixed and a

best match for this profile was calculated by shifting horizontally the remaining profiles, and finally they were averaged to obtain one angular velocity profile for one object. One such angular velocity profile will have ten rows corresponding to the 10 considered joints of five fingers. This process was repeated for all objects and all subjects. At the end, the obtained angular velocity profile was truncated to 0.86 s (from a total of 2.3 s) as remaining time had no useful information because velocities settled to zero by that time.

Next, the angular velocity profiles were used as inputs to a gradient descent algorithm, which is discussed in detail later in this section. A similar algorithm was reported by d'Avella et al. (2002, 2003) except that negative values in angular velocities were allowed here calculation. For each subject, the collected profiles were optimized in eight cases in which increasing number of synergies from 1 to 8 were considered. Following is the method of iterative minimization of reconstructive error. The error is given by

$$E^2 = \sum_s E_s^2 \tag{3}$$

$$\text{with} \quad E_s^2 = \sum_{t=1}^{T_s} || \, \mathbf{v}_s(t) - \sum_{i=1}^{N} c_{si} \mathbf{w}_i (t - t_{si}) \, ||^2$$

where E is the total error, E_s refers to the error per episode, and T_s refers to the duration of an episode.

The optimization algorithm used to minimize the error is the steepest descent method with constant step size. For each subject and for each N (number of synergies), the algorithm was run five times, starting from different initial values of the synergies. Then the results (synergies) from the trial with the minimal error were used for further analysis. The strategies of choosing the initial values of synergies included: (1) random values, (2) the first or last N episodes of the angular velocity profiles, (3) average of all episodes, and (4) optimal synergies from the results obtained for $N - 1$ synergies. The amplitude coefficients started from random values between 0

and 1. The stopping criterion of the algorithm was based on the number of iterations. It was found that after 2000 iterations there was not appreciable decrease in the error in all the above cases.

For better understanding, the algorithm can be broken down to three major steps:

1) Find optimal synergy shifts: Compute the sum of scalar products of s^{th} episode and i^{th} synergy shifted by time t or scalar product of cross-correlation at delay t, for all possible delays. Select the synergy and delay (t_{si}) with highest cross correlation. Subtract from the data the selected synergy (after scaling and time shifting). Repeat this for remaining synergies. This completes one object/episode. Repeat the same for all remaining episodes.

2) Update scaling coefficients: For each episode given the synergies and delays t_{si}, update the scaling coefficients c_{si} by gradient descent.

$$\Delta c_s = -\mu_c \nabla_{c_s} E_s^2 \tag{4}$$

3) Update synergy elements: Given optimal shifts and updated scaling coefficients, update the synergy elements $\mathbf{w}_{i\tau} = \mathbf{w}_i(\tau)$ by gradient descent.

$$\Delta \mathbf{w}_{i\tau} = -\mu_{\mathbf{w}} \nabla_{\mathbf{w}_{i\tau}} E^2 \tag{5}$$

After these three steps, error is calculated and iterated again until the error is reduced to a satisfactory value. For further details please refer to d'Avella et al., (2002).

Using the above optimization method, encouraging results were obtained which not only lead directly to data reduction and simplification but also gave implications to physiological aspects. Shown in the Fig. 11 are the three synergies which linearly combine using different coefficients and shifts as indicated in Fig. 11 to reconstruct the velocity profile as shown in Fig. 12. The above three synergies were task-independent synergies used for 28 different tasks of object reach and grasps. Here positive and negative velocities refer to the movements in the

opposite directions. Along the columns are MCP—metacarpophalangeal, PIP— proximal interphalangeal joints of the five fingers, thumb (T), index (I), middle (M), ring (R), and pinky (P).

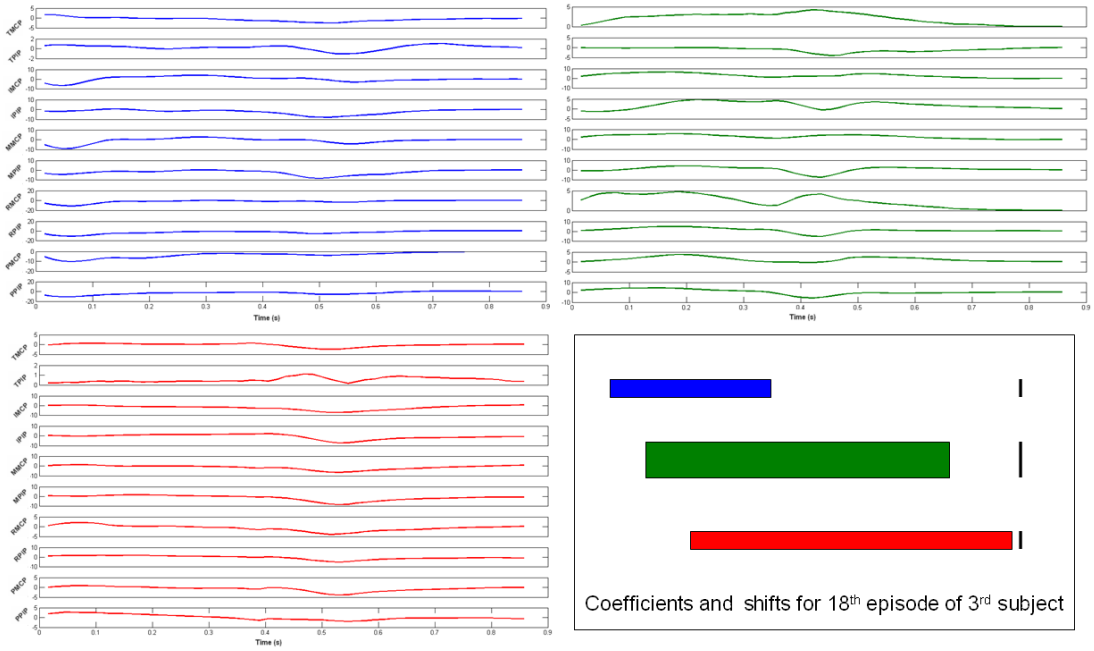

Figure 11. Three synergies (blue, green, red) with shifts and coefficients (in that order)

As mentioned earlier eight cases differing in number of synergies (1–8) were dealt for five subjects. A mean error plot with standard deviation was obtained for all the five subjects as shown in Fig. 13 which implied that using more than three synergies did not add much significant improvement to the reproduction of the original data. Also, there was a noticeable decrease in mean error difference from 1 synergy to 2 synergies (0.7322) to that from 3 synergies to 4 synergies (0.1926).

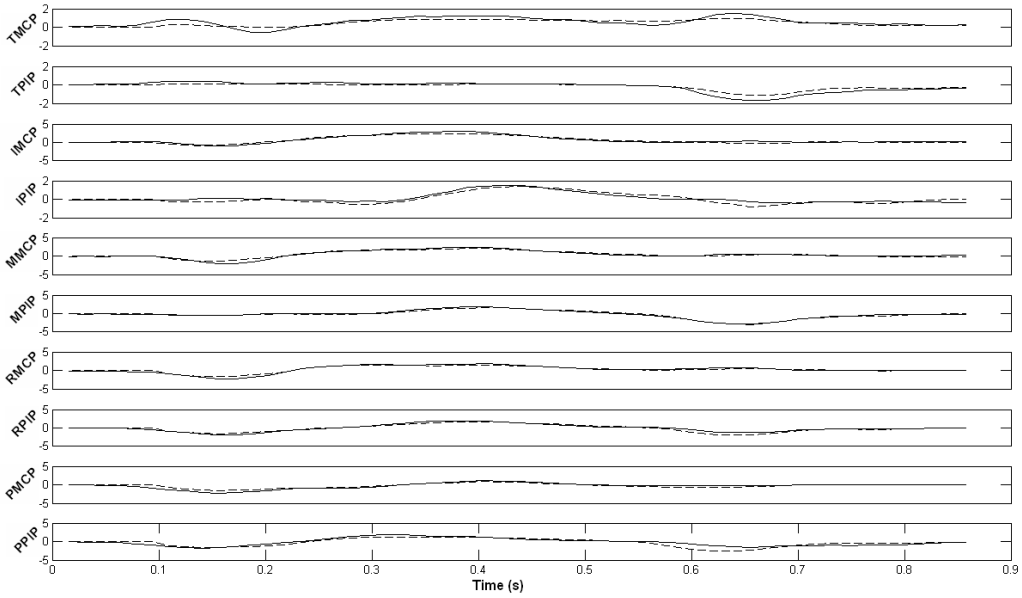

Figure 12. Experimental angular velocity profile (—) is reproduced (---) by using 3 synergies.

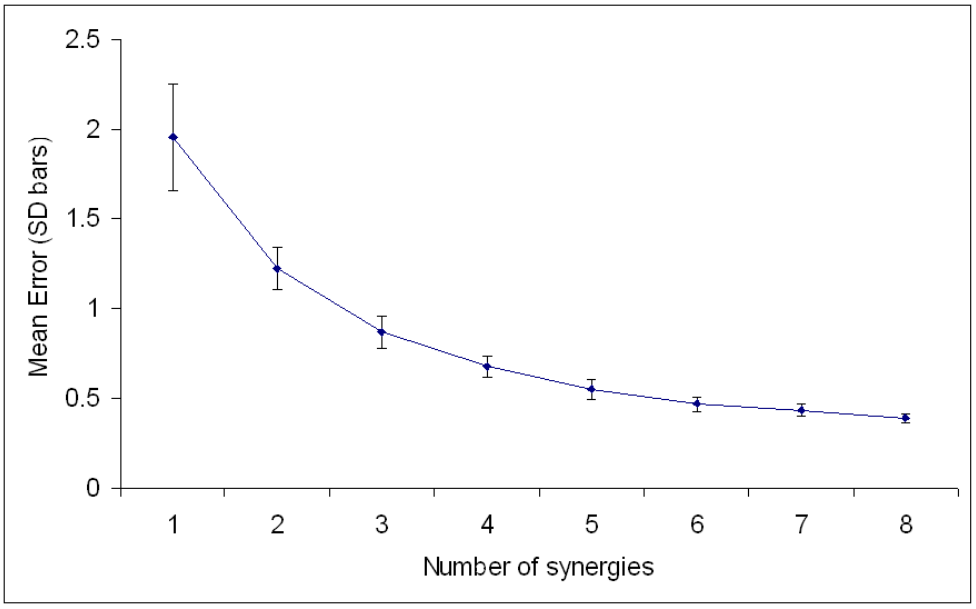

Figure 13. Error plot illustrating sharp decrease in the error difference before 3 synergies.

Within a subject, in different cases with different number of synergies, correlations between synergies were measured which led us to the correlation pyramid as shown in Fig. 14. Nodes in the figure indicate synergies in different cases (e.g. 32—the second synergy in the case of three synergies). Correlations are indicated by thickness of connecting bars between the nodes

following the legend (top right). Pyramid was achieved by fixing one synergy and time-shifting the other until the best correlation was obtained (similar to *Find optimal synergy shifts*). Correlations above 0.5 only were reported in the figure and others were discarded. The correlation pyramid shown here was for one subject but similar trend was seen in all the subjects. It is clearly evident from the figure that there was high correlation between synergies in almost all the cases, except for the later ones (22, 33, 44, 55 and 66). This means as the number of synergies considered increased gradually there was a high correlation between synergies in adjacent cases. In other words synergies in the lower cases were preserved. This ensures (with help of Fig. 13) that considering more than 3 synergies would still be consistent with 3 synergies.

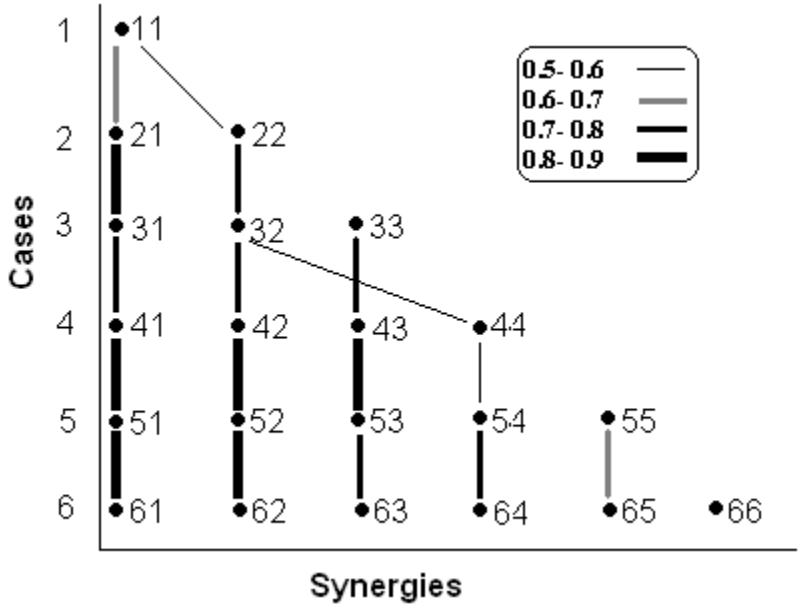

Figure 14. Correlations of synergies depicting synergies are preserved.

In quantitative analyses like principal component analysis, there exists no correlation between the components as they are orthogonal to each other. But in this approach, much similar to radial basis functions there can be similarities between the components. Though we observe correlations between the synergies utilized in the cases where different numbers of synergies

were used, the correlations were not in order. For instance, for one of the subjects, the first synergy in the case of 2 synergies was similar to second synergy in the case of 3 synergies.

From the synergies obtained, in almost all cases the outer joint of thumb was moved only at the end of the task, which indicates that thumb was used as reference throughout the task and moved in finer movements for completion of the grasp. This was verified by experimental angular velocities. During all tasks, opening was observed to be faster and closing slower which was indicated by steep rise in angular velocities during opening.

The successful representation of the original angular velocity profiles using synergies not only is of physiological importance but also leads to a compact set of data facilitating data-traffic intensive applications. Videos of these time-varying synergies can visually explain reach and grasps. The current model is limited only to kinematic features during a small number of reach and grasps tasks; exploring dynamic features in the more general case will make this approach more attractive because of its unique ability in data representation. Also, investigating the concept of synergies in muscle activity of the major muscles during similar experiments using surface electromyography may reveal more details about how central nervous system tackles the high degree of freedom of the hand. This can help in efficient control of future electromyographic hands.

2.4 INHERENT BIMANUAL POSTURAL SYNERGIES

This chapter presents a numerical approach to prove the existence of inherent bimanual postural synergies while performing actions with two hands. Five subjects were tested in two different tasks. The first task was a well coordinated task where each subject screwed nut and bolt using one or both hands. In the second task, subjects were asked to perform several random postures with both hands. Joint angles were measured during the experiment by a pair of data gloves. Principal component analysis (PCA) was performed over the postures obtained during the tasks. In the first task, the number of postural synergies obtained for both hands together was less than the sum of the number of postural synergies for two hands. This is expected intuitively as first task was well coordinated. In the second task where there is no voluntary coordination involved, the number of postural synergies obtained for both hands together was still less than the sum of the number of postural synergies for two hands. This implies that there are innate bimanual synergies wired biomechanically to help brain in bimanual movements.

Coordination is at the core of research in human motor control. Coordination exists at different levels of hierarchy. It is present within joints of hands, arms, within multiple hands, and even within muscles. Coordination has been realized through many compelling conceptual models based on behavioral investigations. One such model is that of synergies which are coordinative structures controlled as a single functional unit (Turvey, 1977). Synergies are hypothesized as tiny modules of movement helping the central nervous system (CNS) in control and coordination of hands, arms, etc. Of these, the most interesting is the architecture of the

---

This work was accepted as R. Vinjamuri, M. Sun, D. Crammond, R. Sclabassi, and Z.-H. Mao. Inherent bimanual postural synergies in hands in Proceedings of the 30th IEEE EMBS Annual International Conference, 2008.

human hand with high degree of freedom; its versatile architecture amazes scientists and engineers even today. Coordination within the joints of the hand itself is very complex and difficult to comprehend, and even intricate is bimanual coordination, the coordination between two hands with coordination within the joints of each hand all happening simultaneously. Synergies have been used by Kelso et al. (1979) to explain synchronous timing of bimanual coordinative movements.

A gradation in levels of difficulty exists in performing bimanually coordinated movements. In day-to-day life we observe many actions involving bimanual coordination. This means some bimanual coordination actions can be performed easily by all. CNS makes most bimanual actions easy and effortless, as though automatic. At the extreme end are musicians (pianists, guitarists, etc.) who can coordinate movements at an unimaginable intricacy. On the other hand, there are some tasks like drawing different shapes with two hands simultaneously (e. g. square with right hand and circle with left hand or vice versa), which need a lot of training.

How is it possible that some bimanual coordination patterns can be performed easily and some are difficult to perform? Consider the coupling of two (right and left) index fingers (Rosenbaum, 1991). At low frequency two fingers can stay in anti-phase (one flexing and other extending), but as we move on to higher frequencies of movement only in-phase coupling is retained. These experiments might suggest that there are some coordination movement patterns built into the neuromuscular apparatus of hands enabling us to perform easily. Other coordination patterns that fall beyond the abilities of neuromuscular apparatus have to be learnt with training over time. It is important to answer such questions because basic coordination is missing in patients with movement disorders such as Parkinson's disease, etc., (Van den Berg et al., 2000).

Postural synergies have been widely proposed. Using matrix factorization methods such as principal component analysis (PCA), dominant postures were obtained which were called postural synergies. Postural synergies were observed during several reach and grasp tasks by many researchers. But none investigated them in the context of bimanual coordination. Here a similar approach using PCA is adapted for obtaining eigen postures (Mason et al., 2001, Thakur et al., 2008) which are the principal components obtained over a large set of postures. Further, postural synergies were obtained in two different tasks—one involved coordination and the other did not involve any coordination. Results support the existence of bimanual synergies in a random postures task which did not involve any coordination. This might indicate the presence of innate bimanual synergies that might be built into the neuromuscular architecture of the hand.

The experimental setup consists of a pair of 5DT data gloves equipped with 14 sensors that can measure angles at ten finger joints including proximal and metacarpal joints and four sensors to measure abduction and adduction between fingers. For the first task involving coordination, large wooden nut and bolt were used as shown in Fig. 15. Arrangement of sensors is also shown in the inset of Fig. 15.

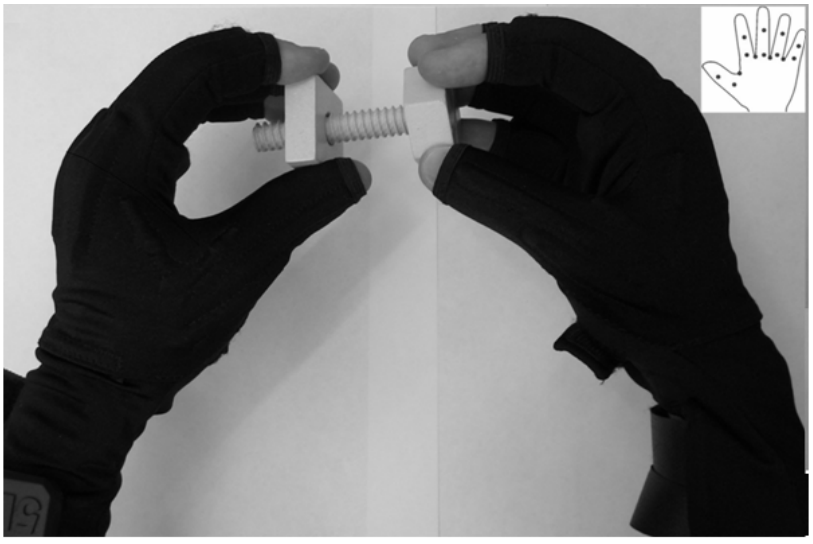

Figure 15. A Subject performing a coordinated task

The experiment consisted of two tasks. First task is a coordination task. Five subjects (including 3 male and 2 female, all right hand dominant) were asked to perform screwing a nut and bolt. At first subjects were asked to use right hand to move and the other hand to grip. This was repeated for left hand. Then they were asked to use both hands to move simultaneously. In day-to-day life, in these types of bimanual coordination tasks, people tend to use their non dominant hand to grip and dominant hand to perform the action. A slight difference was purposefully introduced to involve learning of this simple coordinated task. This learning would ignore previously learned dexterities developed in subjects over time. All subjects have managed to learn it effortlessly.

In the second task all five subjects were asked to pose random dissimilar postures with two hands. Subjects were asked to form postures with both hands at the same point of time and stay still for a few seconds and move on to next posture. No further constraints were imposed on the subjects. Joint angles were recorded during the entire experiment.

In the first task of coordination, all postures (say N in number) collected during the entire action were considered for analysis. Each posture consisted of 14 joint angles corresponding to 14 sensors. As mentioned before, this task was performed under three different cases. For three cases, three matrices (14×N, 14×N, and 28×N) were obtained. Principal component analysis was carried over these matrices. Note that in the third case when both hands were moved, 28 sensors (28×N) were considered.

In the second task where subjects were asked to pose random postures, subjects were asked to pause for a few seconds before moving to next posture. Thus from the joint angles, angular velocities were obtained. Wherever the angular velocities were flat, this corresponded to time when subjects were holding a posture. Thus postures corresponding to these points of time

were collected. From all these postures, three matrices were obtained (14×N, 14×N, and 28×N). Note that unlike the first task, the third matrix here was obtained by cascading the first two matrices one on top of the other. PCA was performed on these matrices.

The above matrices were normalized such that their mean equals 0. This was done by subtracting mean of each row from every element of the row. For each of the normalized matrices covariance matrices were calculated. The eigen values and eigen vectors of covariance matrices were computed. The number of synergies or the number of PC's was computed using the following equation:

$$\frac{\lambda_1 + \lambda_2 + \ldots + \lambda_r}{\lambda_1 + \lambda_2 + \ldots + \lambda_m}, \tag{6}$$

where λ1, …, λr correspond to first r largest eigen values written in the descending order of any covariance matrix, and r is no greater than m, the total number of eigen values. If this fraction exceeds 90% for least possible number of largest eigen values, then the number of eigen values is equal to number of PC's. The computation behind PCA roots from (Jolliffe, 2002).

Six posture matrices were obtained, three for the first task and another three for the second task. PCA was performed on all these matrices. Detailed variation between percentages of variance accounted by PC's along with number of PC's is shown for one of the subjects in Figs. 16 and 17.

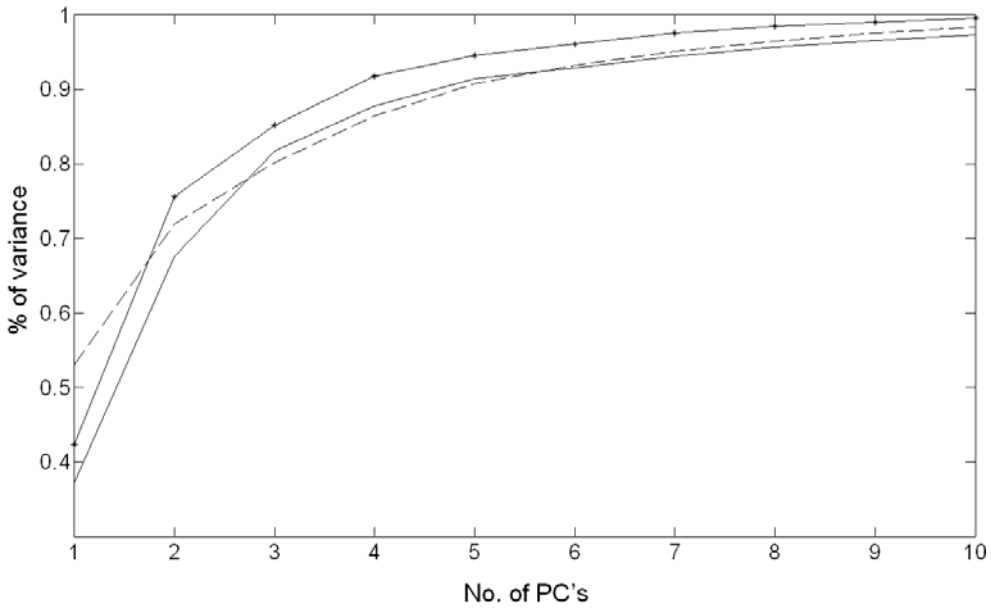

Figure 16. Percentage of variance vs. No. of PCs for Subject 4 during coordination task

Fig. 16 shows the variation in percentage of variance for Subject 4 for coordination task, and Fig. 17 shows the same for random postures task. As observed from Fig. 16, of the coordination task all the three curves (right hand only, left hand only, both hands together) cross 90% of variance at about 4 or 5 PC's. To be precise, variation in left hand crosses at 4 PC's and the rest at 5 PC's. The percentage of variance values are numerically equal to the fraction given in equation (6). For the case of random postures, in Fig. 17 it is observed that the variance curves for right and left hands crossed 90% of variance at about 6 PC's. But both hands together crossed at 9 PC's. For all the subjects the results are summarized in Table 1 for coordination task and Table 2 for the random postures task. The number of principal components corresponds to number of postural synergies or eigen postures, because the eigen vectors are essentially the eigen postures or postural synergies (Mason et al., 2001). From now on principal components will be referred as postural synergies. Eigen vectors (each of length 14 corresponding to 14

sensors/joints in this case) can be further used to extract postural information as discussed in (Thakur et al., 2008).

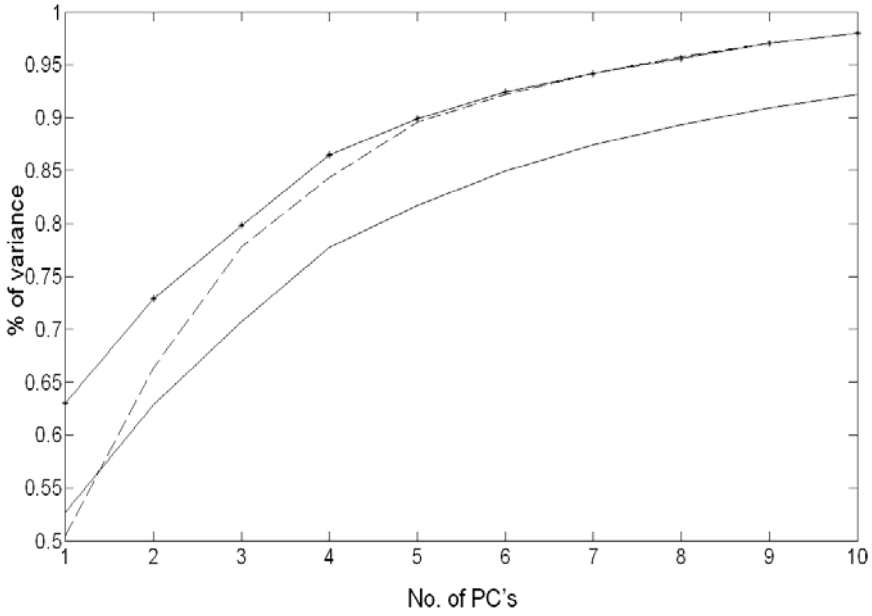

Figure 17. Percentage of variance vs. No. of PCs for Subject 1 during random task

In the first task of coordination, for all the subjects the sum of the number of synergies for right (R) and left hands (L) was always greater than the number of synergies observed for both hands (B) i.e. L+R > B. This is a proof that the task was very well coordinated and the two hands were acting as a single system while performing the task. If there was no coordination, then the sum of the number of synergies for left and right hands independently would have been equal to the number of synergies observed while both hands were acting together (L+R =B). The behavior observed in Table 1 is very much intuitive in the sense that such tasks much similar to everyday tasks are well coordinated.

Table 1. No. of PCs in coordination task

Subjects	Left hand (No. of PCs)	Right hand (No. of PCs)	Both hands (No. of PCs)
Subject 1	4	3	4
Subject 2	5	3	4
Subject 3	4	3	4
Subject 4	4	5	5
Subject 5	4	4	4

In the second task, surprisingly, similar behavior was observed as in the first task. This task is completely different from the first task by nature. The first task makes sure that PCA can be used as a tool to verify the presence of coordination (if L+R > B) and absence of coordination (if L +R = B) by comparing the number of synergies. In the second task, subjects were asked to pose dissimilar postures. In this task there is no voluntary coordination involved. Absence of coordination would imply that the two hands are acting completely independent of each other. In such cases one would expect to see that the number of synergies when both hands are considered together would be equal to the sum of the number of synergies when the hands are considered independently (i.e. B = L+R). On contrary, as seen in Table 2 the sum of the number of synergies in right and left hands was always greater than the number of synergies for both hands for all the subjects (i.e. L+R > B). As this is a random postures task, it is to be noted that the number of postural synergies in general, increased from the coordination task.

Table 2. No. of PCs in random task

Subjects	Left hand (No. of PCs)	Right hand (No. of PCs)	Both hands (No. of PCs)
Subject 1	6	6	9
Subject 2	4	3	5
Subject 3	7	5	10
Subject 4	6	6	9
Subject 5	7	5	9

In the second task, surprisingly, similar behavior was observed as in the first task. This task is completely different from the first task by nature. The first task makes sure that PCA can be used as a tool to verify the presence of coordination (if L+R > B) and absence of coordination (if L +R = B) by comparing the number of synergies. In the second task, subjects were asked to pose dissimilar postures. In this task there is no voluntary coordination involved. Absence of coordination would imply that the two hands are acting completely independent of each other. In such cases one would expect to see that the number of synergies when both hands are considered together would be equal to the sum of the number of synergies when the hands are considered independently (i.e. B = L+R). On contrary, as seen in Table 2 the sum of the number of synergies in right and left hands was always greater than the number of synergies for both hands for all the subjects (i.e. L+R > B). As this is a random postures task, it is to be noted that the number of postural synergies in general, increased from the coordination task.

This chapter adapted a numerical approach using PCA to prove that there are innate bimanual synergies inherently present in the neuromuscular structure of the hands. PCA proved

that bimanual synergies are present in the tasks that did not involve any voluntary coordination. In the cycle of learning sensorimotor skills from infants to adults, dexterity developed (Wiesendanger et al., 2001) is reflected in the random postures task as bimanual synergies. The differences in the number of postural synergies (number of PCs) across different subjects imply that the learning involved is not the same for all subjects. One other possible reason is that the musculoskeletal architectures of hands vary from subject to subject. Unlike the coordination task, random postures task did not necessitate the use of bimanual synergies. This might be a possible answer to the question why some bimanual actions can be easily performed. Those within the abilities of these bimanual synergies can be performed effortlessly where as the other which are beyond these abilities are complex and need training.

Bimanual coordination is damaged in brain lesions (Tuller et al., 1989) and brain disorders (Swinnen et al., 1997). Postural debilitation is evidently seen in patients with movement disorders such as Parkinson's disease, essential tremor, and multiple sclerosis (Vinjamuri et al., 2008c). Differences in postural control and movement performance during goal directed reaching in children with developmental coordination disorders have been studied in (Johnston et al.., 2002). Eigen postures or postural synergies were reported to have physiological and anatomical significance by (Mason et al., 2001 and Thakur et al., 2008). Study of the eigen postures in normal subjects during bimanual coordination and comparing them with bimanual eigen postures of patients will have a potential contribution for rehabilitation. By training, if such lacking eigen postures are learnt by patients, it might be possible to bring back the missing bimanual coordination.

In this chapter a quantitative method using PCA to demonstrate the presence of innate bimanual synergies was presented. For this approach to be useful for rehabilitation purposes the

graphical rendering of the obtained postural synergies is necessary. The study needs to be extended over a large group of subjects to obtain a generalized set of bimanual postural synergies which can be used for training patients with movement disorders.

3.0 MODEL OF CONVOLUTIVE MIXTURES

3.1 DESCRIPTION OF THE MODEL

Modular organization of movement primitives and their weighted summation is very well accepted as a viable strategy adapted by CNS to control numerous degrees of freedom of the peripheral apparatus. A detailed review follows. Here the numerical description of the model is presented.

Previously under the context of time varying synergies (Chap. 2.3) angular velocity was expressed as a weighted summation of M time-varying synergies as follows

$$\mathbf{v}_s(t) = \sum_{i=1}^{M} c_{si}\mathbf{w}_i(t - t_{si}) \tag{7}$$

In this model, the angular velocity profile is expressed as

$$\mathbf{v}(t) = \sum_{i=1}^{N}\sum_{k=1}^{N_i} c_{ik}\mathbf{s}_i(t - t_{ik}), \tag{8}$$

where N is the total number of synergies, N_i is the number of repeats of the i^{th} synergy used in $\mathbf{v}(t)$, and c_{ik} and t_{ik} represent the amplitude coefficient and time shift, respectively, of the k-th repeat of the synergy $\mathbf{s}_i(\cdot)$. The model expressed by Equation (8) can be interpreted in terms of convolutive mixtures (Fig. 18). Each synergy can be considered as an impulse response of some "pattern generator" in the lower-level neural system and connected biomechanical system. The pattern generators are triggered by the source signals (in the format of impulses) created in

the higher-level neural system. It is assumed that (i) the input-output relationship of each pattern generator can be modeled by a finite impulse response (FIR) and (ii) the strengths of the impulses (inputs to the pattern generators) at different times are nongaussian, statistically independent, and identically distributed. Based on these assumptions, a hand movement profile becomes a convolutive mixture of the some source signals through the pattern generators (Fig. 18). Then the techniques of blind separation of convolutive mixtures to identify the source signals and the FIR of the pattern generators can be used. The source signals obtained form blind source separation methods are usually filtered versions of the neural sources. Note that the FIR or input-output relationship of each pattern generator contains information about each synergy, while the source signals contain information about the amplitude coefficients and time shifts, c_{ik} and t_{ik}, of the synergies. This model do not explicitly include feedback, none the less sensory systems can influence the motor output by influencing the delays, weights, and dilations.

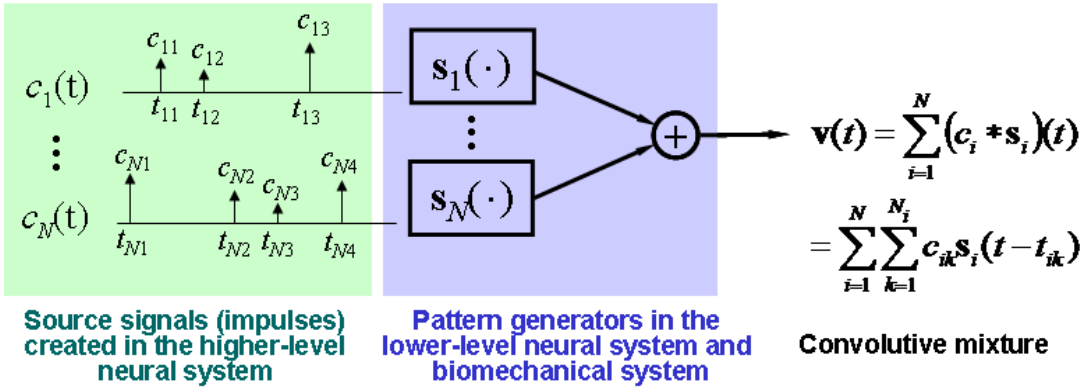

Figure 18. Convolutive mixture model

3.2 NEUROPHYSIOLOGY OF MOVEMENT VARIABLES

In the recent times, several research studies have indicated that motor actions and movements are composed of miniature building blocks called movement primitives, building blocks, synergies or some times called movemes (inspired by phonemes which are building blocks of speech). Movements can be reconstructed by weighted summations of transformations of these building blocks. Current opinion of neurobiology is that new computational methods are needed to advance the understanding of motor compositionality (Flash and Hochner, 2005). It has been observed that combining building blocks to form complex structures is not new but this mechanism has been already in use in the human speech, in the way complex sentences are formed by combining words and words in turn are formed by combining phonemes. This mechanism is not just limited to speech but is also observed in action and cognition.

Movements that are generated by stroke patients (Rohrer et al., 2002) or those that are generated during grasping tasks (Vinjamuri et al., 2007) show that hand trajectory can be composed of a few velocity primitives that are all similar in shape. These infer that these movement primitives are quite stereotypical, with a well-preserved linear relationship between speed and duration (Roitman et al., 2004). During the recovery of stroke patients, they gain better control over their limb, the number of submovements decrease and their temporal overlap increase, giving smoother trajectories (Rohrer et al., 2002). Babies learn to reach and grasp, by smoothly joining together sequential submovements into continuous movements (Rosenbaum, 1991). By a linear superposition of movement segments or by a weighted summation of movement primitives practically any movement can be achieved.

The existence of synergies has been reported not only in humans but also in monkeys during the experiments like prehension tasks. In prehension tasks such as grasping the positions

of the fingers and motions are appropriately selected and preplanned to achieve the goal of the task while securing a stable grasp. Finger movements have been decomposed into basic synergies based on the idea of inverse kinematic computations (Grinyagin et al., 2005). Biomechanical constraints have also simplified complicated hand gestures, such as typing and finger spelling resulting in decomposition of these into elementary units of action called postural synergies. It is reported in (Durr et al., 2003) that reaching movements even in invertebrates are planned in joint space. This was observed when limb targeting in insects was caused by transforming a single movement pattern.

Although the precise anatomical placing of these synergies is difficult, investigators have attempted to present them in behavioral, muscular and neuronal levels. The four mostly possible anatomical sites where the variables for synergistic models can be found in higher level peripheral neural systems are motor cortex, cerebellum, basal ganglia and spinal cord. To be precise these are the representations of movement variables which assist in the modular organization using synergies. Several studies which support the idea of central representations of movement variables like velocities, joint angles are presented. Implications to the convolutive mixtures model are presented in the Chapter 3.3.

3.2.1 Motor cortex

Motor cortex is a term that describes regions of the cerebral cortex involved in the planning, control, and execution of voluntary motor functions. The motor cortex has five main areas, namely, the primary motor cortex (or M1)—responsible for generating the neural impulses controlling execution of movement, the secondary motor cortices, including (1) posterior parietal cortex—responsible for transforming visual information into motor commands (2) premotor

cortex—responsible for motor guidance of movement and control of proximal and trunk muscles of the body and (3) supplementary motor area (SMA)—responsible for planning and coordination of complex movements such as those requiring two hands. Thus motor cortex has been long standing interest for investigators to study the descending sources of movement.

In the cortex of monkeys, electrical microstimulation in primary motor and premotor cortex evoked complex purposeful movements involving many joints and even several body parts. Microstimulation at each site caused the arm to move to a specific final posture (Graziano et al., 2002). It is proposed that there might be a cortical map of joint angles. Neural recording studies have shown that arm motion can be reconstructed from the firing of a population of neurons in the motor areas of the vertebrate cortex (Georgopoulos et al., 1986). Reports based on analyses of both single neurons and neural assemblies have provided evidence for cortical coding which have indicated that neural populations mostly code instantaneous time-varying kinematic variables (e.g. movement direction and velocity). Investigators have proposed that there may be some basis functions in CNS (based on neuronal activity in SMA) that undergo tuning with learning (Padoa-Schioppa et al., 2004) depending on kinematic variables such as position and velocity.

Kalaska et al., (1997) examining the neuronal activity in parietal cortex and also precentral cortical activity proposed that there are spatial representations of limb position, target locations, and potential motor actions are expressed in the neuronal activity in parietal cortex. Also, precentral cortical activity was seen to more strongly express processes involved in the selection and execution of motor actions. These findings suggested that there might be sensorimotor transformations and 'internal models' in cortical control of reaching movements. Kalaska et al., (1997) has indicated that parietal cortex might be responsible in specific for

representations of spatial locations and potential motor actions and that premotor and primary motor cortex are responsible for selection and implementation of motor actions.

Moran and Schwartz, (1999) studied the motor cortical substrate of monkeys associated with reaching when they moved their hands from a central position to targets spaced around a circle. Based on single-cell activity patterns that were recorded in the proximal arm area of motor cortex, they studied the average directional selectivity ("preferred direction") of single-cell activity. Also, they found that the time-varying speed of movement is represented in the cortical activity. A linear model was proposed that described a large portion of the time-varying motor cortical activity during the task. Averbeck and colleagues (2003) recorded neural activity from ensembles of neurons in areas of parietal cortex, while two monkeys copied triangles, squares, trapezoids, and inverted triangles. They used both linear and nonlinear models to predict the hand velocity from the neural activity of the ensembles. The linear model generally outperformed the nonlinear model, suggesting a reasonably linear relation between the neural activity and the hand velocity.

Mason et al., (2001) reported that, although traditionally it was believed that the structure of the primary motor cortex is to control individual muscles, a strict somatotopic representation is not consistent when compared with recent studies. Inactivation and lesion studies also support the concept that M1 is not organized to perform isolated finger movements, even during isolated finger movements. Synergistically multiple fingers are coordinate and act together. Studies support the idea of global control of the hand. They further suggest that the hand is represented as a unit at the premotor cortical unit. The eigen postures observed at the output stage may be represented in the discharge of a population of hand-related motor and premotor cortical cells.

3.2.2 Cerebellum

The cerebellum has attracted the attention of theorists and modelers for many years. The attraction is that the cerebellar cortex has simpler and well defined organization. It has only one output cell, the inhibitory Purkinje cell (P-cell), and four main classes of interneuron; it is also extremely regular in its architecture. Recent investigations based on the evidence from functional imaging, lesion studies, anatomy, and computational modeling support that cerebellum forms a forward model of the motor system (Wolpert et al., 1998). Cerebellar role in co-ordination, motor planning and in predicting the sensory consequences of movements have been studied for a long time. The cerebellum dysfunction leads to pronounced disturbances in movement, posture and balance. It is a relatively massive structure in higher vertebrates. In man, it represents about 10% of the volume of the brain, and it has been estimated to hold more than half of all the neurons in CNS (Miall, 1999). Cerebellum role in motor control and its exact contributions and functions are still under investigation. Models of cerebellum have been proposed showing how the heterosynaptic plasticity of Purkinje cells might be used for motor learning, the physiological details are not clear.

The cerebellar cortex is suggested to acquire internal models of the body and objects in the external world (Ioffe et al., 2007). They have proposed that the cerebellum needs to form an inverse model of the hand/arm system in order to be instrumental in reaching. The role of cerebellum in learning new postural tasks is said to be mainly reorganization of natural synergies .Wolpert et al., (1998) presented two varieties of internal models— forward model and inverse model which are working in parallel in cerebellum. Cerebellar activity was measured by functional magnetic resonance imaging by (Imamizu et al., 2000). Two types of activity were observed. One was spread over wide areas of the cerebellum and was precisely proportional to

the error signal that guides the acquisition of internal models during learning. The other was confined to the area near the posterior superior fissure and remained even after learning. Neuron imaging studies have found that the regional blood flow in the human cerebellum increases significantly at the beginning of learning for a new motor or cognitive task and decreases as the learning proceeds (Imamizu et al., 2000). They proposed that multiple internal models exist and that they compete to learn new environments and tools. During learning, all of these multiple internal models receive a copy of the error signal and only one or a few learn the new transformation, thereby reducing the error signal and localizing the new activity to a distinct region of the cerebellum. According to an electrophysiological study in monkeys (Imamizu et al., 2000), regions near this fissure receive parallel fiber inputs from the premotor and parietal association cortex, and are thus suitable to represent kinematic models of tools.

Thoroughman and Schadmer (2000) proposed a model for Learning of action through adaptive combination of motor primitives. They have proposed that the mathematical properties of the derived primitives resemble the tuning curves of Purkinje cells in the cerebellum. The activity of these cells may encode primitives that underlie the learning of dynamics. Many Purkinje cells simultaneously encode the direction and speed components of velocity. These cells encode hand velocity during planar reaching, firing maximally at preferred velocities distributed in velocity space (Imamizu et al., 2000). This encoding precedes in time the actual movement, suggesting that these cells encode desired velocity.

It has been proposed (Schweighofer et al., 1998) that the role of cerebellum is to synthesize compound movements from simple components to tune its down stream targets so that their functions are performed optimally and to provide feed forward control. Cerebellar damage, results in increased asynergy and intention tremor. These suggest that cerebellum

modulated downstream movement generators and synthesizes compound movements from simpler movements. Kinematic cerebellar reaching deficits, such as poor coordination between shoulder and elbow, curved trajectory, overshoot has been shown to result from an inability to compensate for interaction torques. These strongly suggest the cerebellum provides feed forward motor commands necessary for the proper execution of multijoint movement.

The intermediate cerebellum receives spinal afferents which carry information regarding the state of the arm etc., also receives commands from primary motor, somatosensory and posterior parietal cortex. During reaching movements firing rate of 80% of arm related mossy fibers correlate with joint angle. 33% correlate with velocity. Some are also related to acceleration (Schweighofer et al., 1998). These results suggest and support the idea that cerebellum might be involved in inverse dynamic models. The responses of interpositus neurons are correlated with movement of specific joints (Thach et al.,1982). Cells that fire during reach fire more rapidly during reach. Thus interpositus forms a side path strongly activated during reaching movements which appears to transform kinematic variables into phasic motor commands in body coordinates. Purkinje cell dendrites are linked by parallel fibers forming functionally coupled task specific subgroups that are functional in cerebellar coordination of movement. Such subgroups of Purkinje cells project to discrete areas of cerebellar nuclei possibly influencing synergistic muscles across several joints in the limb.

Cerebellum acts as a comparator of intent and reality (Brooks, 1986). Cerebellum coordinates smooth use of movements in motor performance. Through internal loops it allows for corrections to begin before even movements are initiated. Lateral Cerebellum acts a feedforward model where as intermediate and medial cerebellum act as feedback models to model movements. From lesion studies, it was established that Cerebellum damage leads to loss

of muscle and joint synergies. It also leads to errors in velocities, directions, amplitudes and timing. Dentate, one of the output nuclei of Cerebellum triggers the motor cortex about the onset of movement. Dentate neurons provide a trigger to motor cortex to start intended movement. Also Cerebellum is the chief adjustor of α-γ motor neuron's coactivation. Purkinje cells are also involved in the excitation of α-γ route that determines the muscle tone.

3.2.3 Basal Ganglia

Basal ganglia (BG) and cerebellum are in the side loops to assist motor cortex in evaluating the plans laid out by higher association cortices. BG is involved in the conversion of general motor activity into specific, goal directed motor actions. BG is more commonly referred in Parikinson's disease. Such movement disorders also seem to reveal an important role in the control of hand movements. BG plays an important role in overall scaling and adjusting planned movements. Specifically, the BG (Brooks, 1986) are involved in

1. For simultaneous or successive behavioral use of learned motor acts that are usually chained together by cues interpreted at the higher level
2. For the smooth integration of programmed movements and postures that make up the learned motor acts.

BG has two nuclei Putamen and Caudate. Putamen, in particular deals with scaling the movements (Brooks, 1986). Learned movement patterns are preserved at different speeds. This is made possible by optimal scaling of movement patterns. In our model dilation of synergies can be attributed to as a function of Putamen.

3.2.4 Spinal cord

Traditionally spinal cord is assigned a subservient function during generation of movement and importance is given to supra spinal systems such as motor cortex, basal ganglia and cerebellum. Recent investigations have shown that spinal cord contributes in several aspects of movement that are otherwise attributed to higher neuronal regions. Mussa-Ivaldi and Bizzi (1994) conducted studies on spinalized frogs, and provided evidence that the neural circuits in the spinal cord are organized into a number of distinct functional modules or movement primitives or building blocks. By stimulating two sites in the spinal cord they found that the simultaneous stimulation of two sites leads to the vector summation of the endpoint forces generated by each site separately. This linear behavior is quite significant and provides strong support to the view that CNS may generate a wide repertoire of motor behaviors through the vectorial superposition of a few motor primitives stored within the neural circuits in the spinal cord. The idea that multijoint motor behavior may be organized by CNS through the vectorial summation of independent elements was proposed by Georgopoulos and Schwartz (1986) as mentioned in discussion under motor cortex. These investigators suggested that individual motor cortical neurons specify a desired direction of the hand in space as already discussed under motor cortex. According to their view, the net movement corresponding to a pattern of neural activation in the motor cortex is the vectorial sum of individual primitives.

From the studies related to microstimulation of the spinal cord, the linear combination of the motor outputs generated by different spinal regions was proposed to have major functional implications for the learning and representation of motor behaviors. In particular, linearity suggested that if a system learns to generate a set of different outputs, then the same system is also capable of generating the entire linear span of these outputs. Also because of this linearity,

the controlling system does not need information about the internal structure of the controlled system in order to generate the entire range of possible behaviors.

Tresch et al., (1999) have supported the production of movement by the spinal cord. The CNS is proposed to produce a range of movement through the combination of a small number of 'unit burst generators' organized within the spinal cord. Each of these unit bursters was proposed to control the activation of a small group of synergistic muscles. These units could then be coupled in many different ways to produce a wide range of behavior. The hypothesis that the spinal cord produces movement through the combination of a small number of motor elements is similar to this unit burst generator hypothesis.

Sherrington (1910) first proposed that the responses to cutaneous stimulation might also be used in other classes of movement, such as locomotion. Although the movements produced by the spinal cord in response to cutaneous stimulation are often considered to be simple and stereotyped, it is well established that these responses can be precisely tuned depending on the site of stimulation (Tresch et al., 1999). This flexibility might be used in the movements produced by descending systems.

A recent investigation carried out by Bizzi and colleagues (2000) challenged the traditional architecture of the motor system. Based on the experimental evidences which proved the neurons in spinal cord active during the movement and that this activity was very much similar to the circuitry of supraspinal regions, they suggest that a modular organization of movement primitives may occur in spinal cord. Internal models in skeletomotor system are neuron physiological representations kinematic and dynamic properties of the limbs. Adaptability of the motor system is not just attributed to higher neural system but evidences exist that plasticity of spinal motor system might also function during the adaptation process. Several

observational, lesion and stimulation studies have led to the conclusion that there exists a flexible combination of spinally organized behavioral subunits. The results from their laboratory of experiments proved that spinal cord is active participant in complex functions of motor control such as planning, plasticity and organization of the movement.

3.3 IMPLICATIONS TO THE MODEL OF CONVOLUTIVE MIXTURES

This chapter is a summary of the previous chapter in the sense that, it recapitulates significant physiological conclusions based on the evidences reported in several investigations which might play an important role in bringing an anatomical correlate of the current model.

3.3.1 Neural representations of movement variables

- Reaching movements even in invertebrates are planned in joint space (Durr et al., 2003).
- A cortical map of joint angles (Graziano et al., 2002).
- Spatial representations of limb position, target locations, and potential motor actions in neuronal activity in parietal cortex and precentral cortex by Kalaska et al., (1997), also time-varying speed of movement represented in the cortical activity.
- Arm motion can be reconstructed by firing a population of neurons in the motor areas of the vertebrate cortex (Georgopoulos et al., 1986).
- Single neurons and neural assemblies for cortical coding of instantaneous time-varying kinematic variables (e.g. direction and velocity) by Georgopoulos et al., (1986).
- Basis functions in CNS (based on neuronal activity in SMA) tune, learning (Padoa-Schioppa et al., 2004) kinematic variables such as position and velocity.
- The eigen postures may be represented in the discharge of a population of hand-related motor and premotor cortical cells (Mason et al., 2001)
- During reaching movements firing rate of 80% of arm related mossy fibers correlate with joint angle. 33% correlate with velocity (Schweighofer et al., 1998)

- Purkinje cell dendrites are linked by parallel fibers forming functionally coupled task specific subgroups instrumental in cerebellar movement coordination (Thach et al., 1982)

3.3.2 Linear models

- A linear model that described a large portion of the time-varying velocity and direction in motor cortical activity by Moran and Schwartz, (1999).
- Averbeck and colleagues (2003) recorded neural activity from ensembles of neurons in areas of parietal cortex; The linear model of hand kinematics generally outperformed the nonlinear model, suggesting a reasonably linear relation between the neural activity and the hand velocity.
- Stimulating two sites in the spinal cord, the simultaneous stimulation of two sites leads to the vector summation of the endpoint forces generated by each site separately. Mussa-Ivaldi and Bizzi (1994)
- Multijoint motor behavior may be organized by CNS through the vectorial summation of independent elements (Georgopoulos and Schwartz, 1986).
- The role of cerebellum is to synthesize compound movements from simple components to tune its downstream targets so that their functions are performed optimally and to provide feed forward control (Schweighofer et al., 1998).
- The CNS is proposed to produce a range of movement through the combination of a small number of 'unit burst generators' organized within the spinal cord. Tresch et al., (1999).

- A recent investigation carried out by Bizzi and colleagues (2000) challenged the traditional architecture of the motor system. Based on the experimental evidences which proved the neurons in spinal cord active during the movement and that this activity was very much similar to the circuitry of supraspinal regions, they suggest that a modular organization of movement primitives may occur in spinal cord.

3.3.3 Stroke, lesion studies and disorders

- During the recovery of stroke patients, they gain better control over their limb, the number of submovements decrease and their temporal overlap increase, giving smoother trajectories (Rohrer et al., 2002).
- Regional blood flow in the human cerebellum increases when learning a new motor task suggesting internal models responsible in learning.(Imamizu et al., 2000)
- Cerebellar damage, results in increased asynergy and tremor (Schweighofer et al., 1998)

3.3.4 Summary

A detailed review based on anatomical sites motor cortex, cerebellum, basal ganglia and spinal cord was presented in the previous chapter. In this chapter a classification of significant contributions which support the viability of current model have been grouped under three groups namely representation of kinematic variables, linear models and stroke and disorder studies. Although these were learning lessons, it is hard to comment on the neurophysiological structure of the current model as the current experiments are based peripherally. Never the less, higher level neural systems—posterior parietal cortex, premotor cortex, Purkinje cells in cerebellum and

lower level neural systems—spinal cord and biomechanical systems—muscles can interact for modular organization of synergies to happen. These complex interactions still remain mysterious in the field of neurophysiology even today. It is difficult to pin down precise physiological correlates in current model as it will be a meticulous investigation by itself. The model proposed here can also be readily extended to muscular synergies and is not just limited to postural or kinematic synergies. Current model although proved to be a sufficient mathematical framework to explain joint level kinematics, it is to be extended to include dynamics. It is possible that the current model of convolutive mixtures is criticized as performing nothing more than curve fitting. In refute to this argument, the current convolutive mixtures model expresses joint velocity profiles as a weighted linear combination of time-varying movement modules or primitives. These movement modules when visualized have physiological significance (Chapter 4. 1). This means that the model is not same as rudimentary curve fitting with random signals. Linear combination is some times questioned as there are so many non linearities in neural system. As shown in 3.3.2 linear models have been employed by other investigators and in some cases (Averbeck et al., 2003) linear models outdid non linear models. In solving, how CNS simplifies the problem of managing redundant degrees of freedom of peripheral apparatus, some investigators have proposed complex models. In contrast, in this thesis, based on physiological evidences, a linear combination of synergies was proposed.

In the succeeding chapters, the convolutive mixtures model will be practically implemented in reach and grasp experiments. Also this model is used as an aid in movement disorders and rehabilitation. Realizing this model with practical significance might enable the reader to appreciate the model better.

4.0 REALIZATION OF THE MODEL

The convolutive mixtures model presented in the previous chapter is realized in three different ways in this chapter. First, by simplifying the original model to instantaneous mixtures model, temporal postural synergies were obtained. These are synchronous synergies of angular velocities unlike time-varying synergies presented in Chapter 2.3. Second, by assuming the statistical independence of neural sources, the convolutive mixtures model is utilized in extracting sources responsible for tremor by using blind source separation techniques. Third, the model of convolutive mixtures is realized by utilizing the synchronous synergies presented in 4.1 and l_1-minimizaton algorithm to obtain optimal weighted combination of time-shifted and dilated versions of these synergies.

4.1 TEMPORAL POSTURAL SYNERGIES

In this chapter, by using principal component analysis (PCA) a simplified version of the original convolutive mixtures model is realized. A method to derive kinematic synergies in joint movements of the hand, while performing rapid grasps is demonstrated. Significance of the rapid grasps lies in constraining the synergies to combine instantaneously, leaving no scope for CNS to plan in time-varying space. In this experimental paradigm the convolutive mixtures model is minimized into a weighted summation of synchronous synergies. Hence using PCA to extract

synchronous synergies is justified in this case. This is the main motivation behind this implementation of the model. From the kinematic synergies, with known starting postures of the hand during any task, postural synergies were directly calculated.

Postural synergies of hand obtained by matrix factorization methods like principal component analysis (PCA) have been widely proposed. A few dominant postures were derived that could account for more than 90% of the variance in a collection of number of postures recorded during one or more reach and grasp tasks. By extrapolating these postures, the temporal variation of hand posture during reach and grasp was estimated. Thus the hand postures were visualized across the task time. In this Chapter, a unique method is presented, though by using principal component analysis (PCA), to obtain kinematic synergies in joint velocity profiles. With these kinematic synergies in joint velocities of hand, postural information across the time line was calculated. Instead of estimating by extrapolation, this method is a direct computation of the postures. By this novel method the obtained kinematic synergies in joint velocities of hand resulted in synergies which preserved the postural information across the entire task time. Postural synergies thus obtained, showed various strategies adapted by subjects while grasp.

The concept of synergies (In Greek synergós means working together) received the first numerical representation as a degree of freedom problem by Bernstein (1967). Although synergies were originally defined by Bernstein as high level control of kinematic parameters, different definitions of synergies exist and gradually with time the term has been generalized to indicate the most common patterns observed in the behaviors of muscles, joints, forces, and

---

This work was accepted as R. Vinjamuri, M. Sun, R. Sclabassi, and Z. -H. Mao. Temporal variation of postural synergies of the human hand during grasping in 16th international conference on mechanics in medicine and biology, Pittsburgh, PA.

actions etc. Synergies in hand movements especially present a very complex optimization problem as to how central nervous system (CNS) handles the high degree of freedom hand with over 25 degrees of freedom (Mackenzie and Iberall, 1994). Yet, CNS handles all the movements effortlessly and at the same time dexterously. In an endeavor to solve the problem as to how CNS handles this high dimensional problem, many researchers have proposed numerous concepts of synergies. Some of them which are relevant to current topic are postural synergies (Thakur et al., 2008, Santello et al., 2002, Santello et al.,1998, Todorov et al., 2004, Mason et al., 2001), kinematic synergies in joint movements (Vinjamuri et al., 2007 and Grinyagin1 et al., 2005), and dynamic synergies(Grinyaginl et al., 2005).

With the advent of virtual reality, in recent times postural synergies have been extensively explored but only a few attempts were made to actually visualize postural synergies across time (Santello et al., 2002, Thakur et al., 2008, Santello et al 1998). Many matrix factorization methods such as principal component analysis, singular value decomposition, and discriminant analysis have been used to obtain a few dominant postures in a wide range of postures collected during reach and grasp experiments. But these were all static postures. Temporal postural synergies are not just static postures like eigen postures or principal component postures proposed earlier but are postural variation patterns observed across the time of reach and grasp. The attempts which were made earlier (Thakur et al., 2008, Santello et al., 2002, Mason et al., 2001) were limited to estimation by extrapolation. In (Thankur et al., 2008) postural variation across time was obtained, but was estimated by adding a weighted component of variation to a mean posture. In (Santello et al., 2002 and Mason et al., 2001) also similar estimation was carried out. All the above mentioned attempts to obtain temporal postural synergies remained as estimations but not direct calculations. In this Chapter, a new method to

obtain synergies in angular velocities of fifteen joints of hand is demonstrated. When these kinematic synergies are translated into postures, temporal postural synergies are obtained. The current method led us to direct computation of temporal postural synergies but not approximate estimations. Such direct computations will enable these synergies to play an important role in future rehabilitation.

The experimental setup consists of CyberGlove® equipped with 22 sensors which can measure angles at all the finger joints including distal, proximal and metacarpal joints. For the purpose of this experiment only fifteen of the sensors which correspond to metacarpal, proximal and distal joints of five fingers were considered. Objects (wooden and plastic) of different shapes (spheres, circular discs, rectangles, pentagons, nuts and bolts) and different dimensions were selected based on two strategies. One was gradually increasing sizes of similar shaped objects and the other was different shapes to isolate proximal and metacarpal joints. Some similar sized/shaped objects were intentionally used to observe trends in grasping movements.

A typical experiment consists of grasping the objects of various shapes and sizes. Start and stop times of each task were signaled by computer-generated beeps. In each task, the subject was in a seated position, resting his/her hand at corner of a table and then, upon hearing the beep, grasped the object placed on the table. At the time of the start beep hand is in rest posture and once the subject grasps the object, one is asked to hold it until the stop beep. Each task lasted for 1.732 seconds. Through out the experiment, joint angles were recorded during the experiment by CyberGlove. For each subject forty such tasks were recorded which were as per the criteria mentioned in Materials. After a short recess of about 3-4 minutes, twenty more tasks were collected by picking twenty objects in random order irrespective of their shapes and sizes.

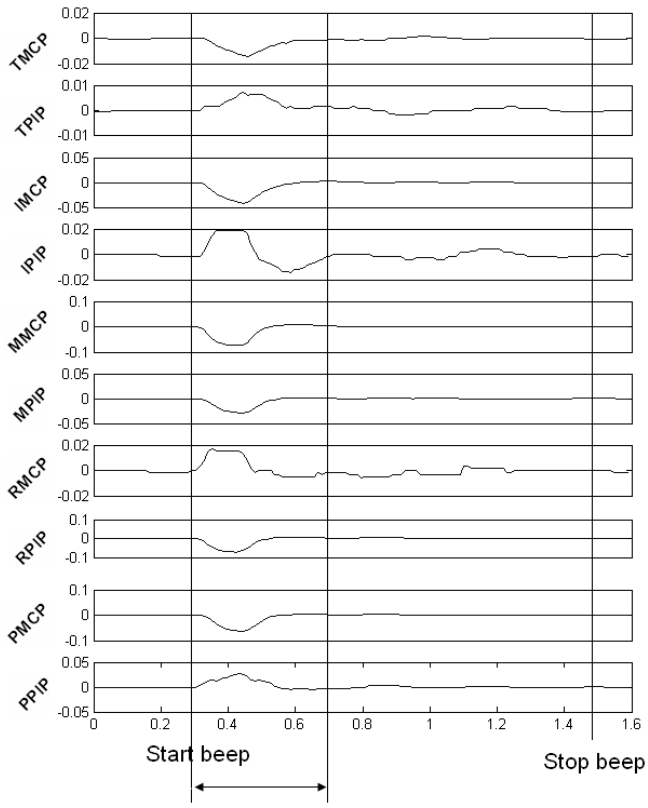

Figure 19. Task profile showing 10/15 joints and Start and Stop signals.

After obtaining the joint angles at various times from the experiment, angular velocities were calculated from them. These angular velocities were filtered from noise. Due to human error all these sixty postures did not exactly start at the same time. A typical task profile which contains the velocity projectile is as shown in the Fig. 19. Only the relevant projectile movement (as indicated in Fig. 19) of the entire velocity profile was preserved and the rest was truncated. Of 1.6 seconds only 0.5 seconds corresponded to the actual movement. Angular velocity profiles of fifteen joints corresponding to one object were cascaded as shown in Fig. 20. Finally one such posture matrix for each subject was obtained. Each row of this matrix contains the velocity profiles of fifteen joints corresponding to one object and forty such different rows form posture matrix for each subject. Please note that although though these are kinematic profiles, they still

preserve the postural information. Each row of the posture matrix corresponds to one start posture and one end posture. The velocity projectile describes the transformation from start posture to end posture. As all start postures are same for all the tasks, we can say that each row of the posture matrix corresponds to one (end) posture.

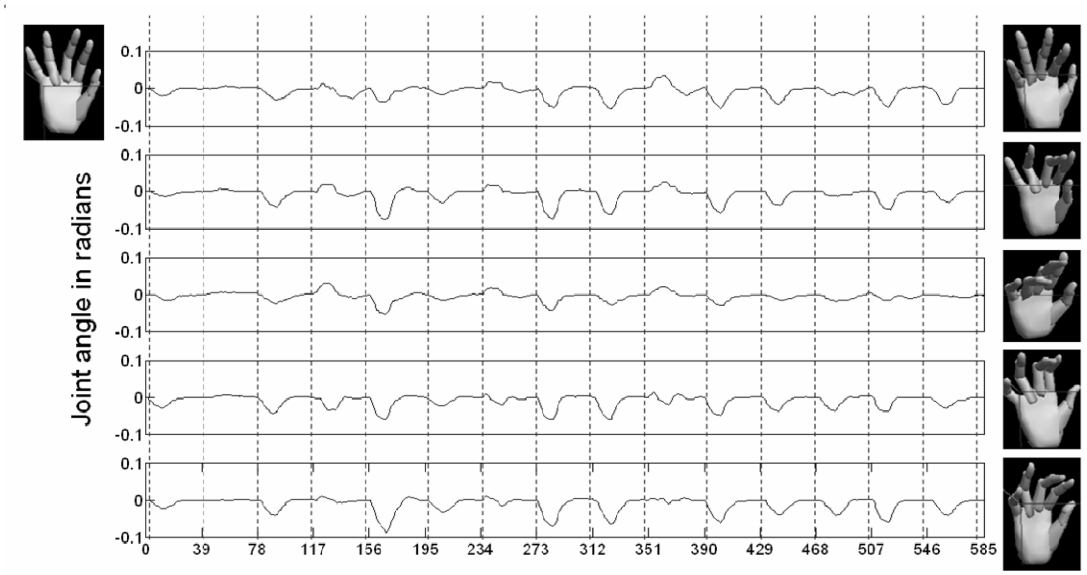

Figure 20. Posture matrix showing formation of five postures from a rest posture.

PCA was run on posture matrix of each subject to obtain principal component postures (we will call them principal postures). These postures are linear combinations of forty training postures which were used for training. Principal postures are very similar in their structure to postures shown in Fig. 20, where velocity projectiles of the joints are cascaded. For each principal posture, all joints are arranged row wise (as shown in Fig. 22) and this is called a synergy. A comprehensive approach to decide the number of principal postures or synergies which are enough to reconstruct the twenty testing postures is presented in Results. By linearly combining these synergies twenty testing tasks were reconstructed. A least square approximation (pinv in MATLAB) was used to find the optimal linear combination of the synergies which can reconstruct the testing movement profiles with minimum error.

A typical task profile which contains the velocity projectile is as shown in the Fig. 19. The bell shaped velocity profiles during reach and grasp have been observed in literature widely. As can be observed, the onset of movement takes place after a short delay which is due to the combined effect of delays in lower neural systems and biomechanical systems. Please note that these delays differed from object to object and obviously from subject to subject. Zero velocity regions correspond to times when there is no movement which is before the start beep and after the grasp.

An illustration of posture matrix was made in Fig. 20. As mentioned earlier, subject started from a relaxed posture and upon a start beep, after a short delay the movement began. After the grasp is completed, subject held posture (end posture) until the stop beep. Only the section of the velocity projectile present in the entire movement of the joint is preserved and the rest is ignored. By cascading such projectiles for all fifteen joints, a row of the posture matrix and hence forth the whole matrix was constructed. Upon performing principal component analysis on this posture matrix, principal components (PCs) were obtained. For all the subjects, on average the first PC accounted for 56% of the total variance. And the first and second PCs together accounted for 82% of the total variance. In order to help determine how many principal components would suffice to account for the variance of the entire training data, a PC-variation chart was plotted as shown in Fig. 21. Error bars indicate standard deviation across five subjects. At about 6 PCs there is not much appreciable improvement in the contribution of higher order PCs. This by itself is not a sufficient evidence to decide on the number of PCs/ synergies. The other criteria used to determine number of synergies will be discussed shortly later.

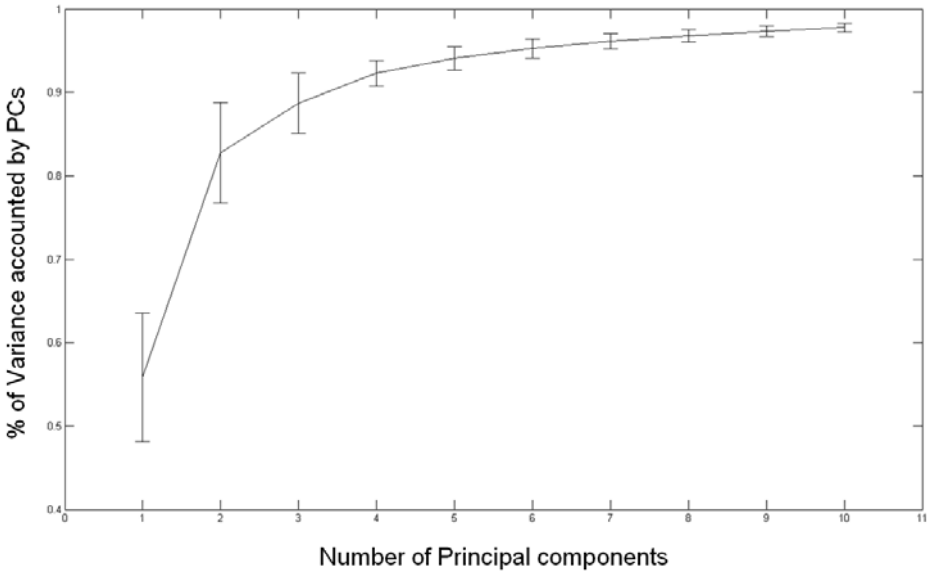

Figure 21. PC variation plot

Angular velocity profiles obtained from the principal component analysis are depicted in Fig. 22. Across the rows are the fifteen joints corresponding to five fingers (three for each). These are the kinematic synergies obtained which show that peak velocities of the grasp are observed at the middle of the task. Acceleration at the beginning of the task, which is generally open loop, followed by deceleration caused due error feedback while reaching the precise position of object, and finally grasp is closed. Only two of the six such angular velocity synergies are plotted in Fig. 22 for Subject 1.

As the observed angular velocity profiles are of fifteen joints, postural information at any time can be obtained given the initial posture. By using these fifteen joints the shape of the aperture of the hand during the entire grasp can be reconstructed. Thus postural synergies from the above kinematic synergies were obtained. A set of six such postural synergies obtained from Subject 1 are depicted in Fig. 23. As can be seen each of the six synergies have their unique function. In the figure four postures indicate 25%, 50%, 75% and 100% of the task times respectively. End posture in each row i.e., for each synergy indicates what type of the grasp is

being achieved by that synergy. Meaning the functionality of the grasp can be implied just by the end posture. Hence such end postures for six synergies in case of remaining four subjects are shown in Fig. 24. As all the subjects performed tasks on the same training objects, there were similarities in synergies adapted, among the subjects. First two synergies were very similar across all the subjects. Fifth and six synergies were again very similar across all the subjects. The end postures of third and fourth synergies were not the same for all the subjects although there were some similarities.

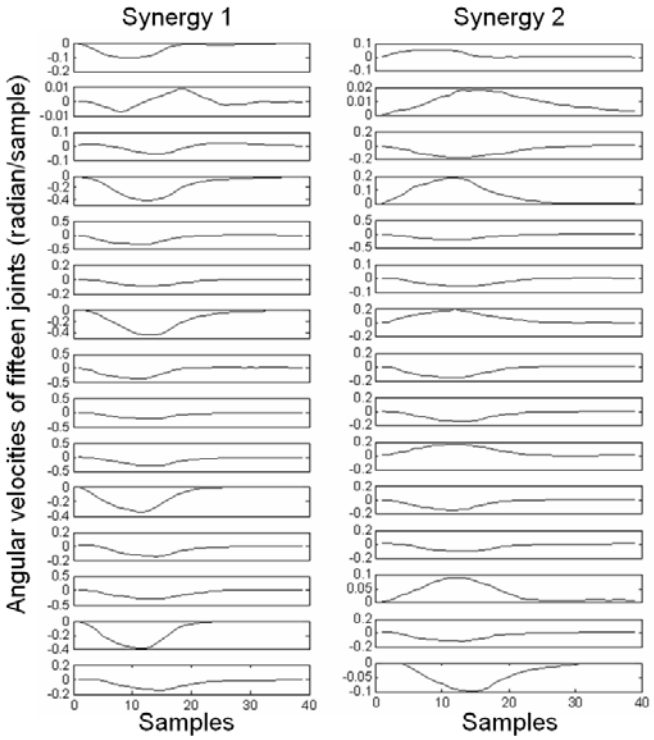

Figure 22. Two synergies in angular velocities obtained from PCA

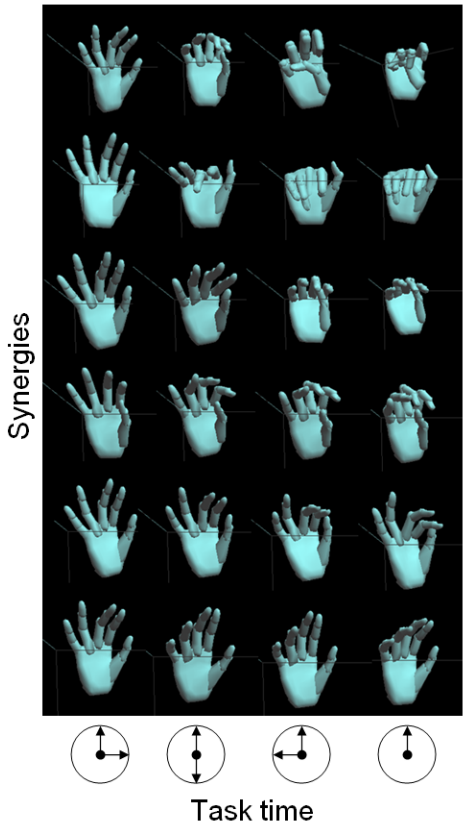

Figure 23. Postural synergies for Subject 1

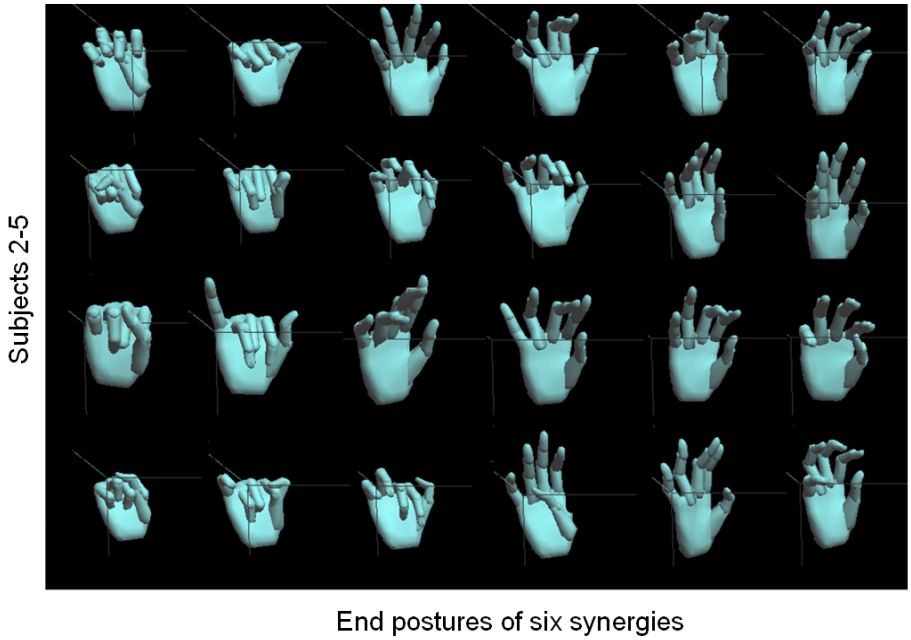

Figure 24. End postures of six synergies

By linearly combining the synergies obtained from PCA, for each subject twenty tasks which comprise the testing data, were reconstructed. One of the best reconstructions is shown in the Fig. 25. As is clearly evident, the reconstruction was very accurate using six synergies in the following task. The reconstruction errors in other cases can be seen in the reconstruction error plot illustrated in Fig. 26. The error bars indicate standard deviation across subjects averaged across twenty testing tasks. The no. of PCs vs. reconstruction error plot also helps in determining the optimal number of PCs. Although it is up to one's discretion about how many PCs can be considered to account for appreciable reconstruction, in this case 6 synergies were proved as sufficient for reconstruction of the testing tasks.

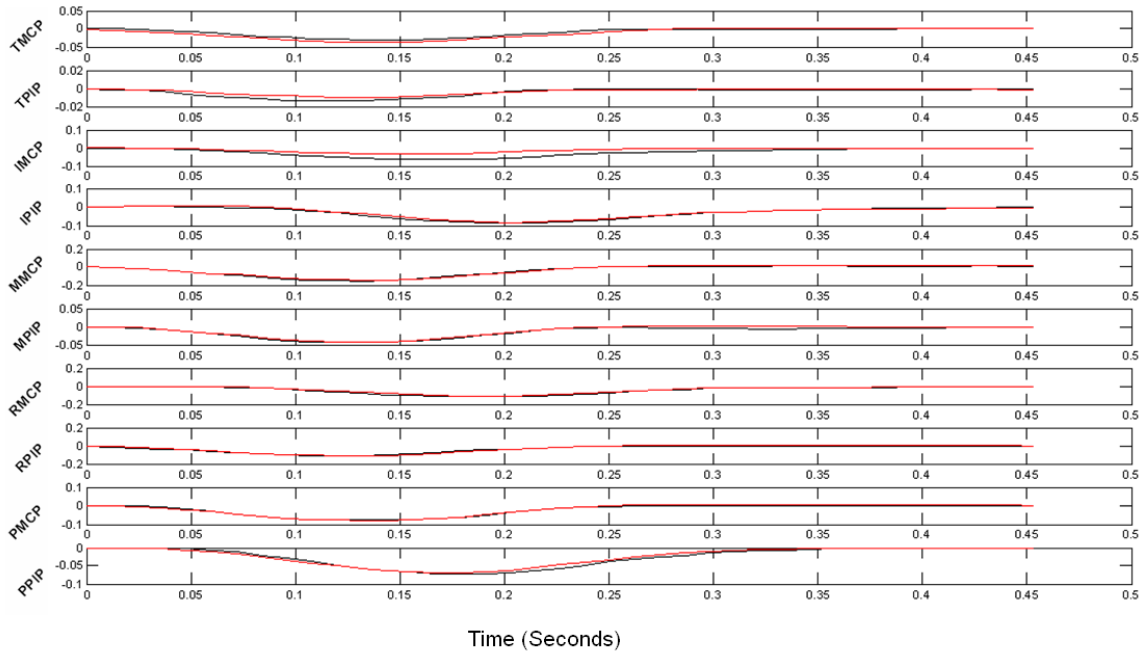

Figure 25. Reconstruction (red) of the original (black) angular velocity profile

In this Chapter, kinematic synergies in velocity profiles of grasping tasks were derived by using PCA. In particular, these kinematic synergies in joint velocities were translated into principal postures. These postures are not just static postures which are dominant across a number of postures recorded during tasks. These postures are temporal variations observed in

hand during a task. Static postures do not contain temporal information. But in this case, principal postures are temporal transformations of hand from a relaxed posture to an object dependent posture. As indicated in Introduction many studies have presented dominant postures or eigen postures but only a few have proposed temporal postural synergies. And even those who have proposed temporal postural synergies have done so using a weighted summation to a mean posture. This becomes just an approximation, but in reality these are not actual temporal postural changes.

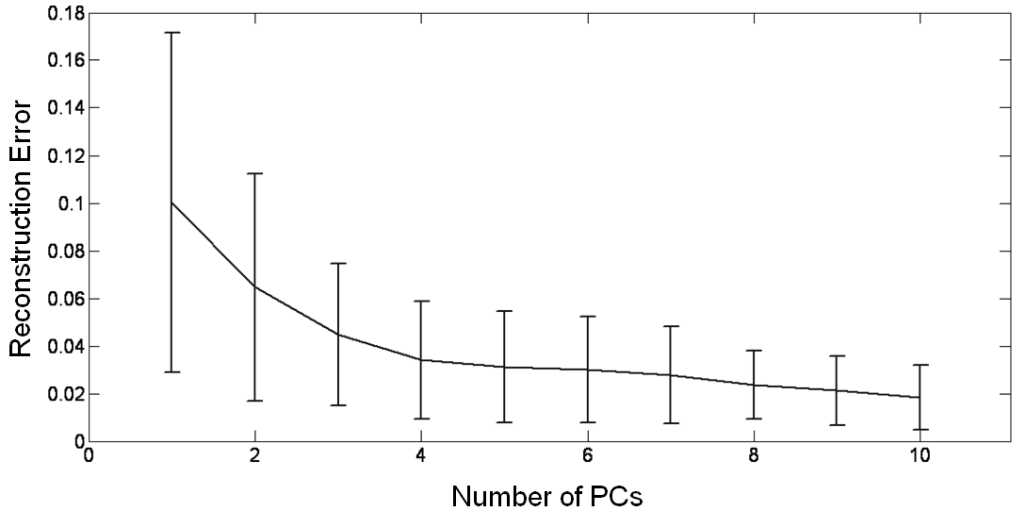

Figure 26. Reconstruction error Vs. Number of PCs plot

Following anatomical insights were obtained from the temporal postural synergies. In Fig. 23, for third, fourth and fifth synergies in this subject, index finger acts as a master in leading the movement and rest of the fingers follow it as slaves. This concept has long been observed and called as enslaving. Implementing such observations in prosthetic hands can greatly reduce the complexity involved in computations. From the end postures of figures Fig. 23 and Fig. 24 it is clearly evident that no single synergy is redundant and that they are all unique. First synergy is a closed fist. Second synergy can be used in tasks like holding a dice, third

synergy in holding small spheres, fourth in cylindrical rods, fifth in precision pinches, and sixth in holding larger spheres/objects. In all of these synergies, it is clearly observed as the size of the grasping object decreases the use of metacarpal joints increases. Meaning in the first two synergies, the metacarpal flexion was dominant when compared to other synergies and got lesser and lesser when moved down. Also for gross major movements only metacarpal joints were involved. For finer and precise movements after major movements, proximal and distal joints were involved respectively. This can be witnessed in fifth synergy.

Postural synergies play an important role in understanding the physiological aspects of the movement. Biologically inspired synergies have already taken an important place in prosthetics (Iftime et al., 2005 and Popovic et al., 2001). In such technologically advancing scenarios, dominant static postures are by themselves not significant unless they are supplied by the information how they can be achieved by collective co ordination in different joints. In Fig. 23 the advantage of presenting the postural variation across the time line can be greatly appreciated. It is important to note here that intermediate postures may seem significant but may not be physiologically meaningful. Meaning dominant static postures proposed earlier need not have physiological meaning. For example in Fig. 23, intermediate posture at 25% time of first synergy is almost similar to end posture of fourth synergy. Although first synergy is aimed to grasp a tiny pearl, its intermediate posture looks very much like fourth synergy that is targeted at grasping a cylindrical rod. Temporal postural synergies eliminate this ambiguity as they supply the postural information across the time line of entire reach and grasp.

Some studies considered synergies as common postural patterns across subjects (Thakur et al., 2008). Should all people use same postural primitives and should they be called synergies? Athletics, calligraphers, artists, musicians have very sophisticated set of skills in hands, which

can adapt to complex movements very easily, what to speak of day to day movements. In such cases, synergies used by skilled professionals need not be same as an average class of people. In such cases the absence of common trends among different people does not mean the absence of synergies but it means that people are adapting different synergies. Some synergies are innate which might be common but some are adaptive as per the changes in environment.

It was very interesting to analyze the utilization of synergies. In all subjects, it was observed that, on average the first synergy was also the best synergy to be used most in all the testing grasps. It is very intuitive in the sense that first synergy involved full flexion for all the subjects. Next in the order were third, fourth and fifth synergies which were not the same for all subjects. Note that in the linear combinations of synergies to reconstruct testing grasps, negative coefficients were obtained for some synergies. What this means is by using first synergy for full flexion and simultaneously, using the other synergies in opposite direction would inhibit the movement and enable the subject to achieve various postures. This degree of inhibition can be controlled by the magnitude of the coefficients in the linear combination. This can be correlated to agonist and antagonist muscles acting simultaneously in opposite directions causing forward movement and at the same time deceleration by negative velocities to control the movement of hand in different tasks.

4.2 QUANTIFICATION OF TREMOR IN MOVEMENT DISORDERS

4.2.1 Blind source separation

In this chapter, by using techniques of blind source separation, we realize the convolutive mixture model. However, it should be noted that the model is mainly targeted at estimation of tremor and cannot account for the characteristics and dynamics of the system under some nonlinear conditions such as output saturation (e.g., maximum force generation) and hysteresis (e.g., rigidity).

The convolutive mixtures model can be expressed by the following equation:

$$y_k(t) = \sum_{i=1}^{m} s_i * f_{ik}(t), \quad k = 1, ..., n \tag{9}$$

where the symbol "*" represents convolution; $y_k(t)$ represents the angle of the k-th joint of the hand at time t, k ranges from 1 to n, and n is the total number of the considered joints of the hand; $s_i(t)$ represents the time sequence of the i-th source signal created in the higher-level neural system, i ranges from 1 to m, and m is the total number of sources; and $f_{ik}(\ .)$ represents the finite impulse response of the filter through which the i-th source acts on the k-th joint of the hand.

The above model is used to extract sources of tremor in hand movements of patients with ET. In ET the tremor sources and the sources responsible for voluntary movement control can be approximately viewed as independent with each other. This assumption is supported by (i) the relative independence of ET from peripheral mechanical reflex mechanisms (Dueschl et al., 2000) and (ii) the existence of central sources responsible only for tremor. Studies have revealed cortical and thalamic involvement in the generation of ET (Raethjen et al., 2007), occurrence of rest tremor in ET (Shahed et al., 2007), thalamic neuronal activity correlated with ET (Hua et al.,

1998), and a strong correlation between tremor in ET and cerebral activity (Hellwig et al., 2001). Although the severity of tremor may depend on the effort to make a movement, the timing of the tremor can be considered independent to that of the voluntary movement. Therefore, it is a reasonable approximation that the tremor sources are statistically independent with the sources for command signals of movement control. Based on this, we can apply the techniques for blind source separation of convolutive mixtures.

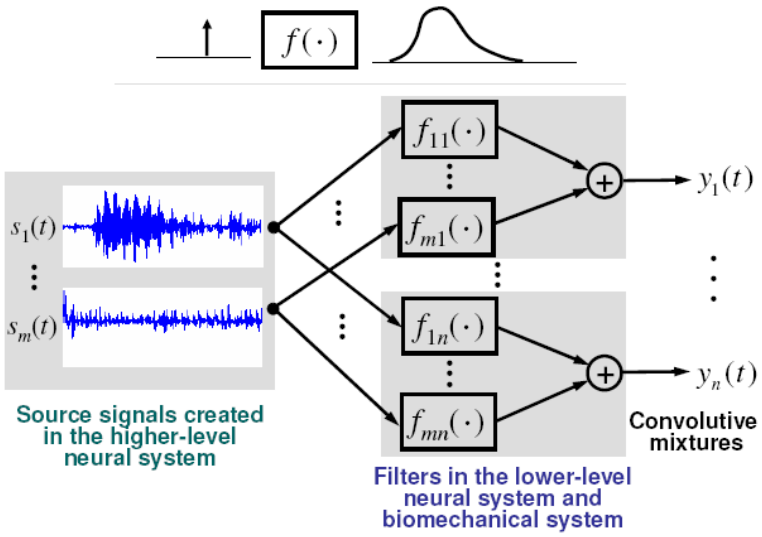

Figure 27. Hypothesized model for generation of hand movement

4.2.2 Current methodologies and limitations

Studies of quantification of the tremor and the degree of severity of diseases with movement disorders like essential tremor (ET) and Parkinson's disease (PD) is one of the major difficulties in clinical evaluation. At present, clinicians are limited by ordinal rating scales such as Unified PD Rating Scale and Fahn-Tolosa-Marin (FTM) Tremor Rating Scale, because such scales are more subjective and open to examiner's interpretation. Researchers are shifting away from ordinal rating scales and are evaluating tremor based on electro-mechanically measured

parameters like stiffness, rigidity, etc. (Patrick et al., 2001) by utilizing computer-aided tools. The behavioral motor characteristics in these movement disorders are infamously unpredictable, especially in advanced stages of the disease, and any contribution to provide better performance would be appreciated by clinicians.

The current methods to measure tremor include accelerometry, electromyography (EMG), computer tracking, tablets, infrared, video cameras, and laser transducers. Though all these methods are better than Likert Scale, which itself is susceptible to problems of sensitivity and reliability, several of them have general drawbacks like bulky machinery (not portable) and time-consuming procedures (e.g., 24-72 hours long EMG recordings). Moreover, it has been reported that accelerometric measurements, besides being one dimensional, suffer from gravitational artifacts (Elble, 2005), EMG provides only a loose measure of tremor amplitude (Rajaraman et al., 2000), and digitizing tablets are deficient in sensitivity to measure tremor (Elble et al., 1990). Apart from the limitations, all the above techniques are useful in specific environments in which they are deployed.

In this study, a data glove is used to measure tremor. Data gloves are precise and easy to use in measurement, as they are wearable and assume the shape of the hand. (Note that hands are affected in 95% of ET patients (Lyons et al., 2005). A similar concept has been already tested previously in (Will et al., 1990) where hand and finger movements were precisely quantized using a VPL data glove in chorea, myoclonus, and tremor. Data gloves have also been used by us

---

This work was revised as R. Vinjamuri, D. Crammond, D. Kondziolka, H.-N. Lee, and Z. -H. Mao. Extraction of sources of tremor in hand movements of patients with movement disorders in IEEE transactions on information technology in biomedicine.

to measure postural and kinematic information for hand movement analysis in normal subjects (Vinjamuri et al., 2006, Vinjamuri et al., 2007).

Quantification of tremor has been achieved by numerical methods such as spectral analysis and time-frequency analysis (Patrick et al., 2001, Riviere et al., 1997, O'Suilleabhain et al., 1998). However, these analyses were performed directly on the experimentally recorded data. They might not achieve optimal quantification of tremor, because tremor is spread across parts of limbs and, at a single site of recording, tremor might not be significant. Although ET is a central tremor that originates from a central source, the tremor is distributed across the limbs (Lyons et al., 2005). Different frequencies of tremor were observed in different limbs (Lyons et al., 2005, O'Suilleabhain et al., 1998). This variation might be due to mechanics of limbs that accentuate tremor differently, although the tremor originates from a single neural source. The distribution of tremor makes it difficult to evaluate, measure, and manage the tremor (Lyons et al., 2005, Anouti et al., 1995). A technique from the blind source separation for convolutive mixtures is proposed here to obtain sources of tremor from joint movements of the hand. In contrast to previous methods, current method attempts to isolate the sources of tremor from a raw data of joint movements that contain tremor distributed across multiple joints of the hand in different movement tasks. These sources can work as miniature windows to view movement disorders.

4.2.3 Implementation

Four subjects, two males (aged 42 and 70 years) and two females (aged 40 and 71 years) with ET were tested in a series of tasks. These subjects recorded 4, 3, 3, and 3 (on a scale of 4) on FTM tremor scales, respectively. All these subjects were informed about the nature of the study and signed institutionally approved consent forms. The experimental setup included a CyberGlove

for the right hand, equipped with 22 sensors which could measure angles at all the finger joints of the hand at a sampling frequency of 64 Hz. Subjects wore this data glove during all the tasks of the experiment. Before the beginning of the experiment, joint sensors were individually calibrated for each of the subjects. Start and stop of the tasks were indicated to subjects by system beeps. The tasks designed for these experimental purposes were motivated by motor examination and daily activities. Tasks included opening and closing the fist naturally, opening and closing the fist at faster rate, opening fist followed by adduction of fingers followed by abduction of fingers followed by closing the fist, repeating the previous task faster, finger tapping, untying shoe laces, drawing Archimedes spiral, drawing pentagon clockwise and then anti-clock wise, drawing letter A, reaching and grasping a cup on the table, and finally signing signatures. Two of the tasks for Subject 2 are illustrated in Fig. 28.

The following steps were performed for data analysis. First, CyberGlove through a PC interface measured the joint angles during different tasks of the experiment. Data collected from the data glove were processed in MATLAB to obtain joint angles of the fingers of the hand. Second, Fourier transforms of the time series of joint angles in each task were calculated, and after a detailed perusal only four of the joints which contribute to major tremor were included for further separation of tremor sources. Other joints were ignored to save computation for blind source separation. An example of four joints selected for Subject 1 was shown in Fig. 29 (Top).Note that these selected joints were different for different subjects. However, the joints included only metacarpophalangeal (MCP) and proximal interphalangeal (PIP) joints. It was reported that hand tremor was observed to be prominent in MCP and PIP joints only (Halliday et al., 1956, Rajput et al., 2004). Distal interphalangeal (DIP) joints were not considered as their movements were dependent to a great extent on movements of their parent PIP joints. Moreover,

it was empirically observed in the analysis that including additional joints did not account for significant improvement as the joints selected already contained major tremor component. Third, all the tasks were cascaded to form a long sequence of tasks, and this sequence was processed with an algorithm for Blind Source Separation of convolutive mixtures through Deflation (BSSD) by Castella et al. (2007). The algorithm was iterative blind source separation using kurtosis real-valued contrast function of cumulants. Kurtosis is a classic measure of nongaussianity, and nongaussianity is used to indicate independence (Hyvarinen et al., 2001). The kurtosis contrast function here allows us to extract one nongaussian and independent source from the mixture at a time. After one source is extracted, its contribution is subtracted from the observations. This iterative process (called deflation) is repeated to extract all the sources. By using filters with finite impulse response, the whole problem becomes finding a least square solution to a linear regression problem (Castella et al., 2007).

So as to justify the independence among the extracted sources, calculated and compared the values of kurtosis for the normalized source signals and joint-angle profiles. The kurtosis of a normalized random variable y, where $E\{y\} = 0$ and $E\{y^2\} = 1$, is defined by $\mathrm{E}\{y^4\}—3(\mathrm{E}\{y^2\})^2 = \mathrm{E}\{y^4\}—3$. As just mentioned, kurtosis can indicate nongaussianity and independence (Hyvarinen et al., 2001). A larger absolute value of kurtosis of y implies a higher nongaussianity of y. According to the central limit theorem, a sum of independent random variables tends to have a probability distribution closer to gaussian than any of the original variables. In other words, an isolated independent source signal tends to have higher nongaussianity than the experimentally recorded data, which are mixtures of independent source signals. Therefore, maximizing nongaussianity, measured by the absolute value of kurtosis, has been used in independent source separation (Hyvarinen et al., 2001). Various filter lengths were tried, and best observed filter

length was used that revealed tremor synchronous with Fourier transform of the experimental data. These filter lengths were obtained based on the following criteria. A tiny finger movement, evoked by an impulse from transcranial magnetic stimulation (TMS), was about 200 ms-300 ms (Gentner et al., 2006). At a sampling frequency of 64 Hz, filter lengths about 12-18 will correspond to this movement. Since a TMS impulse itself has nontrivial duration, the movement evoked by a TMS impulse should last longer than the movement triggered by an ideal impulse. Therefore, the filter lengths that were used (typically 10-15 in length) were slightly shorter than 12-18.

Figure 28. Subject 2 wearing CyberGlove, drawing letter A and Archimedes spiral.

Fourth, time-frequency analysis (TFA) was performed. As a result of source separation, for each subject four sources were obtained from the experimental observations. Of the four sources only one source had substantial component of tremor. The tremor-containing sources were analyzed by fast Fourier transform (FFT)-based TFA using the function *spectrogram* in MATLAB. For comparison, TFA was also performed on the raw joint movement profiles. A Hamming window of length 512 and a 512-point short time FFT were used as parameters.

An example of the joint movement profiles (Subject 1) was shown in Fig. 29 (Top). To the left of the figure are joint movement profiles of the MCP joints of the thumb and index, middle, and ring fingers. In order to make the tremor more visible, the frequency spectra of the same time domain series were plotted in the middle column of Fig. 29 (Top).

Table 3. Kurtosis values of the normalized joint-angle profiles and extracted source signals

Subject	Kurtoses of four joint-angle profiles				Kurtoses of four source signals			
1	4.77	2.21	1.84	2.54	6.14	1.76	1.86	**23.9**
2	2.57	2.47	2.53	1.77	1.65	7.01	1.67	**19.4**
3	2.16	1.51	1.60	1.58	10.3	3.15	1.98	**19.4**
4	4.13	3.68	3.84	2.35	2.06	3.46	8.86	**13.5**

The processed data from MATLAB was streamed through the algorithm of BSSD for convolutive mixtures. During the deconvolution procedure, BSSD used filters which were typically 10-15 in length. For Subject 1, using a filter length of 10, the obtained sources were shown in Fig. 29 (Bottom) along with the frequency spectra. One can clearly witness the source exclusively containing tremor [Source 4 in Fig. 29 (Bottom)]. Tremor was better appreciated for BSSD when compared to direct spectral analysis. To justify independence of the extracted sources, kurtosis values were calculated for the normalized source signals and joint-angle profiles (Table I). The independence of the tremor source (Source 4) can be implied from its kurtosis value (in bold), which is significantly greater than those of the joint-angle profiles. Though analysis of frequency spectrum of the signals provided ready-to-view tremor, it may mislead as the signals are assumed to be stationary. Therefore, in addition to spectral analysis, time-frequency analysis (TFA) was carried out for both the joint movement profiles and the extracted sources, considering the signals as nonstationary. The results were shown in the right

column of Fig. 29. It can be seen that TFA of the source signals (extracted using the convolutive mixtures model) outperformed TFA done directly on experimental recordings from the joint angle profiles. In the case of the other three subjects, the extracted sources were displayed in Fig. 30, and TFA implemented for tremor-containing sources was shown in Fig. 31.

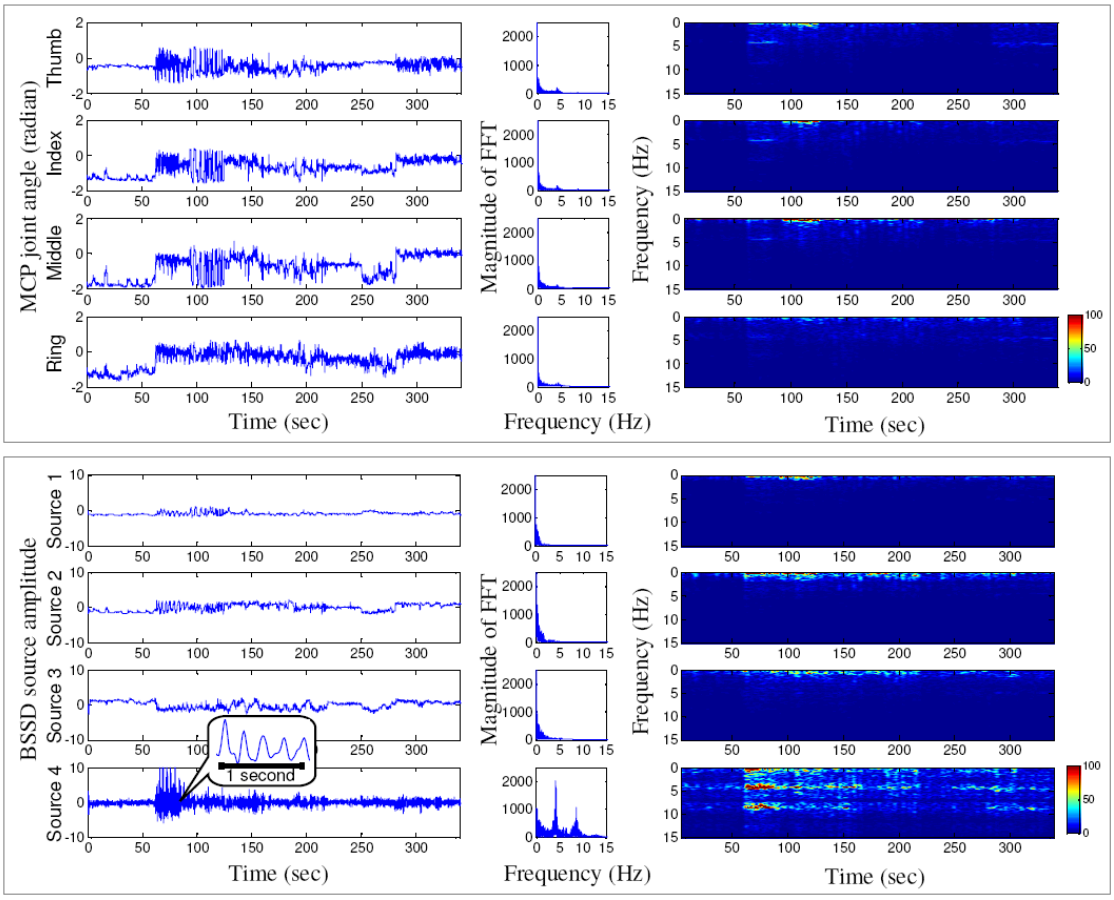

Figure 29. Comparison between direct FFT (top) and BSSD (bottom)

This work was published as R. Vinjamuri, D. Crammond, D. Kondziolka, and Z. -H. Mao. Extraction of neural sources from kinematic profiles of hand movement in NSF Engineering Research and Innovation Conference, Knoxville, TN, 2008.

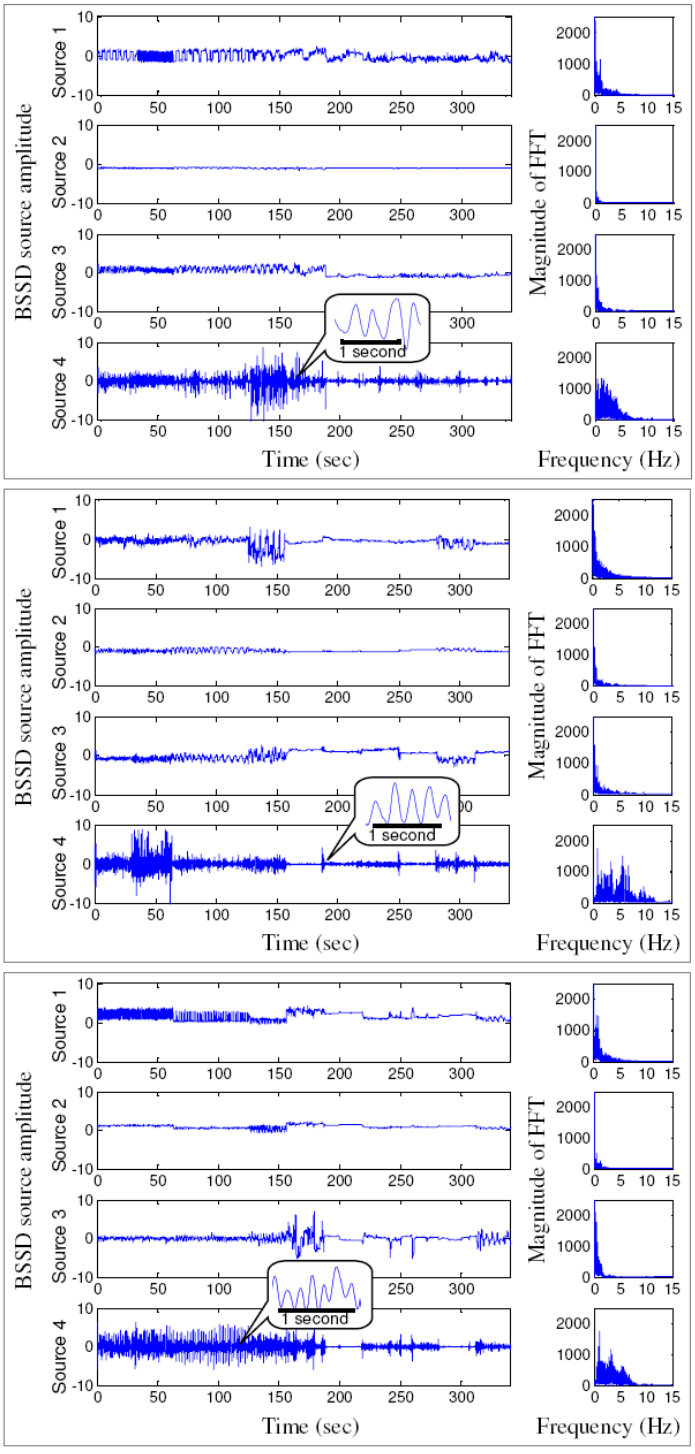

Figure 30. BSSD-extracted sources for Subjects 2-4 (tremor in 4th source)

The filter lengths used for source extraction were 10 for Subject 2, 15 for Subject 3, and 10 for Subject 4, respectively. As noticeably visible, the current model of convolutive mixtures

clearly extracted the sources containing tremor. Multiple components of tremor were observed for all the subjects. It is apparent from the TFA that the tremor was relatively more active in some tasks. This variation cannot be observed in the single frequency spectrum [Fig. 31(Right)] obtained for the entire time series of a source. The variation of tremor seen over time can help clinicians devise better tasks for the tremor to manifest. For instance, in all subjects dominant tremors were observed in finger tapping, opening and closing the fist, and drawing Archimedes spiral.

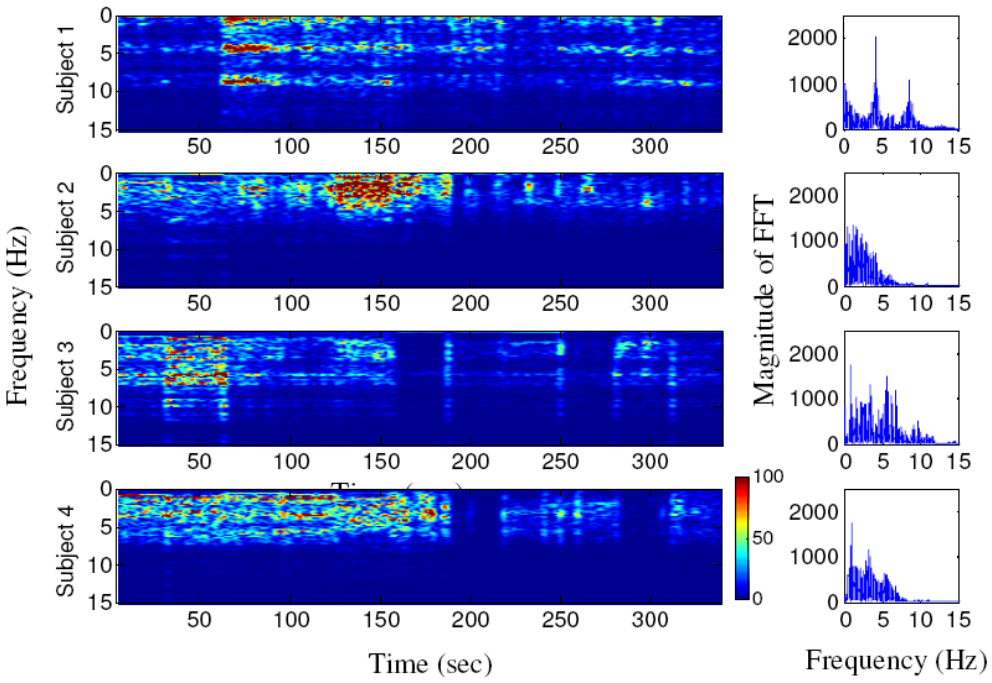

Figure 31. Time-frequency analysis on BSSD extracted tremor sources for all subjects

Essential tremor is accentuated by voluntary movement. The current model of convolutive mixtures was able to extract tremor-containing sources from voluntary movements of hand joints. Four statistically independent sources (per subject) were obtained, of which one source was tremor-exclusive. As witnessed in Fig. 29, tremor was better appreciated in the sources extracted using the current model when compared (by using FFT and TFA) with

experimentally recorded data. This method not only proved significant in tremor detection, but also revealed the sources which might indicate neural activities responsible for tremor generated in the central nervous system. The other sources without tremor might not be exactly the physiological sources for the voluntary movement, but these sources are correlated to the voluntary movement.

1) Multiple components of tremor: It is apparent from time-frequency analysis in Fig. 31 that extracted tremor for all the four subjects had multiple frequency components. This might be due to the sensory feedback which influences the central oscillators (McAuley et al., 2000) (refer to Fig. 1 in (McAuley et al., 2000)). It was observed that subjects had difficulty doing the tasks which needed ample visual guidance. For example, in finger tapping, where subjects had to touch all the fingers with thumb and repeat it as fast as possible, subjects faced difficulty though it appears effortless for normal persons. Multiple components of tremor in ET and other movement disorders were reported by (O'Suilleabhain et al., 1998). In multiple sclerosis, similar behavior was observed by (Liu et al., 1997) where visual guidance was stated as a possible reason.

2) Physiological implications of impulse response: Note that the average length of the selected filters for the four subjects is 11.25 [= (10 + 10 + 15 + 10)/4], which implies that the average duration of the impulse responses of these filters is 11.25/64 × 1000 ms ≈180 ms (sampling rate was 64 Hz). This suggests that a tiny sub-movement of the hand should last for about 200 ms in response to an ideal impulse in the higher-level neural system. Compared with a recent study by Gentner and Classen (2006) (see Fig. 1A in their paper), an estimation of 200 ms is in the same order as 250 ms, the approximate duration of the fastest hand movement evoked by an impulse from transcranial magnetic stimulation.

3) Convolutive vs. Instantaneous mixtures: In the current model joint movements are modeled as convolutive mixtures. Can they also be modeled as instantaneous mixtures? To answer this, blind source separation was carried out using independent component analysis (ICA). For ICA, a FastICA algorithm (version 2.5) (Gavert et al., 2005) was used. The sources obtained for Subject 1 by ICA were shown in Fig. 32. Obviously, ICA outperformed the spectral analysis done directly on the kinematic profiles of hand movements. In the kinematic profiles, tremor can be seen in all joints, but the tremor components were not prominent in the motion of any one of these joints. ICA was able to redistribute the tremor components in the source signals such that the contrast of tremor was more significant in one of the sources. However, ICA could not completely draw out the tremor sources. In comparison, BSSD was able to extract the tremor sources from other sources. One can appreciate BSSD better as shown in Fig. 29—tremor is more apparent in BSSD-extracted source. The advantage of modeling joint movements as convolutive mixtures over instantaneous mixtures can also be supported by the kurtosis values (indicating independence) calculated for source signals extracted by BSSD and ICA, respectively. The kurtosis values of the four source signals extracted by ICA were 1.76, 8.66, 3.65, and 5.54, which are all significantly smaller than 23.9, the kurtosis value of the tremor source extracted using BSSD. ICA has been an efficient technique and been used to separate experimental fMRI in PD (McKeown et al., 2005). The effectiveness of ICA for fMRI data may be due to the fact that the fMRI data directly reflect the neural activities in the brain, which can be well approximated by instantaneous mixtures of some independent source signals. However, when these source signals mix together after passing through the spinal cord and the peripheral nervous and biomechanical structures, the approximation of instantaneous mixture is no longer accurate and thus ICA does not work for this scenario. In contrast, BSSD was effective to detect

tremor sources and extract them from hand movements, because it took into account the dynamics of the peripheral structures and the possible distortion of the source signals by these structures, as discussed in model. Therefore, modeling the movement profiles as convolutive mixtures resulted in better extraction of tremor than as instantaneous mixtures.

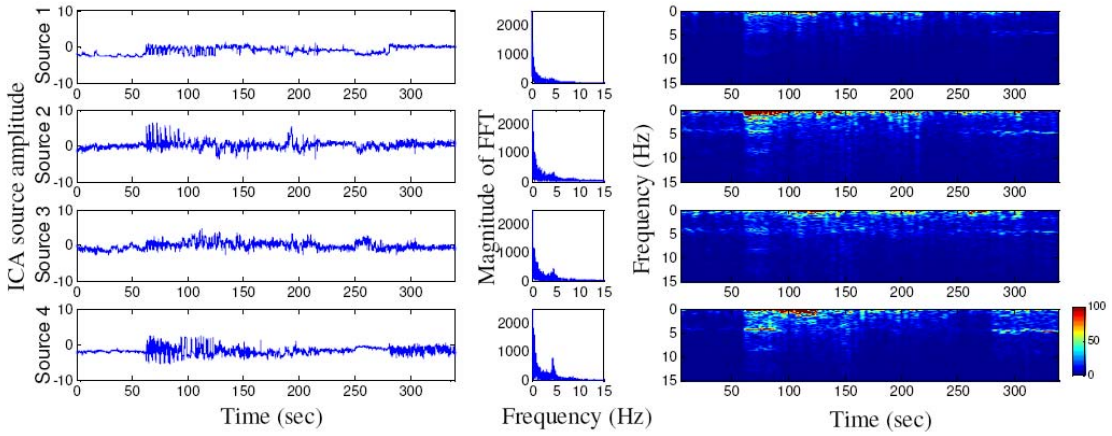

Figure 32. Sources obtained using ICA when modeled as instantaneous mixtures for Subject 1

4) Comparison with contemporary methods: Spectral analysis is popularized for quantification of tremor (Lyons et al., 2005). FFT-based methods have been used frequently because they are computationally inexpensive, but these methods assume the input signals as stationary. In (Rajaraman et al., 2000), Welch's periodogram-based method was used, where power spectral density was estimated for the entire task, ignoring temporal variation of tremor within the task. Current method employing TFA overcomes the above limitations, and the variation of tremor can be seen over time in TFA. TFA was used previously by other investigators as well, but was implemented directly on the experimentally recorded data from muscle activities (O'Suilleabhain et al., 1998). In contrast, current method performed TFA on the tremor sources extracted from the raw experimental data of joint movements. The advantage of using this method was clearly evident in Fig. 29.

5) Correlation between tremor and voluntary movement: For Subject 1 (Fig. 29), the tremor source had a low-frequency component (0.3 Hz, correlated to finger tapping) during the time period from 60 sec to 90 sec. I separately analyzed the finger tapping task by BSSD. As illustrated in Fig. 33 (Top), frequency spectra of joint movement profiles indicated coexistence of frequencies due to task as well as tremor in all joints. However, when processed through BSSD, one can clearly appreciate the separation of task frequency and tremor frequency in spectra of the second and third sources, respectively [Fig. 33 (Bottom)]. Although there was appreciable separation, task frequency was not completely eliminated in the third source, which corresponded to tremor. This implies that the tremor-containing sources included components correlated with voluntary movement. One possible reason is that the current model requires the sources to be statistically independent with each other. However, this cannot be completely satisfied in ET where the amplitude of the tremor may depend on the effort in achieving a task. The correlation between the tremor and voluntary movement was previously observed by (Koster et al., 2002, Hua et al., 2004) in ET. Nevertheless, as mentioned in the model, the timing of tremor can be independent of the voluntary movement—as in the case of rest tremor in ET (Shahed et al., 2007).

Current method was based on a convolutive-mixture model of tremor generation, and was able to attribute tremor to a central source manifested across multiple joints of the hand. Compact representation of sources of tremor, one per subject, was extracted that contained the information of tremor variation across a variety of movement tasks. Clinicians can appreciate this method as this compact representation (a single source of tremor) will ease the diagnosis of the tremor avoiding the trouble of tediously going through numerous experimental data. However, the current method is limited for clinical purposes targeted at quantification of tremor

and may not be applicable for home-based rehabilitation as it is. The method presented is also applicable to Parkinson's disease (PD) as there is evidence of neural sources responsible for tremor: It is reported that in PD central oscillators are responsible for tremor generation (Plenz et al., 1999). The current approach is to be extended over a large group of subjects with various movement disorders.

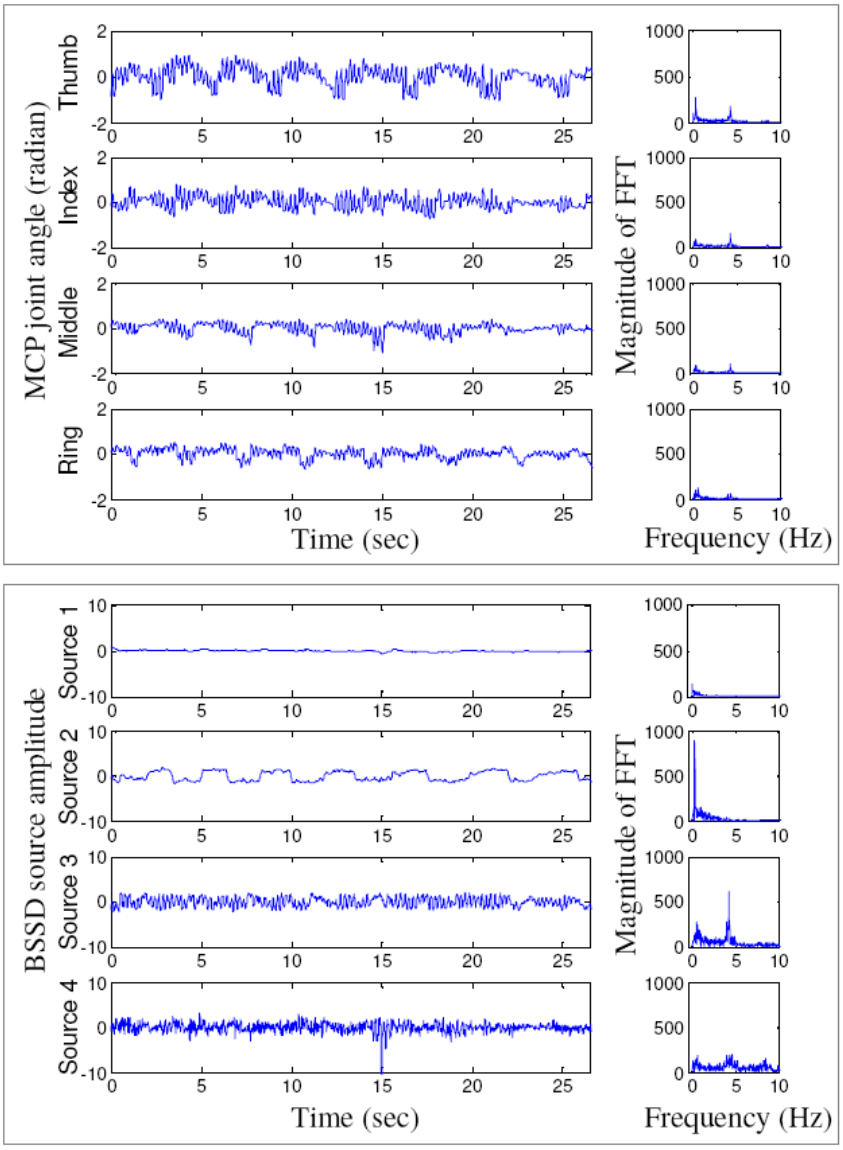

Figure 33. Direct FFT (top) and BSSD (bottom) for finger tapping task for Subject 1

4.3 SELECTION OF SYNERGIES BY l_1— MINIMIZATION

So far the convolutive mixtures model presented in Chapter 3 was realized in two different ways in this chapter. First, by simplifying the original model to instantaneous mixtures, temporal postural synergies were obtained. Second, by assuming the statistical independence of neural sources, the convolutive mixtures model is utilized in extracting sources responsible for tremor by using blind source separation techniques. In this Chapter a numerical method using l_1-minimization is presented to derive an optimal selection of synergies for the convolutive mixtures model. Synergies will be extracted using PCA as discussed in temporal postural synergies (first implementation in Chapter 4.1). Note that these synergies will now be decomposed from a set of hundred rapid grasping movements. These synergies will be used in reconstruction of hundred natural grasping movements (which are slower) and a set of specific movements (which are not grasps).

In Chapter 2.3 the reconstruction of the velocity profile **v**(t), is restricted in the sense that the reconstruction of joint-angular velocity profile does not include repeated use of a synergy—each synergy is used at most once in the generation of an episode of hand movement. Not only reuse of the synergy, but synergies were also dilated (time scaled) before being reused. Here the model is extended to accommodate reuse of synergies, as expressed in the following equation:

$$\mathbf{v}(t) = \sum_{i=1}^{N} \sum_{k=1}^{N_i} c_{ik} \mathbf{s}_i (t - t_{ik}) \tag{10}$$

where N is the total number of synergies, Ni is the number of repeats of the i-th synergy used in **v**(t), and c_{ik} and t_{ik} represent the amplitude coefficient and time shift, respectively, of the k-th repeat of the synergy $s_i(\cdot)$.

4.3.1 Experiment

The experimental setup consists of CyberGlove® equipped with 22 sensors which can measure angles at all the finger joints including distal, proximal and metacarpal joints. For the purpose of this experiment only ten of the sensors which correspond to metacarpal (flexion/extension) and proximal joints of five fingers are used. 25 objects of different shapes, different materials and different dimensions were selected to be used in reach and grasp tasks.

Ten subjects were asked to react spontaneously for system tones by grasping with their fingers 25 objects, starting from a free hand posture and stopping at grasped posture. Each movement was very short and lasted only about half a second. Start and stop were indicated by system tones. At start subject moved his/her fingers and held the posture until stop tone. 25 such grasps were recorded. After a short recess of about five minutes the subject was asked to repeat the experiment. After this, subject was asked to mime grasp (imagining as though subject is grasping the object) all 25 objects and this was repeated again. A total of 100 grasps thus obtained comprised of training data. A similar sequence was followed for testing data to obtain yet another 100 grasps but this time the movements were slow, not rapid as in training data. Also each subject was asked to pose American Sign Language (ASL) numbers (0—9) as shown in Fig. 4 and alphabets (A—Z) as shown in Fig. 34 forming yet another 36 movements which were included in the testing data. The significance of the experiment lies in testing the adaptability of synergies first to natural slower grasping movements; then expanding this adaptability to different movements other than grasps (ASL characters).

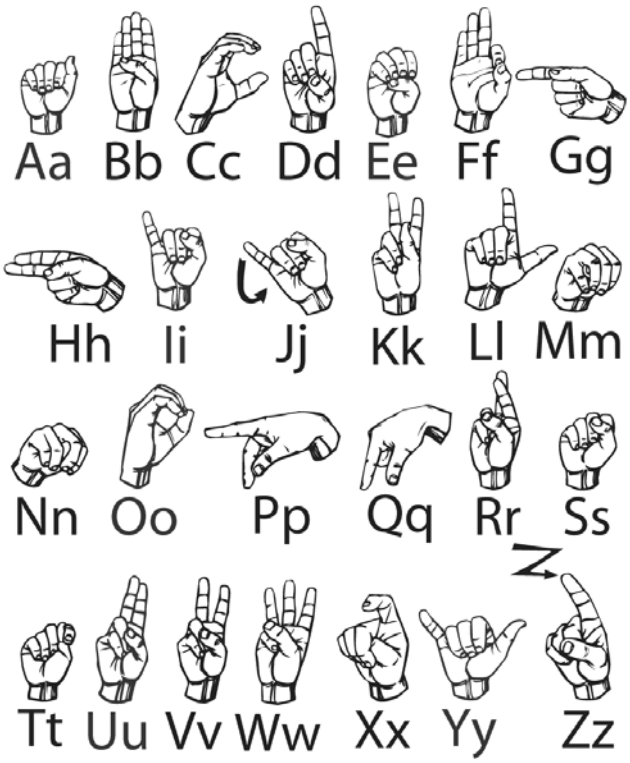

Figure 34. American Sign Language alphabets (adapted from www.wikepedia.org)

4.3.2 l_0-minimization

Data miners and signal processing engineers are interested in finding ways to represent data (signals, images) in the most parsimonious terms in signal analysis; we often consider models proposing that the signal of interest is sparse in some transform domain, such as the wavelet or Fourier domain. Many signals are mixtures of diverse phenomena, and no single transform can be expected to describe them well; instead, models making sparse combinations of generating elements from several different transforms should be considered. An example of l_0-norm minimization problem is shown below.

Minimize $\|x\|_0$ subject to $\boldsymbol{A}x = y$ where $\|x\|_0$ is number of nonzeros in x.

Difficulty in solving the above problem is, in general, solution of the above problem requires enumerating subsets of the library A, looking for the smallest subset able to represent the signal; the complexity of such a subset search grows exponentially with number of elements in the library. l_0-norm is not a true norm. It is not a convex function of x. Instead consider replacing the above problem with l_1- minimization. This is convexification of l_0-minimization (Donoho and Elad, 2003). The added benefit of l_1- minimization is that this can be cast of as linear programming problem and can be solved by modern interior point methods.

4.3.3 Using l_1-minimization

Synergies are extracted by PCA. A standard representation is presented before proceeding to l_1-minimization. Let us assume for a subject, N synergies are obtained. For each synergy, say D dilated versions are allowed. Now there are ND synergies. Again, for each synergy say T shifted versions are allowed. Effectively, there are B (which is equal to product of N, D and T) synergies in total. **M** is the episode which is to be reconstructed as a weighted (where weights are Cs) linear combination of B synergies ($W^1,\ldots,W^B$). Then such equation which is not different from the model of convolutive mixtures (Equation 10) can be expressed as follows:

$$\underset{y}{\begin{bmatrix} M(1,1) \\ M(2,1) \\ \vdots \\ M(j,1) \\ M(1,2) \\ \vdots \\ M(1,k) \\ \vdots \\ M(j,k) \end{bmatrix}_{jk\times 1}} = \underset{A}{\begin{bmatrix} W^1(1,1) & \cdots & W^B(1,1) \\ W^1(2,1) & \cdots & W^B(2,1) \\ \vdots & & \vdots \\ W^1(j,1) & \cdots & W^B(j,1) \\ W^1(1,2) & \cdots & W^B(1,2) \\ \vdots & & \vdots \\ W^1(1,k) & \cdots & W^B(1,k) \\ \vdots & & \vdots \\ W^1(j,k) & \cdots & W^B(j,k) \end{bmatrix}_{jk\times B}} \underset{x}{\begin{bmatrix} C^1 \\ C^2 \\ C^3 \\ \vdots \\ \vdots \\ \vdots \\ \vdots \\ \vdots \\ C^B \end{bmatrix}_{B\times 1}} \tag{11}$$

Now l_1-minimization is used by transforming the above problem into, minimizing l_1-norm subject to equality constraints.

That is

$$\text{Minimize } \|x\|_1 \text{ subject to } \boldsymbol{A}x = y; \text{ where } \|x\|_1 = \sum_i |x_i|$$

This problem is also known as "basis pursuit", finds the vector with smallest l_1-norm that reconstructs the observations y. Such a problem can be recast as a linear programming problem as discussed in (Chen et al., 1999). This means by a sparse selection of synergies this algorithm attempts to solve the reconstruction problem.

4.3.4 Analysis

Synergies are extracted from training data as described in the temporal postural synergies (Chapter 4.1). Readers are requested to refer to that chapter. The remainder of this chapter will be dedicated to results obtained by l_1-minimization assuming that synergies are extracted.

The training data used in obtaining the test synergies were a set of hundred rapid movements. These rapid movements are characterized by higher velocities and shorter durations. Thus the synergies obtained also will have the same features. These synergies were used to reconstruct natural movements. Natural movements are characterized by lower velocities and longer durations. In order to perform best possible approximations in reconstruction of these movements, dilated versions of these synergies are also included in the bank of synergies as mentioned under l_1-minimization section. Dilated synergies are nothing but synergies that are time scaled. Fig. 35 depicts a single joint synergy that is dilated (---) from original synergy (-).

Thus lower velocities can be compensated by multiplying coefficients and longer durations are compensated by dilated versions of synergies.

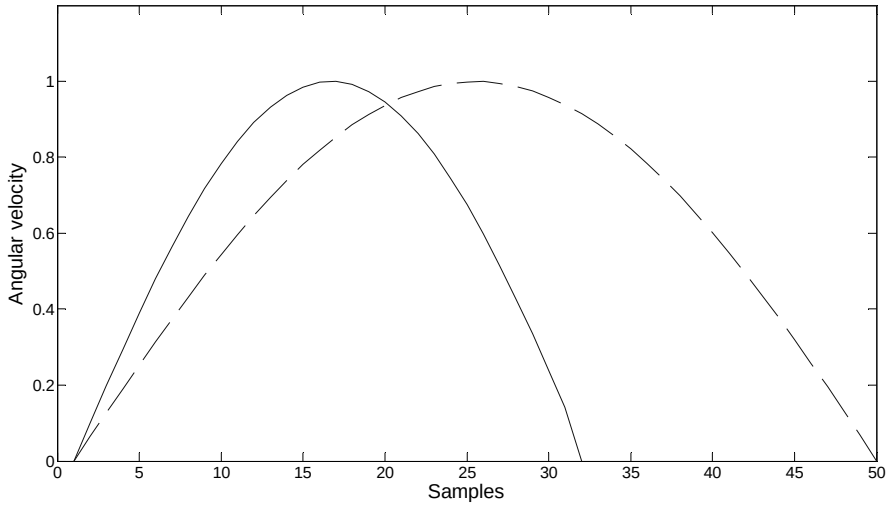

Figure 35. Dilation (---) of synergy (-)

4.3.5 Results

A set of four synergies obtained for one of the subjects is illustrated below in Fig. 36. These synergies were used in reconstruction of the natural or slow movement profiles. Each synergy has ten joints, two joints (metacarpo phalangeal (MCP) and proximal interphalangeal (PIP)) per finger, for thumb (T) and four fingers (I, M, R, P). As learnt from the Figure (Fig. 36) each synergy runs only for a short duration less than half second. Four of the ten synergies are only presented here as they contribute for more than 90% of variance (see Fig. 37) of all the hundred angular velocity profiles included in the training data.

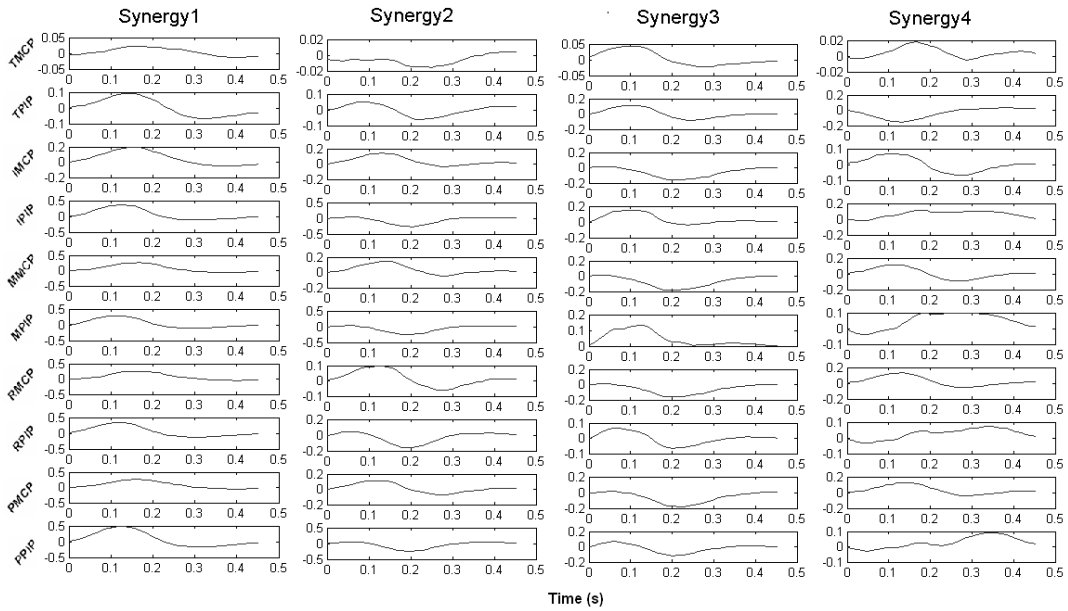

Figure 36. Four of the ten synergies obtained for Subject 1 are shown here.

Ten principal components (PCs) or synergies were obtained for each of the ten subjects. A percentage of variance vs. number of PCs is depicted in Fig. 37 below. This plot shows the percentage of variance accounted by *n* number of PCs. Meaning at 4 PCs, percentage of variance corresponds to that cumulatively accounted by 1 to 4 PCs. Much similar to Fig. 21 adding more number of PCs after about 6 PCs does not contribute to appreciable increase in the percentage of variance or in other words no significant contribution.

A comparison of reconstructions using six synergies and two synergies is shown in the Fig. 38. As a general note all reconstructions are code in black color and original movement in red. In both cases dilations were allowed. The error can be clearly witnessed in thumb and index finger joints. The reconstruction errors were 1.338 (two synergies) and 0.0877 (six synergies).

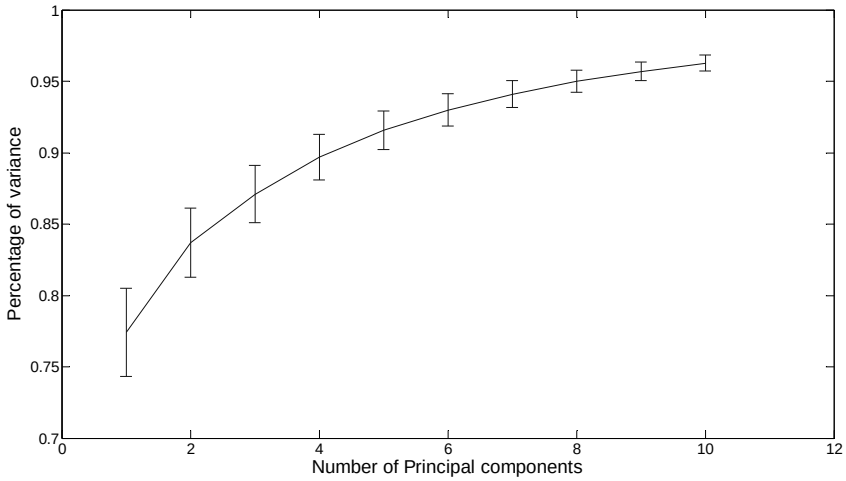

Figure 37. Percentage of variance vs. No. of PCs chart (standard deviation in error bars)

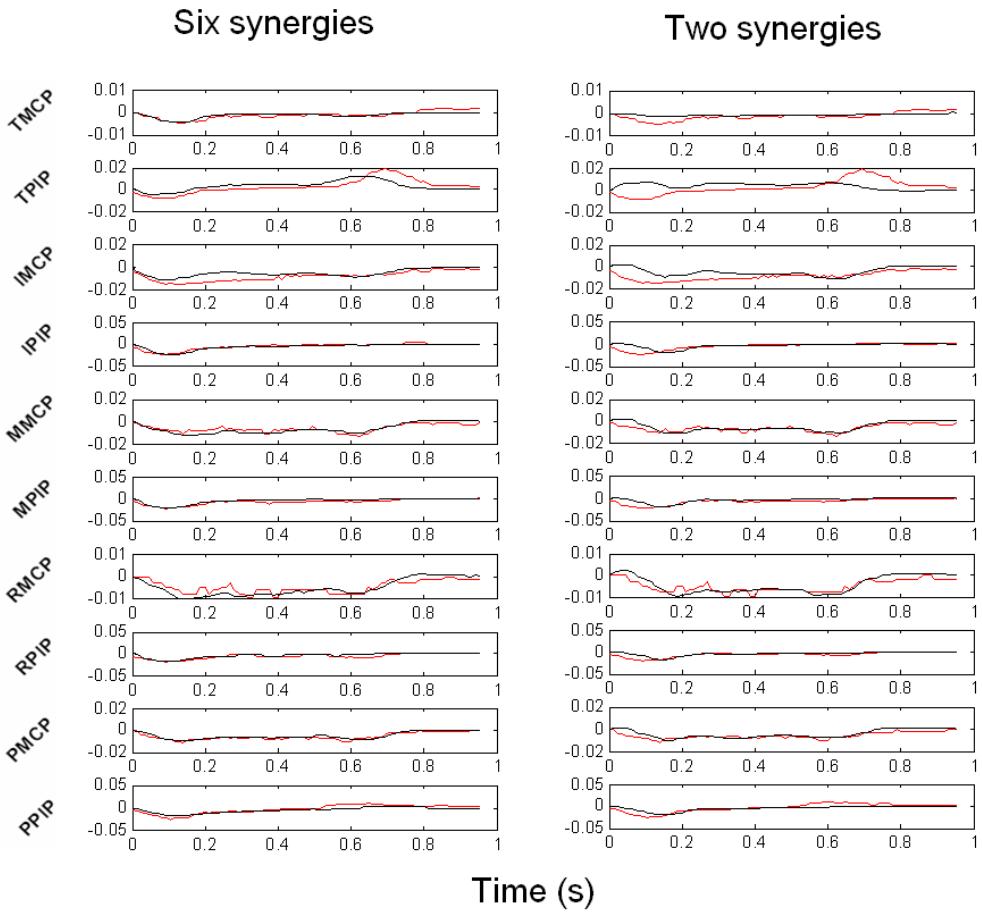

Figure 38. Reconstructions (black) of a natural task (red) with 2 and 6 synergies

Dilation of the synergies increases the adaptability of the synergies to natural or slower movements. For one of the subjects (Subject 10), reconstructions using six synergies one allowing dilation and other without dilation are depicted in Fig. 39. The corresponding reconstruction errors are 0.1225 and 0.0806 respectively. Similar behavior was observed in remaining cases, i. e. when the dilation was allowed it led to appreciable decrease in the reconstruction error.

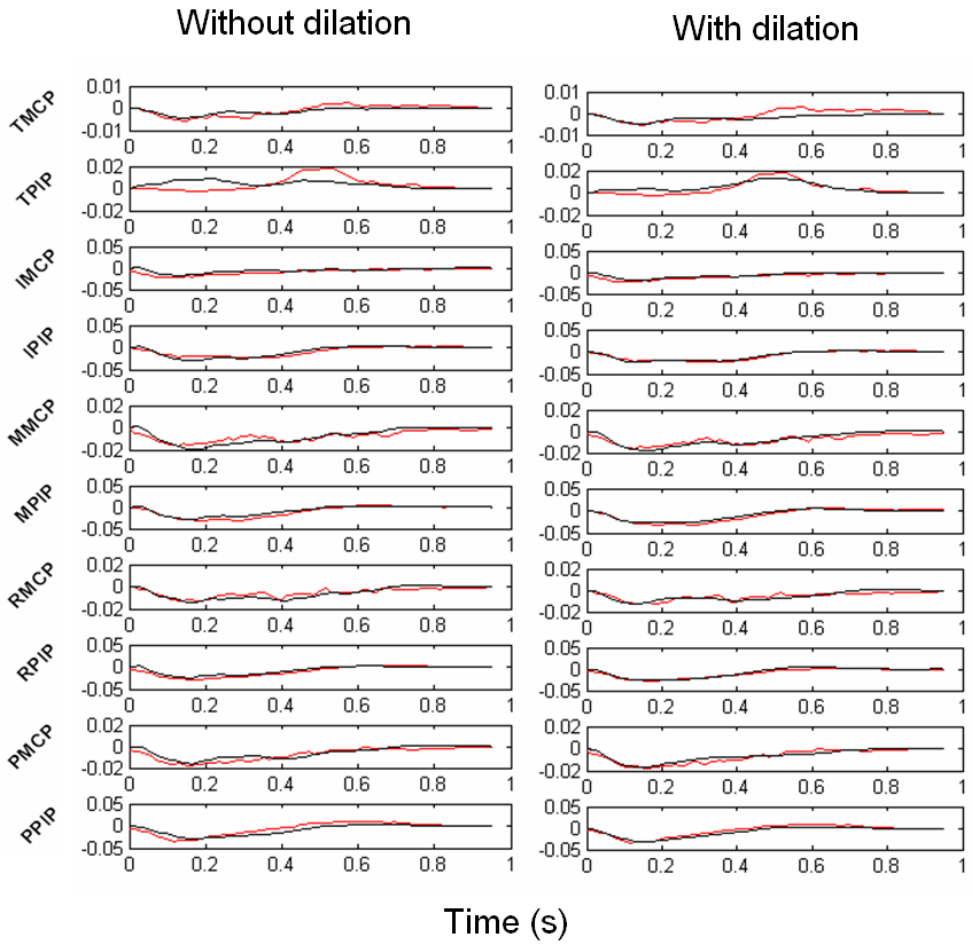

Figure 39. Reconstructions (black) with and without dilations of a natural grasp task (red)

Apart from the reconstructions utilization of synergies was interesting. As mentioned already dilations were allowed for each synergy. Ten dilations were allowed per synergy.

Synergy bank consists of shifted versions of dilated versions of all synergies. Fig. 40 shows the utilization of synergies for one of subjects for five natural tasks. The peaks correspond to the synergies used in reconstruction of a particular task profile. In this particular case 340 versions per synergy (including dilations and shifts). Other than that, Fig. 40 is not self explanatory. This illustration is significant because it contains the important parameters, the coefficients and the shifts appropriate for reconstruction. A brief explanation to appreciate this figure better follows. Six synergies were used in reconstruction of these tasks. For each synergy ten different dilations were allowed. As these dilations were different the number of maximum possible shifts were also different. Meaning, ten dilations allowed were 40, 42, 44, 46, 48, 50, 52, 54, 56, and 58 samples. As the episode length under reconstruction is 82 samples only, the shifted versions are not the same for all the dilated versions of synergies. Hence shifts in that order for each dilated version were 43, 41, 39, 37, 35, 33, 31, 29, 27, and 25 (sum of all these is 340).

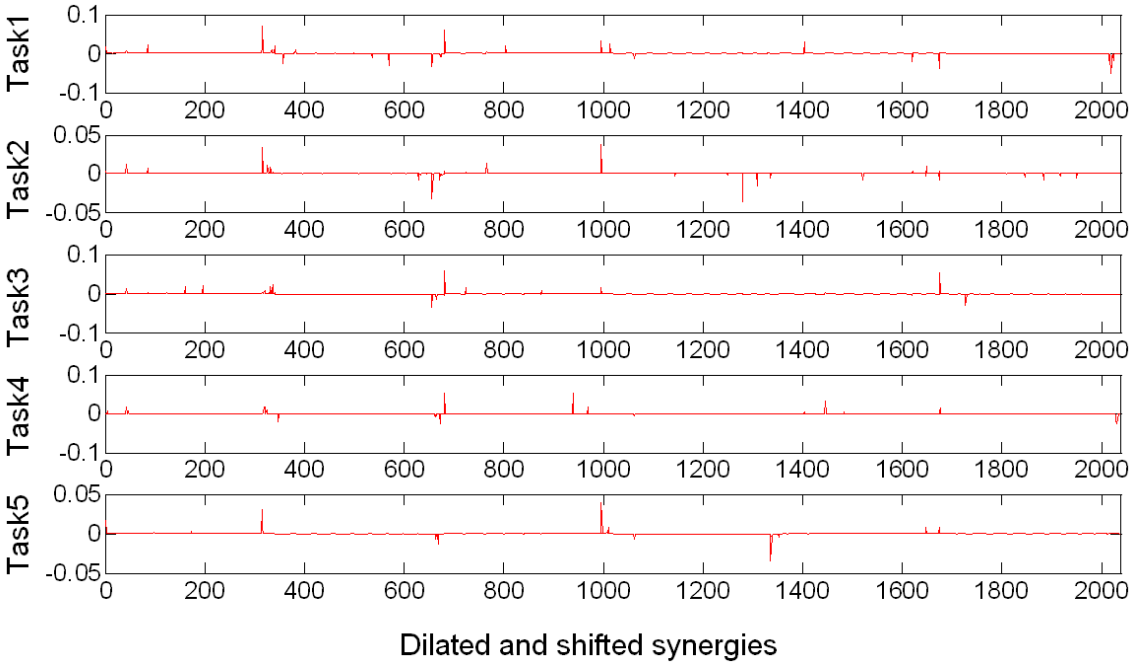

Figure 40. Utilization of synergies in five natural tasks for Subject 8

To simplify let us consider the distribution of coefficients for the first synergy in first task. Fig. 41 depicts the distribution of coefficients. Vertical sections indicate partitions of ten dilated versions of this synergy (D1 to D10). In each section of dilation, there are shifted versions of synergy. This plot can give the information about, which dilated version of this particular synergy was utilized and particular shifts of synergies corresponding to peaks. From the figure it is clear that only D1, D2, D3 and D10 dilations of this synergy have contributed to the reconstruction of the movement. Repeated used of D10 is clearly evident. Note that D5- D9 dilations were not utilized in this particular case.

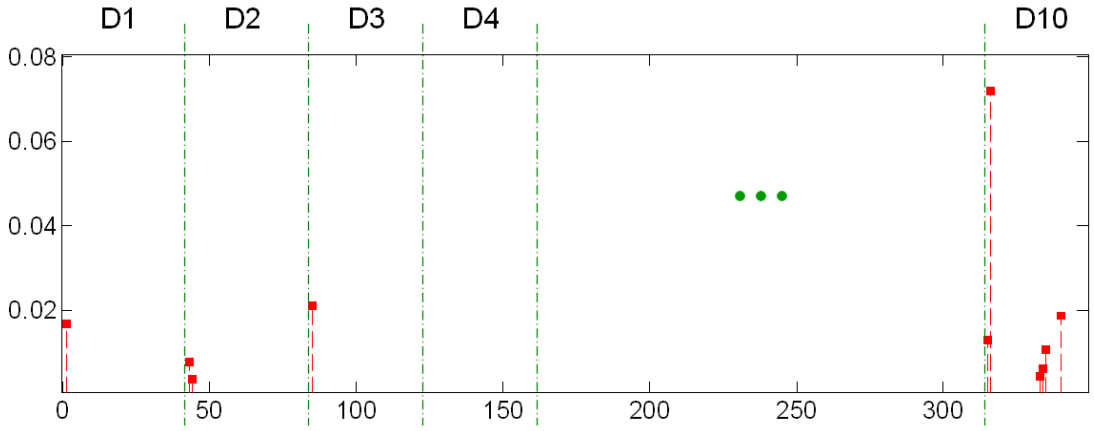

Figure 41. Distribution of coefficients (red stems) in first synergy of the first task of Fig. 40

In order to test the adaptability of these synergies in various paradigms involving tasks which are not grasps, reconstruction of American Sign Language (ASL) characters (10 numbers and 26 alphabets) were also tested. Best and worst constructions are shown below in Fig. 42. The variations in the reconstruction errors across different cases involving increasing number of synergies are shown in Figures 43 and 44 for natural movements and ASL postural movements respectively. The error bars indicate standard deviation across all the subjects and all the tasks. It is observed that maximum reconstruction error for normal movements (0.25) was much smaller

than that of ASL movements (0.42). Although reasonable reconstructions were obtained model performed better in natural grasping movements than ASL postural movements. This might be because the ASL movements for alphabets R, U, V, W, X involved multiple submovements which were not accommodated by limited dilations of synergies. Allowing wider dilations can reconstruct these as well.

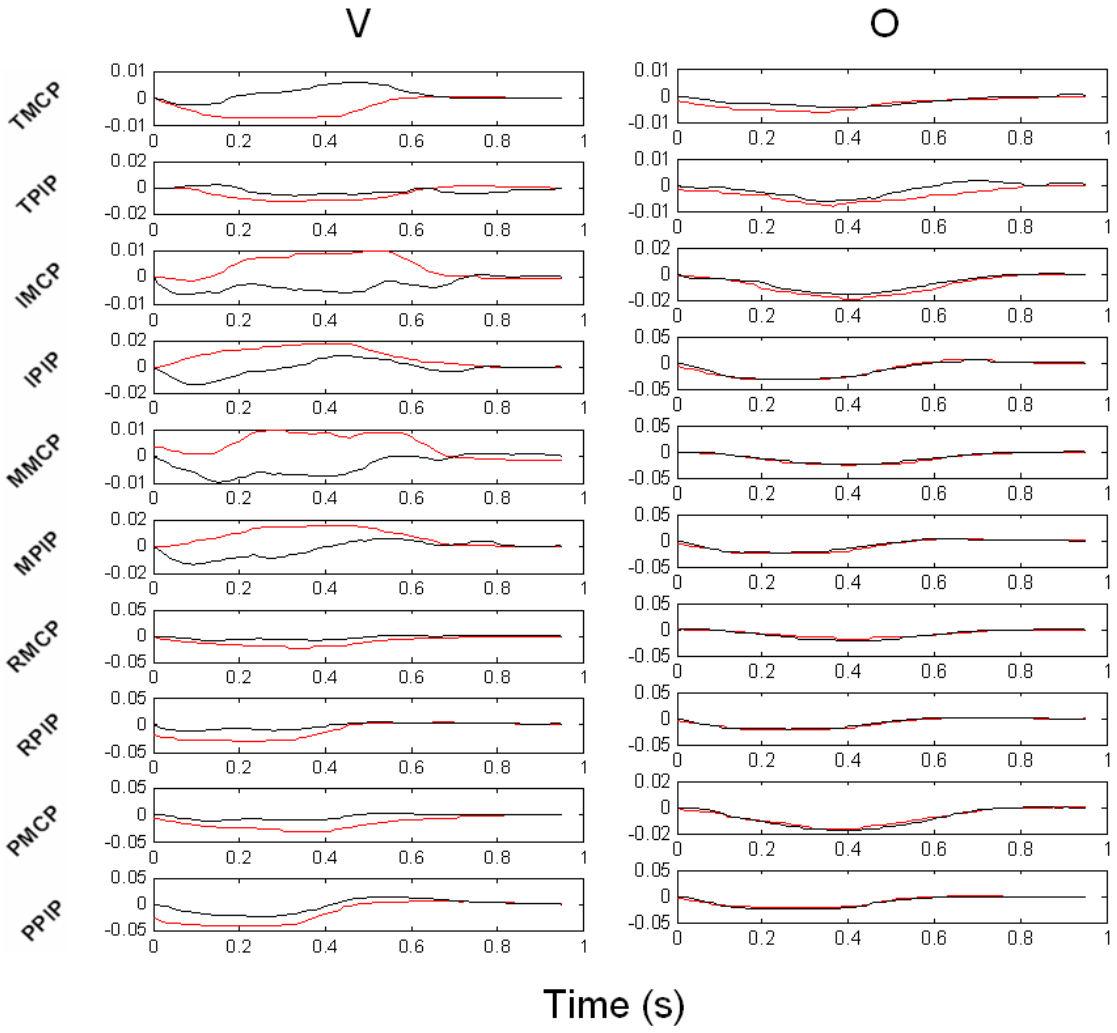

Figure 42. Best (O) and worst (V) reconstructions (black) of ASL postures (red).

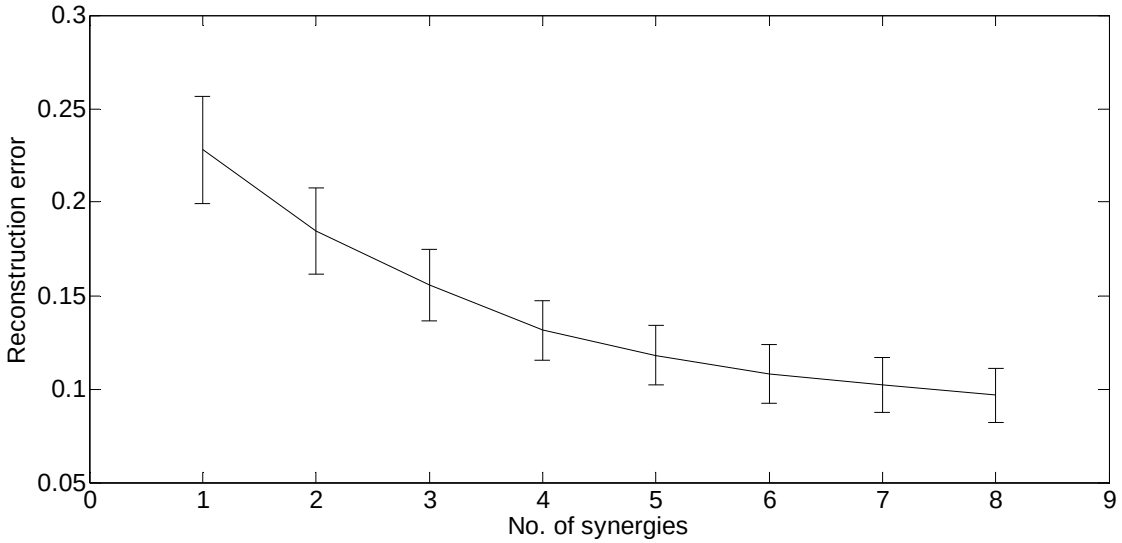

Figure 43. Reconstruction error in natural movements

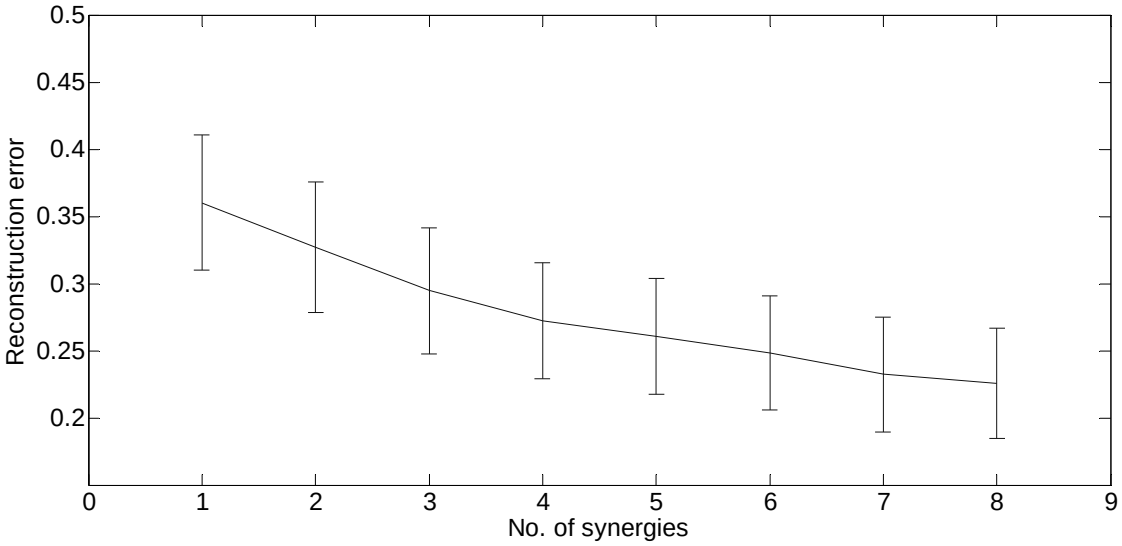

Figure 44. Reconstruction error in ASL movements

Graphical visualizations of the synergies are shown in figures 45 and 46. Fig. 45 shows the transformation of postures of six synergies for Subject 1 along the task time. Each row corresponds to one synergy. Four postures are snapshots of movement at 25%, 50%, 75% and 100% of task times. Synergies from top to bottom are arranged in the order of their contribution (high to low) to the variance of all postural synergies collected for all tasks. It is intuitive that full grasps correspond to significant synergies.

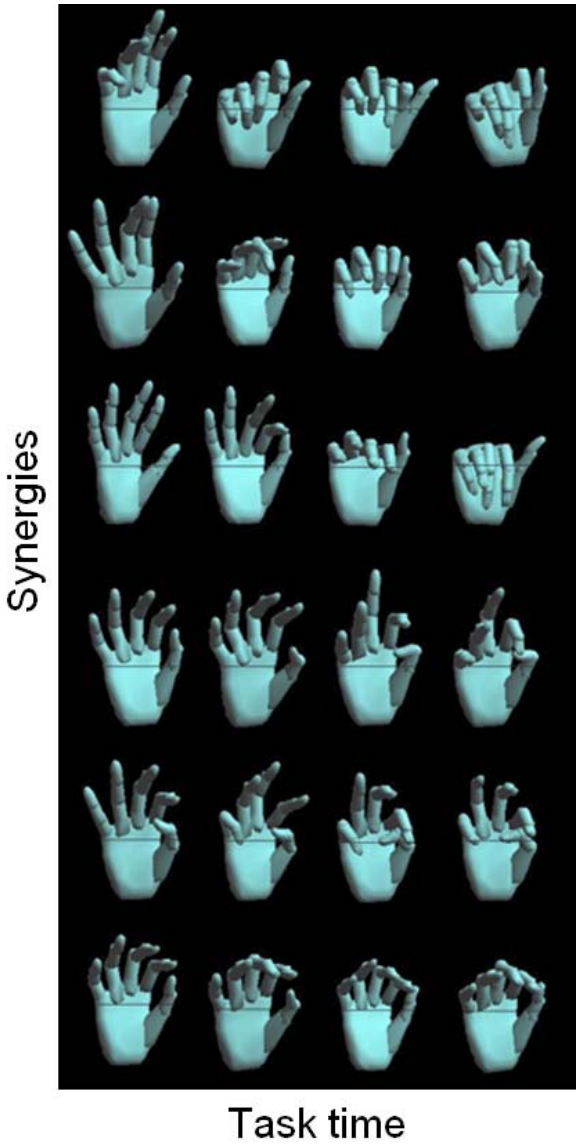

Figure 45. Transformation of postures of synergies along task time

Graphical rendering of synergies for the remaining 9 subjects are shown in Fig. 46. Each row corresponds to one subject. Unlike previous figure, in this figure, postures in each row are snapshots of end postures of six most significant synergies arranged from left to right in the order of their contribution. It is interesting to observe that the most significant synergies in all the subjects correspond to full grasps as seen first 3 columns of Fig. 46.

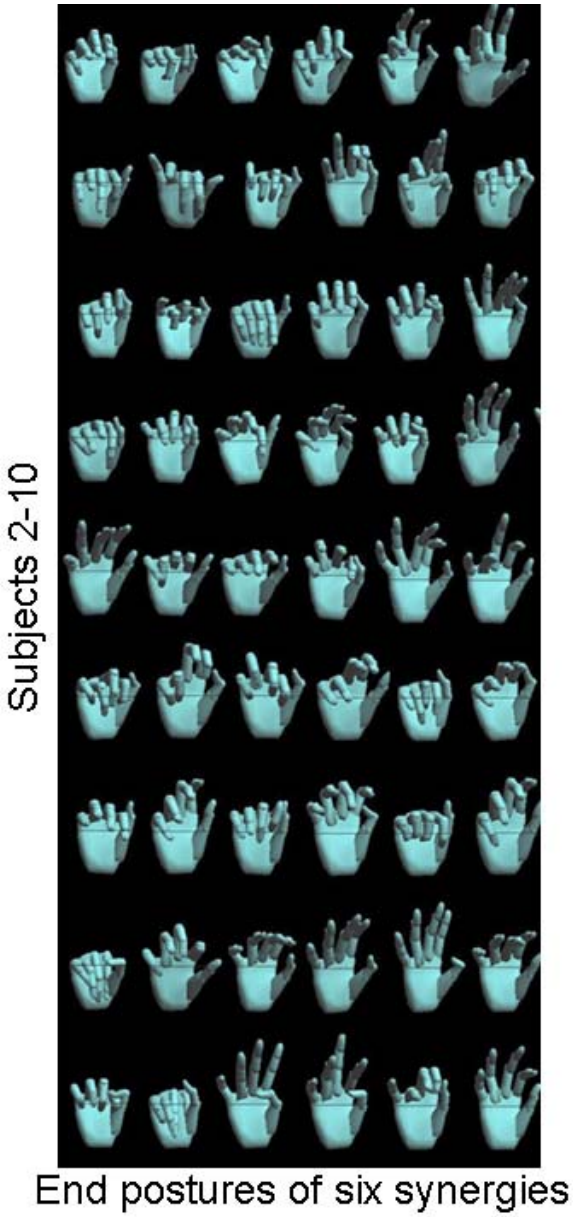

Figure 46. End postures of six synergies for remaining 9 subjects

4.3.6 Discussion

Muscle synergies are widely proposed but kinematic synergies were very often dealt in terms of postural synergies (Santello et al., 2002, Mason et al., 2001 to list a few), although there were kinematic and dynamic synergies observed in (Grinyaginl et al., 2005). Though not using the synergistic models, control and coordination of joint movements (synergistic actions---collective actions) have been reported extensively (Mackenzie and Iberall, 1994). The existence of synergies itself is still debatable, and added to that, synergies have been proposed in different spaces e.g. joint space, muscle space which makes it even more controversial. There are evidences of flexible patterns in joint and muscle coordination observed in movements of frogs and humans which might imply that study in both spaces plays a vital role in understanding the physiology of hand movement.

In this model the concept of multiple recruitments of synergies is introduced. In Fig. 40 and Fig. 41 illustrating the utilization of synergies in reconstruction of a movement, the multiple recruitments are obvious. There have been similar models of combination of movement primitives but none accommodated the possibility of multiple recruitments of synergies. Gorniak et al. (2007) introduced a hypothesis which groups synergies into two types of libraries—one library for day to day actions and another library for learning novel actions. This can be applied to the present case, where CNS borrows the same synergy from one of the libraries more than once at different times with different amplitudes for execution of movement. Also, in (Novak et al., 2002) a movement is expressed as a linear combination of a primary movement and delayed sub movement. Authors observed that the characteristics of shape and symmetry of the primary movement were non different from sub movement. This means that a sub movement may differ in time of recruitment and amplitude and from primary movement. This might suggest that the

same mechanism can be accomplished by a single synergy used multiple times avoiding use of two different primitives (one for primary and other for sub movements) by CNS.

Upon the issue of negative coefficients, physiologically these linear combinations might lead to very meaningful results. Does CNS actually need two different synergies for extension and flexion in velocity space if they are moving at almost same velocity? Extension and flexion are just negation of each other in joint movement space as well as in joint velocity space and other higher kinematic spaces. By allowing negative synergies, the linear combination of primitives is still preserved, but with amplification in negative direction.

Drawing parallels between the convolutive mixtures model and model presented by Novak et al., (2002) [Fig.8 in their paper] implies a similar source signal where HIGH indicates the beginning of primary movement and yet another HIGH would indicate sub movement. Similarly in current model, an impulse would indicate recruitment of a synergy and yet another impulse would infer use of new synergy or shifted or amplified or dilated version of the same.

Characterizing principal components obtained from PCA as synergies leaves a possibility of the synergies to be statistically uncorrelated and not independent. Using ICA to obtain synergies leads to synergies being independent. Unlike PCA, ICA if an algorithm like (d'Avella et al., 2003) is used synergies are correlated much like radial basis functions. It is widely reported that even dexterous humans have difficulty with individuated finger movements which might suggest to some extent that the kinematic synergies might not be strictly independent.

Two different test cases to test two different behaviors of task specificity and task independence were considered. Latash et al, (2007) reported that synergies being learnt are not specific to a particular task but are general dexterities which are adaptable to changes in the external environment. Similar behavior was observed, although not entirely. The reconstruction

error was small in magnitude making them appropriate to be used in reconstruction of grasping tasks as well as ASL postural tasks. This further suggests that some task independent synergies were learnt in the process of learning task specific synergies.

As a last note, addressing the practical viability of the current model, if we were to use the model reported in (Vinjamuri et al., 2007) in prosthesis it might suffer serious problems of performance due to computational time and optimization problems like converging to local minima. Given these problems, running with different initial conditions as suggested in (d'Avella et al., 2003) might not be a practical solution given the time constraints. This model overcomes these problems. Moreover reconstruction error was further minimized by using more number of synergies i.e. considering more principal components which are computationally inexpensive.

An improved model of combination of movement primitives which can accommodate multiple recruitments of synergies was proposed in the current model. Extending this approach to broader area of behavior (beyond tasks) specific and behavior independent synergies would significantly help in understanding the physiology of movement.

5.0 CONCLUSION

Indeed hand makes mind and mind makes hand. Here I have attempted to identify motor primitives and their formation and analyzed collective action of the same which leads to the formation of entire movement profiles in human hands. This study of neural control in general promotes understanding of the brain, the most miraculous controller in the world. Understanding control of human hand has potential applications in neural prostheses and design of dexterous robotic hands.

Current research has significant impacts in various fields of robotics, telesurgery and rehabilitation. First this will promote understanding of neural organization and mechanism for hierarchical control of movements. Effort in this direction will enable us to design brain-like circuits and brain-machine interfaces that can be used in prosthetics, aiding stroke victims, handicapped individuals, and those with brain or spinal cord damages. Second, inspired by the neural principles for handling problems of high complexity and dimensionality, this research will provide insights for the control of large-scale engineering systems. The neural principles will have potential applications in a broad range of areas, such as air traffic management, and exploration with a large number of robots. Third, both the experimental study and theoretical analysis on hand movement will give insights to the development of "alternative control": People may create additional control or communication channels based on translation of hand postures into command signals. The additional channels will allow human operators such as surgeons and

pilots to be more versatile and flexible in device manipulation. Therefore, this research can stimulate the development of interface devices that may replace the conventional keyboards, mice, and joysticks with improved transmission speed.

BIBLIOGRAPHY

Anouti A, Koller WC (1995). Tremor disorders-diagnosis and management. West Journal of Medicine 162, 510–513.

Averbeck BB, Chafee MV, Crowe DA, Georgopoulos AP (2003a). Neural activity in prefrontal cortex during copying geometrical shapes - I. Single cells encode shape, sequence, and metric parameters. Exp Brain Res 150, 127-141.

Averbeck BB, Crowe DA, Chafee MV, Georgopoulos AP (2003b). Neural activity in prefrontal cortex during copying geometrical shapes - II. Decoding shape segments from neural ensembles. Exp Brain Res 150, 142-153.

Averbeck BB, Chafee MV, Crowe DA, Georgopoulos AP (2005). Parietal Representation of Hand Velocity in a Copy Task. Journal of Neurophysiology 93, 508-518.

Barré JA, Reys L (1920). Le syndrome parkinsonien post-encéphalitique. Le bulletin medical i, 351–356.

Bernabucci I, Conforto S, Capozza M, Accornero Neri, Schmid M, D'Alessio T (2007). A biologically inspired neural network controller for ballistic arm movements. Journal of Neuroengineering Rehabilitation 4, 1-17.

Bernstein N (1967). The Co-ordination and Regulation of Movement. Pergamon, Oxford.

Bizzi E, Tresch MC, Saltiel P, d'Avella A (2000). New perspectives on spinal motor systems. Nature Reviews Neuroscience 1, 101-108.

Bizzi E (2007). Motor Primitives and Rehabilitation. Virtual rehabilitation 27, 20-22.

Braido P, Zhang X (2004). Quantitative analysis of finger motion coordination in hand manipulative and gestic acts. Human Movement Science 22, 661-678.

Brooks V (1986). The neural basis of motor control. Oxford.

Castella M, Rhioui S, Moreau E, Pesquet JC (2007). Quadratic higher-order criteria for iterative blind separation of a mimo convolutive mixture of sources. IEEE Transactions on Signal Processing 55, 218–232.

Chen SS, Donoho DL, Saunders MA (1999). Atomic decomposition by basis pursuit. SIAM J. Sci. Comput 20, 33-61.

Cole KJ, Abbs JH (1986). Coordination of three-Joint digit movements for rapid finger-thumb grasp. Journal of Neurophysiology 55, 1407-1423.

Dana CL (1887). Hereditary tremor: a hitherto undescribed form of motor neurosis. The American journal of the medical sciences, 386-393.

Degeorges R, Oberlin C (2003). Measurement of three-joint-finger motion: reality or fancy? A three-dimensional anatomical approach. Surg. Radiol. Anat. 25, 105-112.

Deuschl G, Elble RJ (2000). The pathophysiology of essential tremor. Neurology 54, S14–S20.

Dietz V, Hillesheimer W, Freund HJ (1974). Correlation between tremor, voluntary contraction, and firing pattern of motor units in Parkinson's disease. Journal of Neurology, Neurosurgery, and Psychiatry 37, 927–937.

Durr V, Matheson T: (2003). Graded limb targeting in an insect is caused by the shift of a single movement pattern. Journal of Neurophysiology 90, 1754-1765.

Elan DL (2000). Essential tremor. Archives of neurology, 1522-1524.

Elble RJ (2005). Gravitational artifact in accelerometric measurements of tremor. Clinical Neurophysiology 116, 1638–1643.

Elble RJ, Sinha R, Higgins C (1990). Quantification of tremor with a digitizing tablet. Journal of Neuroscience Methods 32, 193–198.

Ferrell WR, Milne SE (1989). Factors affecting the accuracy of position matching at the proximal interphalangeal joint in human subjects. Journal of Physiology 411, 575-583.

Flash T, Hochner B (2005). Motor primitives in vertebrates and invertebrates. Current Opinion in Neurobiology 15, 660–666.

Fukumoto I (1986). Computer simulation of Parkinsonian tremor. Journal of Biomedical Engineering 8, 49-55.

Gavert H, Hurri J, Sarela J, Hyvarinen A (Oct. 2005). FastICA version 2.5,[Online]. Available: http://www.cis.hut.fi/projects/ica/fastica/

Gentner R, Classen J (2006). Modular organization of finger movements by the human central nervous system. Neuron 52,731–742.

Gorniak SL, Zatsiorsky VM, Latash ML (2007). Hierarchies of synergies: an example of two-hand, multi-finger tasks.

Goodwin GC, Graebe SF, Salgado ME (2001). Control System Design. Prentice Hall, Upper Saddle River, NJ.

Gourie-Devi M, Venkataram BS (1983). Concept of disorders of muscles in Charka Samhita, an ancient Indian medical treatise - relevance to modern myology. Neurology (India), 13-14.

Graziano MSA, Taylor CSR, Moore T, Cooke DF (2002). The cortical control of movement revisited. Neuron 36, 349-362.

Grinyagin IV, Biryukova EV, Maier MA (2005). Kinematic and dynamic synergies of human precision-grip movements. Journal of Neurophysiology 94, 2284-2294.

Halliday AM, Redfearn JWT (1956). An analysis of the frequencies of finger tremor in healthy subjects. Journal of Physiology 134, 600–611.

Hauser H, Neumann G, Ijspeert AJ, Maass W (2007). Biologically Inspired Kinematic Synergies Provide a New Paradigm for Balance Control of Humanoid Robots. Humanoids, Pittsburgh, USA.

Hellwig B, Haubler S, Schelter B, Lauk M, Gushlbauer B, Timmer J, Lucking CH (2001). Tremor-correlated cortical activity in essential tremor. Lancet 357, 519–523.

Hua SE, Lenz FA, Zirh TA, Reich SG, Dougherty PM (1998). Thalamic neuronal activity correlated with essential tremor. Journal of Neurological Neurosurgical Psychiatry 64, 273–276.

Hua SE, Lenz FA (2004). Posture-related oscillations in human cerebellar thalamus in essential tremor are enabled by voluntary motor circuits. Journal of Neurophysiology 93, 117–127.

Hyvarinen A, Karhunen J, Oja E (2001). Independent Component Analysis. John Wiley & Sons, Inc., New York.

Iftime SD, Egsgaard LL, Popovic MB (2005). Automatic determination of synergies by radial basis functions artificial neural network for the control of a neural prosthesis. IEEE Transactions on neural engineering and rehabilitation, 482-489.

Imamizu H, Miyauchi S, Tamada T, Sasaki Y, Takino R, Pütz B, Yoshioka T, Kawato M (2000). Human cerebellar activity reflecting an acquired internal model of a new tool. Nature 403, 192-195.

Ioffe ME, Chernikova LA, Ustinova KI (2007). Role of cerebellum in learning postural tasks. The cerebellum 6, 87-94.

Jerde TE, Soechting JF, Flanders M (2003a). Biological constraints simplify the recognition of hand shapes. IEEE Trans. Biomedical Engineering 50, 265-269.

Jerde TE, Soechting JF, Flanders M (2003b). Coarticulation in fluent finger spelling. Journal of Neuroscience 23, 2383-2393.

Johnston LM, Burns YR, Brauer SG, Richardson CA (2002). Differences in postural control and movement performance during goal directed reaching in children with developmental coordination disorder. Human Movement Science 21, 583–601.

Jolliffe IT (2002). Principal Component Analysis (2nd edition), New York: Springer.

Jones L (1997). Dexterous hands: human, prosthetic, and robotics. Presence: Teleoperator and Virtual Environments 6, 29-56.

Kalaska JF, Scott SH, Cisek P, Sergio LE (1997). Cortical control of reaching movements. Current Opinion in Neurobiology 7, 849-859.

Kawato M, Gomi H (1992). The cerebellum and VOR/OKR learning models. Trends Neuroscience 15, 445-453.

Kelso JAS, Southard DL, Goodman D (1979). On the coordination of two-handed movements. Journal of Experimental Psychology 5, 229–238.

Koster B, Deuschl G, Timmer LJ, Guschlbauer B, Lucking CH (2002). Essential tremor and cerebellar dysfunction: abnormal ballistic movements. Journal of Neurology, Neurosurgery and Psychiatry 73, 400–405.

Kunesch E, Binkofski F, Freund HJ (1989). Invariant temporal characteristics of manipulative hand movements. Experimental Brain Research 78, 539-546.

Latash ML, Scholz JP, Schöner G (2007). Toward a New Theory of Motor Synergies, Motor Control 11, 276-308.

Lee WA (1984). Neuromotor synergies as a basis for coordinated intentional action. Journal of Motor Behavior 16, 135–170.

Likert R (1932). A Technique for the Measurement of Attitude. Archives of Psychology 140, 1-55.

Liu X, Miall C, Aziz TZ, Palace JA, Haggard PN, Stein JF (1997). Analysis of action tremor and impaired control of movement velocity in multiple sclerosis during visually guided wrist-tracking tasks. Movement Disorders 12, 992–999.

Lyons KE, Pahwa R (2005). Handbook of Essential Tremor and Other Tremor Disorders. New York, USA: Taylor and Francis Group.

Mackenzie CL, Iberall T (1994). The Grasping Hand. North-Holland.

Maier MA, Hepp-Reymond MC (1995). EMG activation patterns during force production in precision grip. II. Muscular synergies in the spatial and temporal domain. Experimental Brain Research 103, 123-136.

Mason CR, Gomez JE, Ebner TJ (2001). Hand synergies during reach-to-grasp. Journal of Neurophysiology 86, 2896-2910.

McAuley JH and Marsden CD (2000). Physiological and pathological tremors and rhythmic central motor control. Brain 123, 1545–1567.

McKeown MJ, Hu YJ, Wang ZJ (2005). ICA denoising for event-related fMRI studies in Proceedings of the IEEE Engineering in Medicine and Biology 27th Annual Conference 1, 157-161.

Miall RC (1999). The cerebellum and visually controlled movements, IEE Workshop on Self-Learning Robots III Brainstyle Robotics: The Cerebellum Beyond Function Approximation 2, 1-5.

Moran DW, Schwartz AB (1999). Motor Cortical Representation of Speed and Direction During Reaching. Journal of Neurophysiology 82, 2676-2692.

Morasso PG (2000). Motor control models: learning and performance. In International Encyclopedia of the Social and Behavioral Sciences, Section: Mathematics and Computer Sciences, Marley AAJ, Section Ed. Pergamon Press.

Mosier KM, Scheidt RA, Acosta S, Mussa-Ivaldi FA (2005). Remapping hand movements in a novel geometrical environment. Journal of Neurophysiology 94, 4362-4372.

Mussa-Ivaldi FA, Giszter SF, Bizzi E (1994). Linear combination of primitives in vertebrate motor control. Proc. Natl Acad. Sci. USA 91, 7534-7538.

Novak KE, Miller LE, Houk JC (2002). The use of overlapping submovements in the control of rapid hand movements. Exp. Brain. Res.144, 351–364.

O'Suilleabhain PE, Matsumoto JY (1998). Time-frequency analysis of tremors. Brain 121, 2127–2134.

Padoa-Schioppa C, Li CSR, Bizzi E (2004). Neuronal activity in the supplementary motor area of monkeys adapting to a new dynamic environment. Journal of Neurophysiology 91, 449-473.

Patrick SK, Denington AA, Gauthier MJA, Gillard DM, Prochazka A (2001). Quantification of the UPDRS rigidity scale. IEEE Transactions on Neural Systems and Rehabilitation Engineering 9, 31–41.

Paulignan Y, Frak VG, Toni I, Jeannerod M (1997). Influence of object position and size on human prehension movements. Experimental Brain Research 114, 226-234.

Penfield W, Rasmussen T (1950). The cerebral Cortex of Man: A Clinical Study of Localization of Function. Macmillan, New York.

Plenz D, Kital ST (1999). A basal ganglia pacemaker formed by the subthalamic nucleus and external globus pallidus. Nature 400, 677–682.

Popovic M, Popovic D (2001). Cloning of Biological synergies improves control of elbow neuro-prosthesis. IEEE_M_EMB, 74-81.

Pouget A, Sejnowski TJ (1997). Spatial transformations in the parietal cortex using basis functions. Journal of Cognitive Neuroscience 9, 222-237.

Raethjen J, Govindan RB, Kopper F, Muthuramanan M, Deuschl G (2007). Cortical involvement in the generation of essential tremor. Journal of Neurophysiology 97, 3219–3228.

Rajaraman V, Jack D, Adamovich S, Hening W, Saged J, Poizner H (2000). A novel quantitative method for 3D measurement of Parkinsonian tremor, Clinical Neurophysiology 111, 338–343.

Rajput A, Robinson CA, Rajput AH (2004). Essential tremor course and disability: a clinicopathologic study of 20 cases. Neurology 62, 932–936.

Riviere CN, Reich SG, Thakor NV (1997). Adaptive Fourier modeling of quantification of tremor. Journal of Neuroscience Methods 74, 77–87.

Rohrer B, Fasoli S, Krebs HI, Hughes R, Volpe B, Frontera WR, Stein J, Hogan N (2002). Movement smoothness changes during stroke recovery. Journal of Neuroscience 22, 8297-8304.

Roitman AV, Massaquoi SG, Takahashi K, Ebner TJ (2004). Kinematic analysis of manual tracking in monkeys: characterization of movement intermittencies during a circular tracking task. Journal of Neurophysiology 91, 901-911.

Rosenbaum DA (1991). Human Motor Control, New York: Academic Press, Inc., 1991.

Rouiller EM (1996). Multiple hand representations in the motor cortical areas. In Hand and Brain: The Neurophysiology and Psychology of Hand Movements, Wing AM, Haggard P, Flanagan JR, Eds. Academic Press, Boston, MA, 99-124.

Saltiel P, Wyler-Duda K, d'Avella A, Ajemian RJ, Bizzi E (2005). Localization and connectivity in spinal interneuronal networks: the adduction-caudal extension-flexion rhythm in the frog. Journal of Neurophysiology 94, 2120-2138.

Santello M, Flanders M, Soechting JF (2002). Patterns of hand motion during grasping and the influence of sensory guidance. Journal of Neuroscience 22, 1426-1435.

Santello M, Soechting JF (1997). Matching object size by controlling finger span and hand shape. Somat. Mot. Res. 14, 203-212.

Schieber MH, Santello M (2004). Hand function: peripheral and central constraints on performance. Journal of Applied Physiology 96, 2293-2300.

Schweighofer N, Arbib MA, Kawato M (1998). Role of the cerebellum in reaching movements in humans. I. Distributed inverse dynamics control. Eur J Neurosci. 10, 86-94.

Sebelius FCP, Rosen BN, Lundborg GN (2005). Refined myoelectric control in below- elbow amputees using artificial neural networks and a data glove, Journal of Hand Surgery 30A, 780-789.

Shahed J Jankovic J (2007). Exploring the relationship between essential tremor and Parkinson's disease. Parkinsonism and Related Disorders 13, 67–76.

Smutz WP, Kongsayreepong A, Hughes RE, Niebur G, Cooney WP, An KN (1998). Mechanical advantage of the thumb muscles. Journal of Biomechanics 31, 565-570.

Swinnen SP, Van Langendonk L, Verschueren S, Peeters G, Dom R, De Weerdt W (1997). Inter limb coordination deficits in patients with Parkinson's disease during the production of two-joint oscillations in the sagittal plane. Movement Disorders 12, 958–968.

Thakur PH, Bastian AJ, Hsiao SS (2008). Multidigit movement synergies of the human hand in an unconstrained haptic exploration task. Journal of Neuroscience 28, 1271–1281.

Thoroughman KA, Shadmehr R (2000). Learning of action through combination of motor primitives. Nature 407, 742-747.

Todorov E, Ghahramani Z (2004). Analysis of the synergies underlying complex hand manipulation. Proc. Annu. Conf. IEEE Engineering in Medicine and Biology Society 2, 4637-4640.

Todorov E, Jordan MI (2002). Optimal feedback control as a theory of motor coordination. Nature Neuroscience 5, 1226-1235.

Tresch MC, Saltiel P, Bizzi E (1999). The construction of movement by the spinal cord. nature neuroscience 2, 162-167.

Tuller B, Kelso JAS (1989). Environmentally-specified patterns of movement coordination in normal and split-brain subjects. Experimental Brain Research 75, 306–316.

Turvey MT (1977). Preliminaries to a theory of action with reference to vision, in Perceiving, Acting and Knowing: Toward an Ecological Psychology (R. Shaw and J. Bransford, editors), Hillsdale, NJ: Erlbaum, 211–265.

Valero-Cuevas FJ, Johanson ME, Towles JD (2003). Towards a realistic biomechanical model of the thumb: the choice of kinematic description may be more critical than the solution method or the variability/uncertainty of musculoskeletal parameters. Journal of Biomechanics 36, 1019-1030.

Valero-Cuevas FJ, Zajac FE, Burgar CG (1998). Large index-fingertip forces are produced by subject-independent patterns of muscle excitation. Journal of Biomechanics 31, 693-703.

Van den Berg C, Beek PJ, Wagenaar RC, Wieringen PCW (2000). Coordination disorder in patients with Parkinson's disease: a study of paced rhythmic forearm movements, Experimental Brain Research 134, 174–186.

Vinjamuri R, Mao ZH, Sclabassi R, Sun M (2006). Limitations of surface EMG signals of extrinsic muscles in predicting postures of human hand. IEEE International Conference of the Engineering in Medicine and Biology Society, New York City, NY.

Vinjamuri R, Mao ZH, Sclabassi R, Sun M (2007). Time-varying synergies in velocity profiles of finger joints of the hand during reach and grasp. IEEE International Conference of the Engineering in Medicine and Biology Society, France.

Vinjamuri R, Sun M, Crammond D, Sclabassi R, Mao ZH (2008a). Inherent bimanual postural synergies in hands. International Conference of the Engineering in Medicine and Biology Society, Vancouver, Canada.

Vinjamuri R, Sun M, Sclabassi R, Mao ZH (2008b). Temporal variation of postural synergies of the human hand during grasping. 16th international conference on mechanics in medicine and biology, Pittsburgh, PA, USA.

Vinjamuri R, Crammond D, Kondziolka D, Mao ZH (2008c). Extraction of neural sources from kinematic profiles of hand movement, Proceedings of NSF Engineering Research and Innovation Conference, Knoxville, TN.

Warner DJ, Will AD, Peterson GW, Price SH, Sale EJ, Linda CAL (1990). The VPL data glove as a tool for hand rehabilitation and communication. Ann. Neurol. 28, 272.

Weiss EJ, Flanders M (2004). Muscular and postural synergies of the human hand. Journal of Neurophysiology 92, 523-535.

Werbos P (2005). Neural networks that actually work in diagnostics, prediction and control: common misconceptions vs. real-world success. A tutorial presented at IEEE Industrial Electronics Conference.

Wiesendanger M, Serrien DJ (2001). Toward a physiological understanding of human dexterity. News Physiological Science 16, 228–233.

Will AD, Warner DJ, Peterson GW, Price SH, Sale EJ, Linda CAL (1990). Quantitative analysis of tremor and chorea using the VPL data glove. Annals of Neurology 28, 299.

Wing AM (1996). Anticipatory control of grip force in rapid arm movements. In: Haggard P, Wing AM, Flanagan JR (eds) Hand and brain: neurophysiology and psychology of hand movement. Academic Press, San Diego, 301–324.

Wolpert DM, Miall RC, Kawato M (1998). Internal models in the cerebellum. Trends in Cognitive Sciences 2, 338-347.